Transcriptional regulation of tissue separation during gastrulation of *Xenopus laevis*

Dissertation

submitted to the

Combined Faculties of the Natural Sciences and for Mathematics of the Ruperto-Carola University of Heidelberg, Germany

for the degree of

Doctor of Natural Sciences

presented by

Dipl.-Biol. Isabelle Köster

Dissertation

submitted to the

Combined Faculties of the Natural Sciences and for Mathematics of the Ruperto-Carola University of Heidelberg, Germany

for the degree of

Doctor of Natural Sciences

presented by

Dipl.-Biol. Isabelle Köster

born in Pforzheim, Germany

Date of oral examination: 12 November 2010

Transcriptional regulation of tissue separation during gastrulation of *Xenopus laevis*

Referees:

Prof. Dr. Herbert Steinbeißer

Prof. Dr. Thomas Holstein

Table of contents

1 Summary

During *Xenopus* gastrulation, the involuting mesoderm gets into contact with the inner layer of the blastocoel roof. However, the two tissues do not fuse but remain separated from each other by Brachet's cleft. Key molecules for tissue separation are Paraxial Protocadherin (PAPC) and the *Xenopus* Frizzled 7-receptor (xFz7), which contribute to non-canonical Wnt-signalling and activate Rho, JNK and PKC.

To determine whether PAPC and xFz7 also play a role in regulating the transcription of target genes to elicit tissue separation, microarray analysis was performed on the Agilent *Xenopus* oligo microarray system. I compared the transcriptomes of wildtype animal caps to animal caps in which tissue separation behaviour was induced by the overexpression of PAPC and xFz7. In animal cap tissue ectopically expressing PAPC and xFz7, I identified 56 upregulated and 58 downregulated genes. The array results were confirmed for a subset of these genes by qRT-PCR and "whole mount" *in situ*-hybridisations.

Among the group of downregulated genes, I identified xGit2 and xRhoGAP 11A, two GTPase-activating proteins (GAP) for small GTPases. Both proteins are not described in *Xenopus* yet and were named after their human homologues Git2 and RhoGAP 11A. xGit2 and xRhoGAP 11A are expressed in the dorsal ectoderm, and their transcription is downregulated in the involuting dorsal mesoderm by PAPC and xFz7. Overexpression of xGit2 and xRhoGAP 11A inhibits RhoA activity and impairs convergent extension movements as well as tissue separation behaviour. Therefore I propose that Rho activity in the involuting mesoderm is enhanced through inhibition of xGit2 and xRhoGAP 11A transcription by PAPC and xFz7. xRhoGAP 11A and xGit2 are restricted to the dorsal ectoderm by PAPC and xFz7, while Rho signalling is inhibited.

Zusammenfassung

Während der Gastrulation in *Xenopus laevis* kommt das einwandernde Mesoderm in direkten Kontakt mit der inneren Schicht des Blastocoeldaches, doch die beiden Gewebe verschmelzen nicht miteinander, sondern bleiben durch die Brachet'sche Spalte getrennt. Schlüsselmoleküle für das Gewebstrennungsverhalten sind das Paraxiale Protocadherin (PAPC) und der *Xenopus* Frizzled 7-Rezeptor (xFz7), die zu nicht-kanonischen Wnt-Signalwegen beitragen, indem sie RhoA, JNK und PKC aktivieren.

Um herauszufinden, ob PAPC und xFz7 auch eine Rolle bei der transkriptionellen Genregulation spielen, um Gewebstrennungsverhalten hervorzurufen, wurden Microarrayexperimente auf dem Agilent *Xenopus* Microarray-System durchgeführt. Dabei habe ich das Transkriptom von animalen Kappen des Wildtyps mit dem Transkriptom von animalen Kappen, in denen Gewebstrennungsverhalten durch die Überexpression von PAPC und xFz7 induziert worden war, verglichen. In animalem Kappengewebe, das PAPC und xFz7 ektopisch exprimierte, identifizierte ich 56 hoch und 58 herunter regulierte Gene. Die Ergebnisse der Microarrays wurden für einen Teil dieser Gene durch qRT-PCR und „whole mount" *in situ*-Hybridisierung bestätigt.

In der Gruppe der herunter regulierten Gene identifizierte ich xGit2 und xRhoGAP 11A, zwei GTPase aktivierende Proteine (GAPs) für kleine GTPasen. Beide Proteine sind in *Xenopus* bisher nicht beschrieben, und wurden daher nach ihren humanen Homologen Git2 und RhoGAP 11A benannt. xGit2 und xRhoGAP 11A werden im dorsalen Ektoderm exprimiert. Ihre Transkription wird im involutierenden dorsalen Mesoderm von PAPC und xFz7 herunter reguliert. Überexpression von sowohl xGit2 als auch xRhoGAP 11A hemmt die RhoA-Aktivität und behindert konvergente Extensionsbewegungen sowie Gewebstrennungsverhalten während der Gastrulation. Daher schlage ich vor, dass die RhoA-Aktivität im involutierenden Mesoderm durch die Hemmung der Transkription von xGit2 und xRhoGAP 11A durch PAPC und xFz7 verstärkt wird. xRhoGAP 11A und xGit2 werden durch PAPC und xFz7 auf das dorsale Ektoderm beschränkt, wo die RhoA-Signalgabe gehemmt ist.

2 Introduction

During embryogenesis, the vertebrate embryo develops from a single cell, the oocyte, into a multicellular animal with a distinct three dimensional feature. This single cell, which is initially divided into several smaller, similar looking cells, ultimately forms different tissues and organs with clearly defined functions. Therefore, the cells have to differentiate, and, in order to separate from cells with other roles, boundaries must be established that prevent the mixing of different cell types.

The corner stone for differentiation and border formation is set at gastrulation, when the three germ layers are established. Morphogenetic movements re-structure the embryonic body plan and initial tissue boundaries are formed. This is controlled by intracellular signalling pathways which are to date quite well, but not yet fully characterised. Constantly, new components are identified and, furthermore, already well known components show new functions.

In order to find novel components of the morphogenetic machinery, I used genome-wide screening in *Xenopus laevis*, the African clawed toad, and characterised those candidates functionally.

2.1 Gastrulation establishes the three germ layers

Vertebrate embryos share a set of important stages during their development. After fertilisation of the oocyte, rapid cell divisions cleave the zygote into multiple smaller cells without increasing its cell mass. At the end of this cleavage, the embryo consists of several thousand cells and contains a liquid-filled cavity, the blastocoel (Fig. 1A). The embryo is now called blastula. Subsequently, gastrulation establishes the basic three dimensional body plan of the vertebrate embryo by concerted action of morphogenetic cell movements and results in the rearrangement of the three germ layers: the ectoderm covers the outside, the endoderm has moved inside and the mesoderm is placed in between the endoderm and the ectoderm. Gastrulation has been intensively studied in the amphibian *Xenopus laevis* which is used as a model organism in this study.

In *Xenopus*, gastrulation starts on the future dorsal side of the blastula embryo by the formation of a slit-like groove, the blastopore. This groove is achieved by the apical constriction of the so-called bottle cells in the dorsal marginal zone. Through the blastopore, the endodermal cells that line the prospective archenteron involute inside the embryo (Fig. 1B). Endodermal cells are followed by the mesodermal cells of the marginal zone. The driving force of involution is the vegetal rotation movement of the endodermal cell mass (Winklbauer and Schurfeld, 1999). The endoderm moves actively towards the blastocoel roof and so it is positioned opposite the ectoderm (Fig. 1A, blue arrows). This movement surges the mesendodermal cells inwards, which invaginate through the blastopore and migrate along the blastocoel roof (BCR) anteriorly.

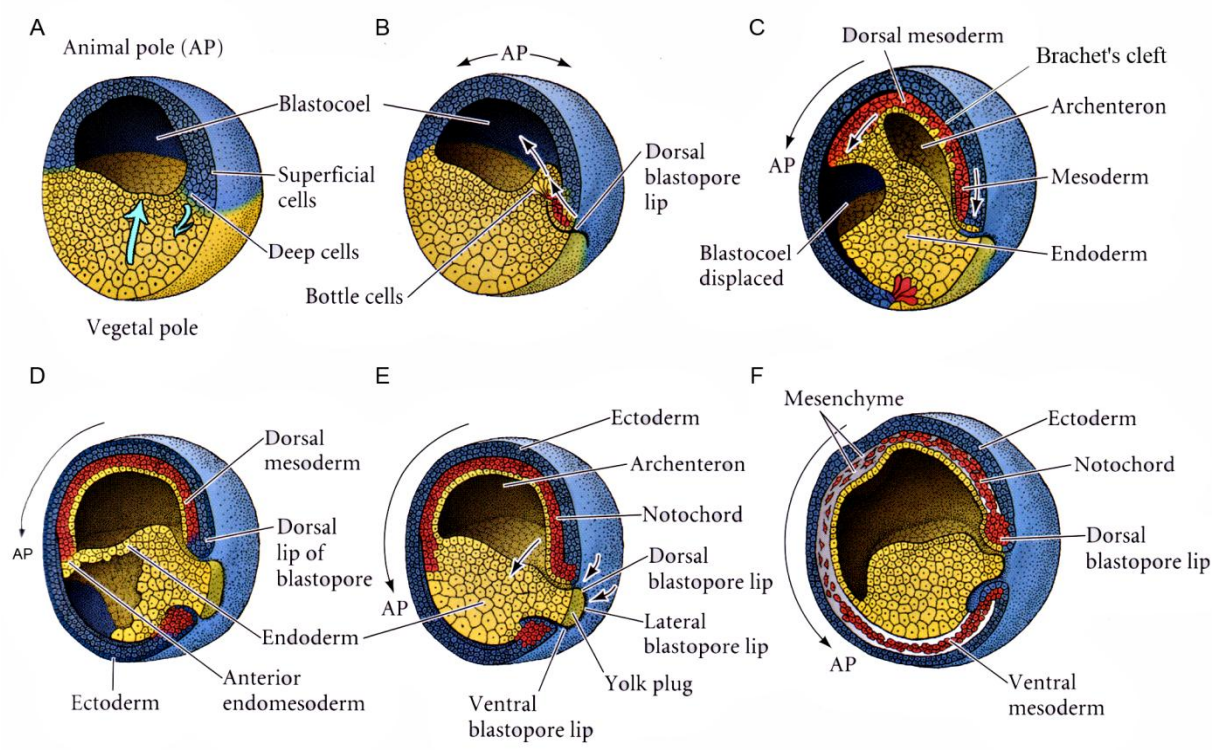

Fig. 1: Cell movements during *Xenopus* gastrulation. (A) Blastula embryo. The animal hemisphere is built from ectodermal cells, the vegetal pole from endodermal cells. Light blue arrows show the vegetal rotation movement of the endoderm. (B) Gastrulation starts in the dorsal marginal zone by vegetal rotation of the endoderm and the formation of bottle cells. (C, D) The endoderm moves in anterior direction along the BCR. (E, F) By epiboly the ectoderm spreads over the embryo and drives blastopore closure. Adapted from (Gilbert, 2006).

The blastopore lip is constantly being built from new cells. The first cells to involute are the cells of the anterior mesoderm which will become head structures, followed by chordamesoderm that forms the notochord and the somites. Gastrulation movements start dorsally, but the blastopore expands laterally towards the ventral side of the embryo, until it forms a ring-like structure. Meanwhile, the ectoderm undergoes epiboly. By radial cell intercalations, the ectoderm spreads vegetally and narrows the blastopore, until it converges at the animal pole and is closed at the end of gastrulation (Fig. 1C-F). At this time, the whole embryo is covered by ectodermal cells (Keller et al., 1992; Keller et al., 2000; Davidson et al., 2002; Keller, 2005).

2.1.1 Convergent extension movements elongate the axis

Convergence and extension (CE) is a common way during chordate development to achieve a rapid change in tissue shape. The body axes of nematodes, ascidians, teleosts, amphibians, birds and mammals are elongated by this type of coordinated cell movements (Schoenwolf and Alvarez, 1989; Sausedo and Schoenwolf, 1994; Keller et al., 2000; Munro and Odell, 2002; Glickman et al., 2003). It also occurs during germ band extension in *Drosophila* development (Irvine and Wieschaus, 1994).

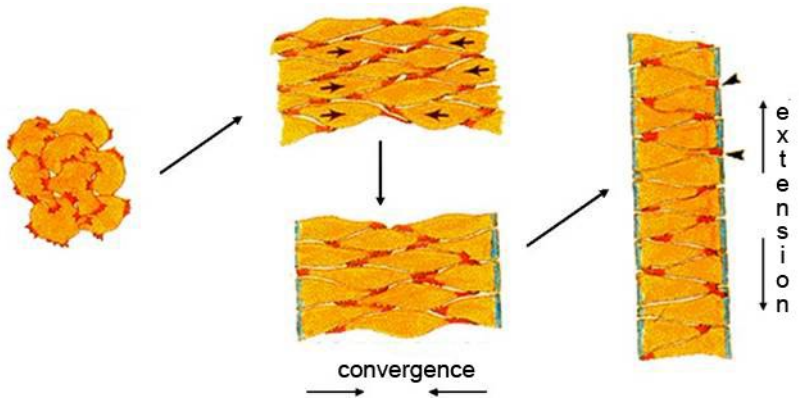

Fig. 2: Convergence and extension movement of the involuting mesodermal cells. Multipolar cells acquire a bipolar shape, and converge at the dorsal midline. By cell intercalations, the tissue is elongated in the anterior-posterior direction. Adapted from (Keller et al., 2000).

In *Xenopus* gastrulation, the involuting mesodermal cells undergo convergent extension movements after internalisation, thus elongating the anterior-posterior body axis. Multipolar cells with randomly oriented protrusive activity acquire a bipolar shape and align themselves mediolaterally, perpendicular to the anterior-posterior axis (Fig. 2). The bipolar tips of these cells exert their protrusive activity on the neighbouring cells and pull themselves between each other. By cell intercalations, the tissue narrows in the mediolateral direction and elongates in the perpendicular direction. Individual cells only have to cover small distances, while this movement achieves a quick elongation of the tissue (Keller et al., 1992; Keller et al., 2000; Wallingford and Harland, 2001; Keller, 2002; Wallingford et al., 2002).

Convergent extension movements also appear in tissue explants of the dorsal marginal zone, indicating that these movements are independent of external tissues or substrates and driven by internal forces (Keller et al., 1992). The regulation of CE movements has been intensively studied in *Xenopus* and zebrafish embryos.

2.1.2 Tissue separation forms the boundary between mesoderm and ectoderm

Tissue boundaries become more and more important during development for the establishment and maintenance of the body plan and the formation of organs. Separation behaviour prevents cell mixing and helps to define borders between different tissues. In metastasising tumours, the opposite, a massive dissolution of tissue boundaries, is observed.

The first separation event in *Xenopus* development occurs when the mesendodermal cells involute through the blastopore and start to migrate along the BCR in anterior direction. The mesendodermal and ectodermal cells do not fuse, but stay separated from each other by a physical barrier, the so-called Brachet's cleft (Fig. 3). The anterior part of Brachet's cleft is formed by the vegetal rotation movement of the endoderm before gastrulation starts (Winklbauer and Schurfeld, 1999), while the posterior part of the cleft is formed by the mesendodermal cell mass when they turn around the blastoporus lip and involute inside the embryo (Wacker et al., 2000).

How this separation behaviour is achieved and regulated, is so far only weakly understood (Wacker et al., 2000; Winklbauer et al., 2001; Medina et al., 2004). Although there is a fibronectin network covering the blastocoel roof, the fibronectin fibrils are not dense enough to just physically separate ectoderm and mesendoderm (Nakatsuji and Johnson, 1983). Moreover, cell adhesion molecules like EP/C and XB/U cadherin are expressed on both sides of the cleft, and tissue separation behaviour is obviously not a simple matter of differential cell adhesion (Choi et al., 1990; Angres et al., 1991; Ginsberg et al., 1991; Herzberg et al., 1991), although it has been shown that a local downregulation of cadherin mediated adhesion is sufficient to induce separation (Wacker et al., 2000).

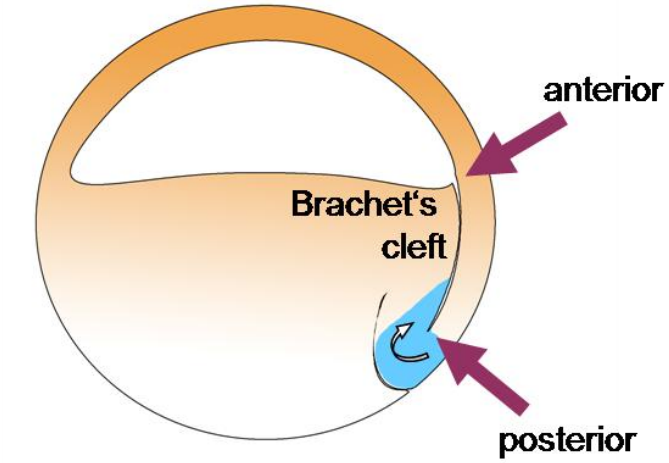

Fig. 3: Brachet's cleft formation in *Xenopus* embryos. During gastrulation the involuting mesodermal cells (blue) stay separated from the ectoderm of the blastocoel roof by Brachet's cleft. The anterior and posterior ends of the cleft are marked by red arrows. The white arrow indicates the migration direction of the involuting mesoderm.

The tissue separation (TS) of the involuting cells develops during invagination through the blastopore and spreads from the anterior to the posterior mesoderm in parallel to the internalisation movements. Cells that have not turned around the blastopore lip yet are indiscriminate and sink into the BCR substratum in an *in vitro* BCR assay (for detailed explanation see 5.3.4). But once they involute, these cells acquire their specific separation behaviour. It has also been shown that activin, which induces dorsal mesoderm, is able to induce separation behaviour in indiscriminate animal cap cells, but the ventral mesoderm inducer FGF cannot do so (Wacker et al., 2000; Jungwirth, 2009). The two transcription factors Mix.1 and gsc, which play a role in the specification of dorsal mesoderm and whose expression patterns coincide with the region of tissue separation, promote TS behaviour in the anterior mesoderm and act as transcriptional repressors in this context (Lemaire et al., 1998; Latinkic and Smith, 1999; Wacker et al., 2000). The *Xenopus* Paraxial Protocadherin (PAPC) and the Frizzled-7 receptor (xFz7) have also been identified as regulators of the TS machinery and are able to induce separation behaviour independent of mesoderm induction (Winklbauer et al., 2001; Medina et al., 2004).

Cells of the blastocoel roof have to develop a repulsion behaviour prior to the involution of the mesoderm (Wacker et al., 2000). An *in vitro* assay showed that early blastula BCR cells are indiscriminate, and cells of the endoderm and the involuted mesoderm, cells that already show

separation to mature BCR cells, would mix with the cells of the early animal cap. Only at stage 9, shortly before gastrulation starts, the cells start to repel endo- and mesoderm. Recently, it was shown that Ephrin mediated signalling is involved in the regulation of the repulsion behaviour of the ectoderm (Jungwirth, 2009).

2.2 Signalling pathways control convergent extension and tissue separation

Convergent extension movements and tissue separation are regulated by a number of well known intracellular signalling pathways. It has been shown that CE is controlled by BMP signalling (Myers et al., 2002), as well as the canonical (Kühl et al., 2001) and non-canonical Wnt-pathways (Torres et al., 1996; Wallingford and Harland, 2002; Veeman et al., 2003). Furthermore, *Xenopus* Paraxial Protocadherin (PAPC) and the Frizzled-7 (xFz7) receptor play a crucial role in regulation of convergent extension as well as tissue separation during *Xenopus* gastrulation (Kim et al., 1998; Djiane et al., 2000; Medina et al., 2000; Medina and Steinbeisser, 2000; Sumanas and Ekker, 2001; Unterseher et al., 2004; Medina et al., 2004).

2.2.1 Wnt-signalling pathways and morphogenesis

Wnt signalling pathways play a crucial role in regulating morphogenetic movements during *Xenopus* gastrulation. The best known pathway is the **canonical** or **Wnt/β-catenin pathway** (Fig. 4, middle). By binding of the Wnt proteins to their receptor of the frizzled family (Logan and Nusse, 2004), the dishevelled protein is activated which in turn inhibits the activity of glycogen synthase kinase-3β (GSK-3β). Active GSK-3β phosphorylates β-catenin and prevents its dissociation from APC that marks it for degradation by the proteasome. By inactivation of GSK-3β, β-catenin accumulates in the cell, enters the nucleus where it binds to transcription factors of the Lef/TCF family and activates the transcription of target genes (Miller, 2002; Huelsken and Behrens, 2002) like Nodal-related 3 (Xnr3) and siamois (Brannon and Kimelman, 1996; Carnac et al., 1996; McKendry et al., 1997; Fan et al., 1998). Wnts that activate this pathway belong to the Wnt-1 class.

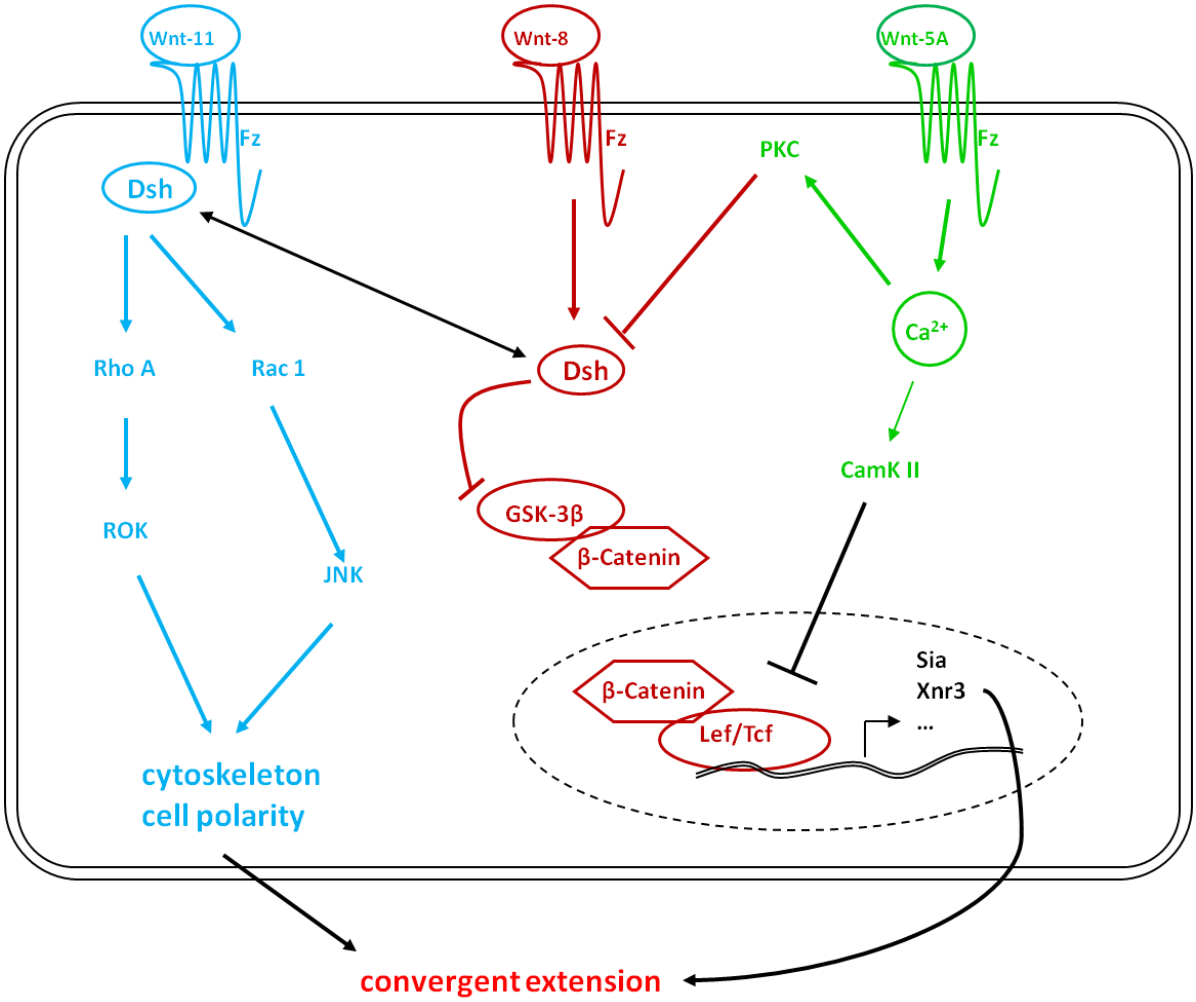

Fig. 4: Wnt signalling pathways during *Xenopus* gastrulation. Wnt/PCP-signalling is displayed in light blue, Wnt/β-catenin-signalling in red and Wnt/Ca^{2+}-signalling in green.

The canonical Wnt-pathway is involved in many processes in early development like the establishment of the anterior-posterior body axis, patterning of the nervous system and induction of neural crest. One of its earliest roles is the breaking of the embryonic symmetry and establishing the Nieuwkoop centre by accumulation of β-catenin in the dorsal side after cortical rotation (Huelsken and Birchmeier, 2001; Darken and Wilson, 2001; Geng et al., 2003). Overactivation of the Wnt/β-catenin pathway in the ventral embryo leads to axis duplication in *Xenopus*. The canonical Wnt-pathway also plays a role in the regulation of convergent extension as it activates the transcription of Xnr3 which has been shown to regulate morphogenetic movements (Kühl et al., 2001).

Apart from the canonical Wnt-pathway, several **β-catenin-independent Wnt-pathways** exist in vertebrates that are important for morphogenetic movements (Kühl et al., 2000; Kühl, 2002; Tada et al., 2002; Wang et al., 2006; Kestler and Kühl, 2008). Wnts that activate these non-canonical Wnt-signalling comprise the Wnt-5A class.

One of those pathways resembles the **Planar Cell Polarity (PCP) pathway** (Fig. 4, left) that has first been described in *Drosophila* and which regulates the organisation of the ommatidia in the fly eye or the polarity of epithelial cells within the plane of the epithelium like the *Drosophila* wing hairs (Klein

and Mlodzik, 2005; Jenny and Mlodzik, 2006). PCP signalling also involves the activation of Dishevelled through Frizzled receptors, but it requires a different set of intracellular signalling transducers like Strabismus and Prickle. Downstream of Frizzled, Dishevelled is translocated to the cell membrane and the small GTPases RhoA and Rac1 and c-jun N-terminal kinase (JNK) are activated. This leads to cytoskeletal rearrangements and cell shape changes. Dishevelled functions as a molecular switch between canonical and Wnt/PCP signalling and its different protein domains are responsible for the different pathways. The DIX domain that has similarities to Axin is active in Wnt/β-catenin signalling, the DEP domain which regulates the activity of small GTPases is in charge of signalling in the PCP pathway. The PCP pathway is characterised by recruitment of Dsh to the cell membrane (Axelrod et al., 1998). While in *Drosophila* no Wnt has been described to be active in PCP signalling, it has been shown in vertebrates that Wnt-5 and Wnt-11 are involved in its activation (Kühl, 2002; Veeman et al., 2003). Proper PCP signalling is indispensable for convergent extension movements and regulates mediolateral cell polarity during this process (Wallingford et al., 2000). Perturbation of this non-canonical Wnt-pathway in either way leads to the disruption of convergent extension movements. In addition, it has been shown, that activation of RhoA is important for tissue separation (Medina et al., 2004).

In vertebrates, a third Wnt pathway has been described which is commonly referred to as the **Wnt/Ca^{2+}-pathway** (Fig. 4, right). By activation of Wnt-5A, a G-protein coupled mechanism releases Ca^{2+}-ions from the endoplasmatic reticulum and calcium sensitive proteins like PKC and CamK II are activated (Kühl et al., 2000; Sheldahl et al., 2003). Activation of this pathway blocks CE and it antagonises canonical Wnt-signalling on different levels (Kühl et al., 2000). PKC is able to inhibit dishevelled function, whereas CamK II operates on the level of the Lef/Tcf transcription factors. Furthermore it has been shown, that PKC is activated by xFz7 in the context of tissue separation behaviour during *Xenopus* gastrulation (Winklbauer et al., 2001).

Regulation of morphogenesis requires a fine-tuned crosstalk of all Wnt-signalling cascades. Canonical Wnt-signalling is required for the establishment of the anterior-posterior body axis and also regulates CE through Xnr3. PCP signalling is required for the establishment of mediolateral cell polarity in the tissue that undergoes CE movements and the Wnt/Ca^{2+}-pathway inhibits canonical Wnt-signalling and antagonises it from the ventral side. Only the sensitive balance of all three pathways enables proper morphogenetic movements.

2.2.2 PAPC and xFz7 regulate convergent extension and tissue separation

Two molecules have been identified to play a role in non-canonical Wnt-signalling and they both are involved in the control of convergent extension and tissue separation: the *Xenopus* Paraxial Protocadherin (PAPC) and the *Xenopus* Frizzled-7 (xFz7) receptor (Winklbauer et al., 2001; Medina et al., 2004).

Receptors of the Frizzled family are seven-transmembrane-domain receptors that bind secreted glycoproteins of the Wnt-family and activate the intracellular signalling cascades (Logan and Nusse, 2004). The frizzled proteins have a cysteine-rich extracellular domain that acts as Wnt-binding site,

seven transmembrane domains and an intracellular C-terminus that differs in size and is responsible for signal transduction into the cell.

The ***Xenopus* Frizzled 7 (xFz7)** receptor is a maternally expressed member of the frizzled family and can activate both canonical and non-canonical Wnt-signalling pathways, depending on the context (Djiane et al., 2000; Sumanas et al., 2000; Medina et al., 2000). The maternal xFz7 transcripts are localised animally. Zygotic xFz7 expression peaks at gastrula embryos (stage 10 to 11) and transcripts are preferentially found on the dorsal side. As gastrulation proceeds, xFz7 forms a ring in the marginal zone. During neurulation its expression gets restricted to three domains: an anterior domain, a posterior domain in the tailbud region and the prospective pronephros (Medina et al., 2000).

xFz7 can interact with Wnt proteins of the Wnt-1 and the Wnt-5A class. Depending on the ligand, xFz7 is able to activate all three different Wnt-signalling cascades. xFz7 specifically synergizes with xWnt-8b in the induction of secondary body axes, a typical phenotype of the Wnt/β-catenin-pathway (Medina et al., 2000). Additionally, xFz7 is also able to induce non-canonical Wnt-pathways, as it is able to recruit PKC to the plasmamembrane in a G-protein coupled manner (Medina et al., 2000; Medina and Steinbeisser, 2000). Finally, xFz7 interacts with xWnt-11 in the activation of Wnt/PCP-signalling and it is able to recruit dishevelled to the plasma membrane (Djiane et al., 2000; Medina and Steinbeisser, 2000). Overexpression of xFz7 results in disturbed morphogenetic movements, as activin treated AC explants do not elongate when xFz7 is coexpressed (Medina et al., 2000). Furthermore it was shown, that knockdown of xFz7 results in ventralised embryos and defects in dorsoventral patterning and convergent extension movements (Djiane et al., 2000; Sumanas et al., 2000; Sumanas and Ekker, 2001).

The **Paraxial Protocadherin (PAPC)** is a member of the cadherin superfamily. Cadherins are a large family of type I transmembrane proteins for Ca^{2+}-dependent homophilic cell-cell adhesion. They consist of five extracellular cadherin domains (EC), a transmembrane domain and a highly conserved cytoplasmic domain including a β-catenin binding site that links classical cadherins to the actin cytoskeleton (Halbleib and Nelson, 2006).

Like classical cadherins, protocadherins are type I transmembrane proteins. In contrast to classical cadherins, the extracellular domain of protocadherins is composed of six or seven EC domains and their cytoplasmic domain is structurally diverse (Halbleib and Nelson, 2006). The PAPC belongs to the superfamily of Protocadherins and it consists of six EC domains, a transmembrane domain and a structurally unconserved cytoplasmic C-terminus (Fig. 5). Initially it has been isolated in a screen for genes that are specifically expressed in the dorsal blastopore lip of *Xenopus* (Bouwmeester et al., 1996) and it is involved in mediating cell adhesion, convergent extension and tissue separation during gastrulation.

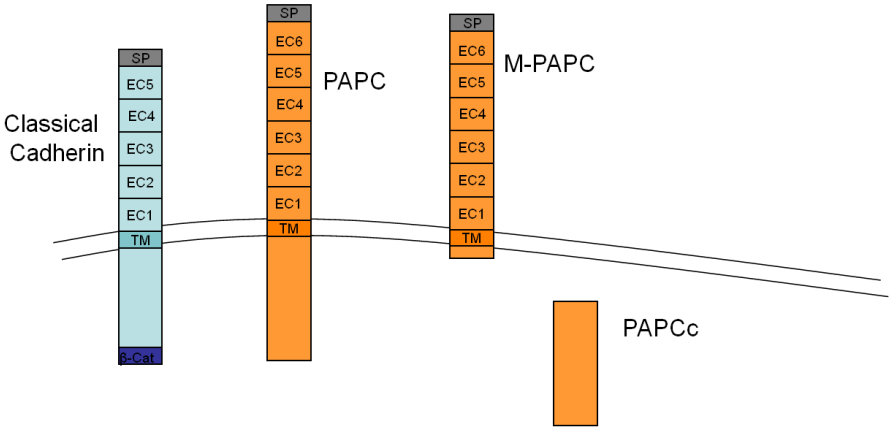

Fig. 5: Protein structure of PAPC compared to that of classical cadherins. M-PAPC is a truncated mutant of PAPC that lacks most of the intracellular domain. PAPCc consists only of the cytoplasmic domain and lacks extracellular and transmembrane domains of full-length PAPC.

PAPC expression starts at blastula stage (stage 8) in the dorsal marginal zone. Its expression domain expands during gastrulation to the entire mesodermal mantle. In the notochord PAPC expression is switched off. At stage 13, when the involution of the mesodermal mantle is complete, expression of PAPC is exclusively found in the trunk mesoderm that undergoes CE movements and the head mesoderm that undergoes direct migration is separated from the trunk mesoderm by a sharp border of PAPC expression. During somitogenesis, PAPC is expressed in the forming somites and switched off after their completion (Kim et al., 1998; Kim et al., 2000).

This complex expression pattern of PAPC is regulated by a number of different factors. Expression in the paraxial mesoderm is induced by the T-box transcription factor VegT, which itself is induced by Bvg1 and activin. In the notochord, PAPC is repressed by xNot, and the repression in the anterior mesoderm results from cerberus, a secreted factor that promotes head formation (Kim et al., 1998). Furthermore, it has been shown that PAPC is a target gene of Lim1, an organizer specific protein that is involved in the regulation of morphogenetic movements (Hukriede et al., 2003). Recently, an alternative non-canonical Wnt-5A/Ror2 pathway has been identified, that also positively regulates PAPC expression (Schambony and Wedlich, 2007).

It has been shown, that PAPC has a function in mediating cell adhesion and cell sorting, as cells injected with full-length PAPC or M-PAPC (Fig. 5), a truncated mutant that lacks the cytoplasmic domain of PAPC, are able to sort out from wildtype cells. However, this effect is due to the downregulation of C-cadherin activity by endocytosis rather than a direct effect of PAPC as a cell adhesion molecule (Kim et al., 1998; Chen and Gumbiner, 2006; Berger, 2009).

PAPC regulates convergent extension movements and cell polarity of the involuting mesoderm. Loss of PAPC inhibits the elongation of TGF-β induced animal caps (Kim et al., 1998; Medina et al., 2004) and the constriction of Keller open face explants of the dorsal marginal zone (Unterseher et al., 2004). This regulation depends on the cytoplasmic domain of PAPC, as M-PAPC cannot rescue these phenotypes. Furthermore, it has been shown that PAPC possesses signalling function and this is responsible for proper CE movements. PAPC is able to activate c-jun N-terminal kinase (JNK) and the small GTPase RhoA, while it inhibits Rac activity (Unterseher et al., 2004; Medina et al., 2004). These

are downstream components of Wnt/PCP signalling which is crucial for the regulation of morphogenetic movements. Recently, we have shown, that sprouty (spry), an FGF inhibitor that also blocks CE by interfering with PCP pathway in a yet unknown mechanism, binds intracellularly to PAPC and that this interaction inhibits spry function and enhances PCP signalling (Wang et al., 2008).

PAPC and xFz7 are key molecules for tissue separation (Winklbauer et al., 2001; Medina et al., 2004). Loss of PAPC as well as loss of xFz7 induces a loss of the posterior part of Brachet's cleft indicating their role in the regulation of tissue separation. Yet the two proteins are not redundant, as knockdown of PAPC cannot be rescued by xFz7 or vice versa. Our group has shown, that the regulation of RhoA by PAPC is crucial for proper tissue separation (Medina et al., 2004), while xFz7 activates PKC to elicit TS (Winklbauer et al., 2001).

Furthermore, it has been shown, that xFz7 and PAPC act synergistically in the activation of TS in the involuting mesoderm. While neither protein is able to induce sufficient separation in indiscriminate ectodermal AC cells, cells coexpressing both proteins stay separated from the BCR substratum in the *in vitro* BCR assay (Medina et al., 2004). Notably, mesoderm induction is not necessary for this separation behaviour. Immunoprecipitation assays revealed that the extracellular domains of PAPC and xFz7 can interact and it has been shown that the interaction is necessary for proper TS behaviour, as the ectopic separation behaviour induced by the combined expression of PAPC and xFz7 is lost, when their physical interaction is inhibited. Furthermore, the adhesive properties of PAPC are dispensable for TS, as combined expression of xFz7 and M-PAPC is not able to induce separation behaviour.

Mesodermal cells injected with a morpholino against xFz7 did not show separation behaviour in the *in vitro* BCR assay (Wacker et al., 2000; Winklbauer et al., 2001). This effect could be rescued by PKC, a downstream component of the Wnt/Ca^{2+}-pathway but not by downstream components of PCP signalling, which shows that xFz7 activates PKC to induce separation behaviour. In the context of tissue separation, PAPC contributes to PCP signalling whereas Xfz7 activates PKC. The influence of PAPC and xFz7 mediated non-canonical Wnt-signalling on convergent extension and tissue separation is summarised in Fig. 6.

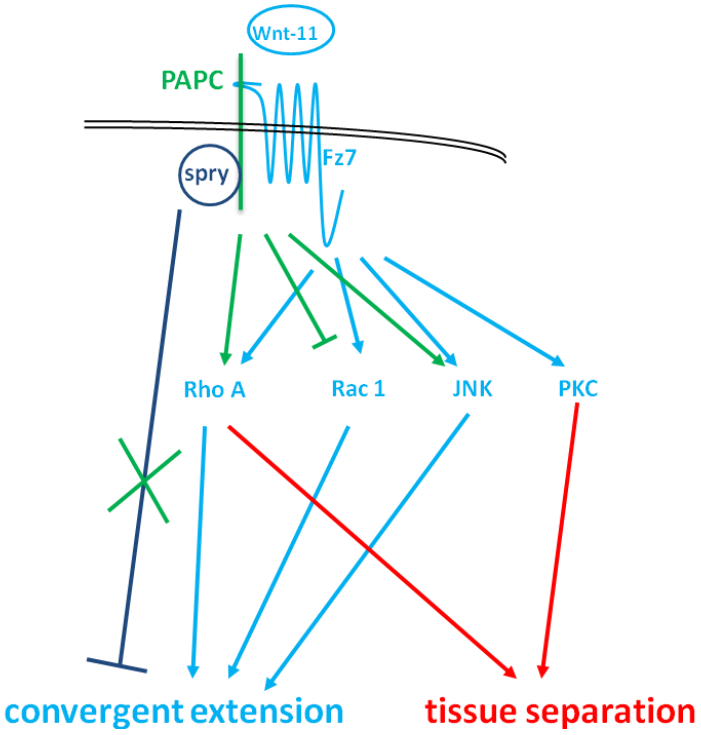

Fig. 6: Summary of PAPC and xFz7 mediated signalling in CE and TS. Light blue indicates non canonical Wnt signalling that leads to convergent extension, green indicates PAPC mediated signalling and red indicates signalling leading to tissue separation behaviour. PAPC promotes CE by sequestering spry (dark blue).

2.3 Aim of this study

PAPC and xFz7 synergise in the activation of tissue separation in the involuting mesoderm during *Xenopus* gastrulation. It has been shown that they interact physically and functionally. They both activate β-catenin independent Wnt-signalling and the signalling properties of both are required for this process, yet the pathways which they induce are not redundant. For the regulation of TS by PAPC, the activation of the small GTPase RhoA is indispensable. Loss of Brachet's cleft by knockdown of PAPC can be rescued by RhoA. xFz7 regulates tissue separation by the activation of PKC (Winklbauer et al., 2001; Medina et al., 2004). However, the molecular mechanisms of how these signalling pathways influence tissue separation are unclear.

As tissue separation occurs after midblastula transition (MBT) when the transcription of zygotic genes has started, it is possible that PAPC and xFz7-mediated signalling could alter gene transcription and regulate the expression of genes involved in tissue separation behaviour.

Therefore the aim of this study was to investigate differential gene expression in wildtype animal cap cells and animal cap cells displaying ectopic separation behaviour induced by PAPC and xFz7 overexpression by microarray analysis. Target genes were to be investigated regarding their possible impact on tissue separation and morphogenesis by functional assays.

3 Results

3.1 PAPC and xFz7 mediate the transcription of target genes

During embryogenesis tissue boundaries become visible and maintain the embryonic body plan. The first tissue boundary occurs when the involuting mesendodermal cell mass comes into contact with the multilayered blastocoel roof, but the two tissues do not fuse and stay separated by Brachet's cleft. In order to achieve tissue separation, the ectoderm develops a repulsive behaviour after midblastula transition, while the dorsal mesoderm develops separation behaviour during invagination (Wacker et al., 2000).

It is known that Paraxial Protocadherin (PAPC) and Frizzled 7 (xFz7) are key components in this process and are sufficient to induce ectopic separation behaviour in *Xenopus* animal cap cells (Winklbauer et al., 2001; Medina et al., 2004). PAPC and xFz7 act in a non-canonical Wnt signalling pathway and their signalling properties are required for proper tissue separation. Yet the molecular mechanism of how they achieve this is unclear.

Since tissue separation occurs after midblastula transition (MBT) when zygotic gene transcription has started it is likely that the zygotic gene expression is required, and PAPC and xFz7 could alter this gene transcription either by non-canonical Wnt-signals or direct regulation of gene transcription. A yeast-two hybrid screen for interaction partners of PAPC, revealed SMARCD1 (Hsiao et al., 2003; Oh et al., 2008), a nuclear mediator of gene transcription, as a potential interaction partner of the intracellular domain of PAPC (Wang, 2007) which suggests that PAPC is involved in mediating gene transcription. In order to determine whether PAPC and xFz7 mediated signalling activates the specific transcription of target genes in the context of tissue separation, I performed microarray analysis on the Agilent *Xenopus laevis* 60-mer oligo microarray.

3.1.1 Microarray analysis of PAPC and xFz7 induced animal caps

To investigate whether PAPC and xFz7 affect gene transcription in the ectoderm, I compared the transcriptomes of animal cap cells ectopically expressing PAPC and xFz7 with wild type (WT) animal cap tissue using the Agilent *Xenopus laevis* 60-mer oligo microarray. 4-cell-stage embryos were injected animally with 400 pg PAPC and 300 pg xFz7 mRNA, amounts sufficient to induce tissue separation (Medina et al., 2004). Animal caps were explanted at the blastula stage (stage 9), cultured until control embryos reached stage 10.5, and RNA was extracted from WT and injected tissues. The RNA was amplified and cRNA was directly labelled with Cy3 (WT) and Cy5 (injected).

The microarray experiments were repeated in three biological replicates. Data analysis was performed using Rosetta Resolver software with the help of Dr. Henner Friedle (Agilent technologies, Karlsbad, Germany). Those genes that were regulated significantly in all three replicates (p=0.01) were further analysed. I found 56 genes that were upregulated in PAPC and xFz7 expressing animal cap cells (Fig. 7A), and 58 genes that were significantly downregulated (Fig. 7B). The genes were then

categorised according to their predicted or established functions by a similarity search in DNA and protein databases.

In both groups, about 25% of the genes were unknown ESTs (expressed sequence tags) or hypothetical proteins which are not characterised further. Additionally, genes with many different functions were identified, like transcription factors, proteins involved in signal transduction or RNA and DNA binding proteins. Among the upregulated genes, there were some proteins that could be involved in cell surface binding and cell adhesion. Among the downregulated genes a group of genes that are involved in Rho and small GTPase signalling especially attracted my attention, as convergent extension and tissue separation are sensitive to Rho signalling (Veeman et al., 2003; Unterseher et al., 2004; Medina et al., 2004).

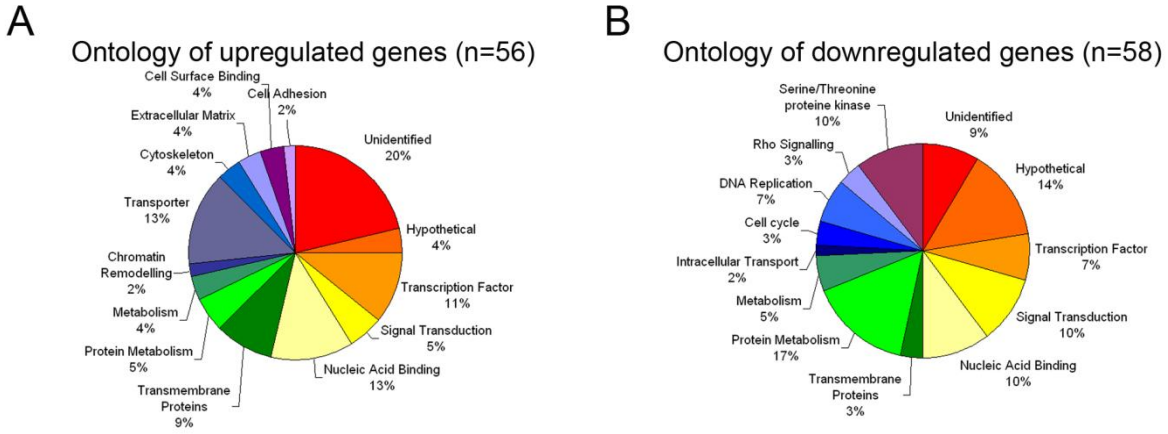

Fig. 7: Ontology of upregulated (A) and downregulated (B) genes in PAPC and xFz7-expressing *Xenopus* animal caps (st.10.5) identified by microarray analysis. The intersections of those genes that were regulated in all three biological replicates (p=0.01) are shown. Up and downregulated genes were categorised according to the predicted or established functions of the proteins acquired by similarity search against DNA and protein databases.

3.1.2 Confirmation of the regulation of target genes

To validate the specificity of the microarray experiments, five upregulated and downregulated candidate genes were chosen for further qRT-PCR analysis (Table 1 and Table 2). These candidates were chosen, because they looked promising to play either a role in tissue separation or in transcriptional regulation derived from their known or predicted gene functions.

The chosen group of upregulated genes therefore consisted mainly of transcriptions factors and transmembrane proteins with cell-cell interaction domains (Table 1). Xnlrr-1, the *Xenopus laevis* neuronal leucine-rich repeat protein, has a leucine rich extracellular domain that often plays a role in cell-adhesion. It is expressed in the developing eye, diencephalon, hindbrain and the spinal cord (Hayata et al., 1998). xOct-91 is a homeobox transcription factor which suppresses mesoderm formation (Hinkley et al., 1992). The homeobox transcription factors xGATA-2 and xGATA-3 are known as regulators of hematopoietic-specific gene transcription (Kelley et al., 1994). Recently, a role for GATA proteins in early gastrulation and mesendoderm migration has been published (Fletcher et al., 2006). BC077967 is an unknown protein with a fibronectin type III-like binding domain, which might be associated in cell-matrix-adhesion, and was hereafter called FNIII-like protein.

Accession number	Sequence name	Sequence description	Prospective function
BC059292	xnlrr-1	*Xenopus laevis* neuronal leucine-rich repeat protein	cell surface binding
M60077	xoct-91	X.*laevis* xoct-91	homeobox transcription factor
M76564	XGATA-2	X.*laevis* GATA-binding protein (XGATA-2) gene	transcription factor
M76565	XGATA-3	X.*laevis* GATA-binding protein (XGATA-3) gene	transcription factor
BC077967	"FNIII-like"	*Xenopus laevis* MGC80995 protein	membrane protein with FNIII-like binding domain

Table 1: List of further analysed upregulated genes

In the group of downregulated genes, one subgroup specifically caught my interest, because these genes are involved in the regulation of small GTPase signalling: two unknown GTPase activating proteins (GAPs) - one specific for RhoA, the other specific for the small GTPase Arf - and a guanine nucleotide exchange factor (GEF) homologous to human Larg (Kristelly et al., 2004). As morphogenetic processes like convergent extension and tissue separation are sensitive to small GTPase signalling (Wallingford et al., 2000; Wallingford et al., 2002; Veeman et al., 2003; Tahinci and Symes, 2003; Unterseher et al., 2004; Medina et al., 2004; Kwan and Kirschner, 2005; Wang et al., 2006; Tanegashima et al., 2008), I focussed on these genes (Table 2). The two GAP proteins, named xRhoGAP 11A and xGit2, were further investigated functionally in chapter 3.2. Additionally, I examined the neural inducing transcription factor Sox-2 (Kishi et al., 2000; Sasai, 2001) and the protein kinase XeWee-1A which is involved in cell cycle control (Mueller et al., 1995).

Accession number	Sequence name	Sequence description	Prospective function
BC070822	xRhoGAP 11A	*Xenopus laevis* hypothetical protein MGC83907	Rho-GAP
AY211396	Larg	*Xenopus laevis* guanine nucleotide exchange factor (Larg)	Rho-GEF
BC073412	xGit2	*Xenopus laevis* hypothetical protein MGC80878 protein	Arf-GAP protein with multiple domains
BC076717	Sox-2	*Xenopus laevis* Sox-2 gene	transcription factor
BC081031	XeWee-1A	*Xenopus laevis* Wee1A kinase	Serine/Threonine protein kinase

Table 2: List of further analysed downregulated genes.

Using qRT-PCR, the regulation of the candidate genes by PAPC was confirmed. 400 pg of PAPC-mRNA and 300 pg of xFz7-mRNA were injected both alone and in combination animally into 4-cell embryos. At stage 9, animal caps were dissected, cultured until stage 10.5 and total RNA was isolated and reverse transcribed. The cDNA was used for qRT-PCR.

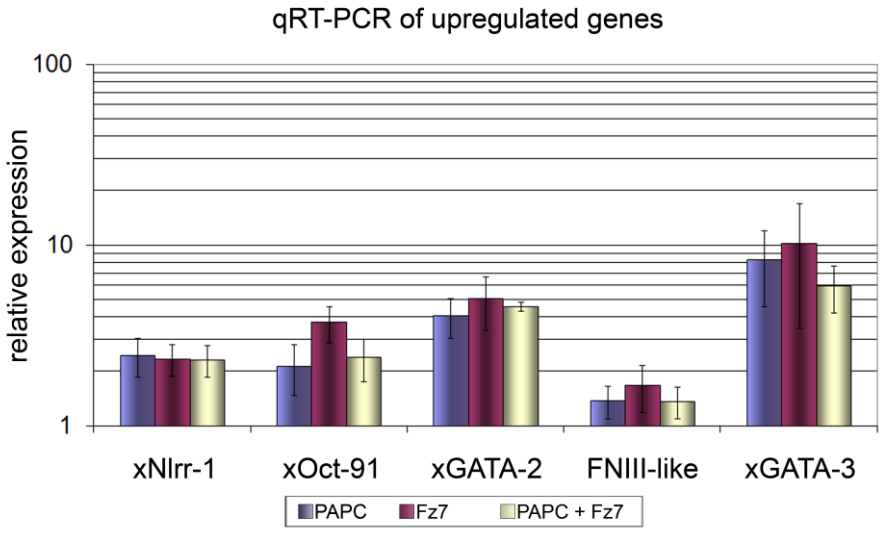

Fig. 8: qRT-PCR of upregulated genes. Upregulation of microarray candidate genes by PAPC and xFz7 was validated by qRT-PCR. 400 pg PAPC and 300 pg xFz7 were injected animally either alone or in combination. Relative expression levels were normalised to uninjected control ACs. Averages from three independent experiments were taken. Standard error is indicated.

Most of the genes that were upregulated in the microarrays also showed an upregulation in the qRT-PCR (Fig. 8). Surprisingly, overexpression of PAPC or xFz7 alone was sufficient to induce the same degree of upregulation that was seen, when PAPC and xFz7 were injected together. XNlrr-1 was regulated about 2.5-fold. xOct-91 was similarly upregulated by PAPC or the combination of PAPC and xFz7, but xFz7 alone was able to upregulate xOct-91 almost 4-fold. xGATA-2 was regulated 4- to 5-fold. The highest regulated gene was xGATA-3, whose expression level could be increased 8- to 10-fold. For the unknown membrane protein FNIII-like regulation by PAPC and xFz7 could not be confirmed. Therefore, it was considered as false positive.

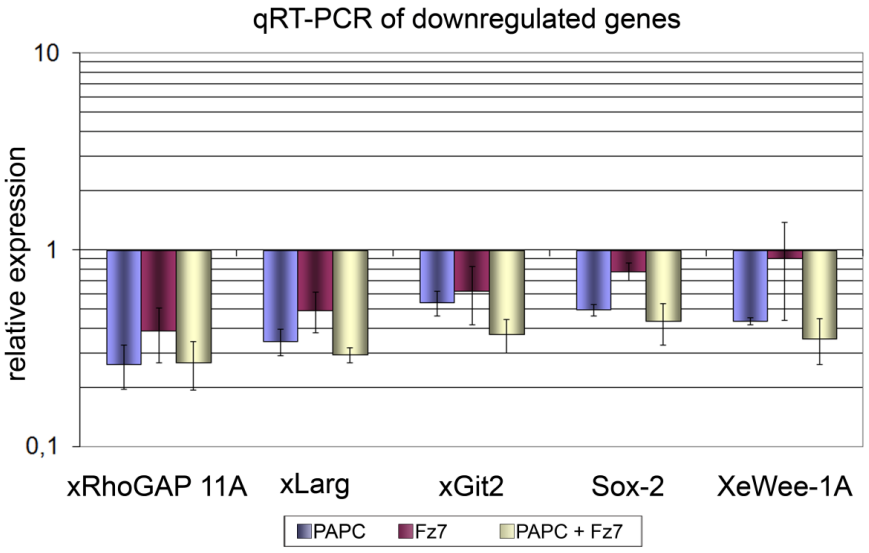

Fig. 9: qRT-PCR of downregulated genes. Downregulation of microarray candidate genes by PAPC and xFz7 was validated by qRT-PCR. 400 pg PAPC and 300 pg xFz7 were injected animally either alone or in combination. Relative expression levels were normalised to uninjected control ACs. Averages from three independent experiments were taken. Standard error is indicated.

I could verify the regulation by PAPC and xFz7 also for downregulated genes (Fig. 9). PAPC and xFz7 reduced the expression levels of xRhoGAP 11A, Larg, xGit2, Sox-2 and XeWee-1A to 30-50% of their wildtype expression levels. Like for the upregulated genes, PAPC or xFz7 injection alone was sufficient to reduce the expression levels of these genes. But remarkably, xFz7-overexpression was not as potent in downregulating the candidate genes as PAPC. xFz7 was able to reduce gene expression levels of xRhoGAP 11A, xGit2, xLarg and Sox-2 only to 40-80% of wildtype levels. XeWee-1A wasn't downregulated at all by xFz7.

3.1.3 Temporal and spatial expression of target genes

To test whether the identified target genes are coexpressed with xFz7 or PAPC, which would make a regulation possible *in vivo*, their temporal and spatial expression patterns were examined by RT-PCR and whole mount *in situ* hybridisation. Total RNA of 5 embryos each from different developmental stages (st.7: morula; st.9: late blastula; st.10: early gastrula; st.11: mid gastrula; st.12: late gastrula; st.17: neurula; st.21: tailbud stage; st.33: tadpole stage) was isolated, reverse transcribed and subjected to RT-PCR (Fig. 10).

The developmental RT-PCR of the upregulated genes revealed that xGATA-2, xOct-91 and Xnlrr-1 were upregulated during gastrulation and after MBT when zygotic gene expression has started. Their expression continues from this moment. xOct-91 is upregulated at stage 10, the beginning of gastrulation, its expression peaks at stage 11 but vanishes again after that. These expression pattern are agree with the microarray results that suggest that these genes are positively regulated by PAPC and xFz7. FNIII like (BC077967), whose regulation by PAPC and xFz7 was not confirmed in qRT-PCRs (Fig. 8), shows a persistent expression throughout all embryonic stages (Fig. 10A).

The downregulated genes XeWee-1A, xGit2, xRhoGAP 11A and xLarg were expressed maternally and showed a decrease at the beginning of gastrulation (Fig. 10B). xGit2 and xRhoGAP 11A are functionally characterised in chapter 3.2. The kinase XeWee-1A regulates the control of the cell cycle which needs to be impeded for proper gastrulation (Mueller et al., 1995). Early *Xenopus* development is characterised by rapid cell divisions. After MBT, cell divisions are slowed down, and cells that undergo morphogenetic movements like the cells in the involuting marginal zone don't divide at all. This corresponds to the fact that a gene that is involved in cell cycle regulation is found among the genes downregulated by PAPC and xFz7.

Sox-2 is upregulated at stage 9 after MBT. Nevertheless, this is no contradiction to its downregulation by PAPC and xFz7. Sox-2 is a transcription factor that induces neural tissue in the prospective neuroectoderm (Kishi et al., 2000; Sasai, 2001). As shown by qRT-PCR, Sox-2 is downregulated by PAPC and xFz7 or PAPC alone. xFz7 alone is not sufficient to decrease Sox-2 expression levels (Fig. 9). As a neural marker gene, Sox-2 is expressed in the ectoderm where xFz7 localisation can be found as well, but not in the mesoderm where PAPC and xFz7 are expressed together. Therefore a local downregulation of Sox-2 in the involuted mesendoderm might be due to the regulation by PAPC and xFz7. I assume that PAPC and xFz7 restrict the expression of Sox-2 to the prospective neural tissue.

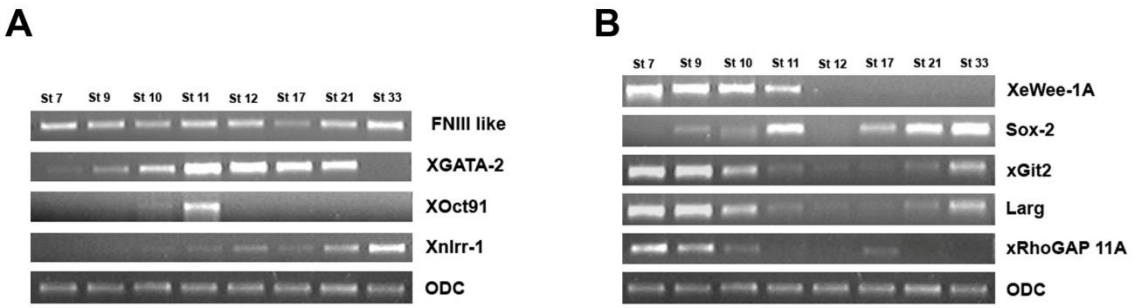

Fig. 10: Temporal expression pattern of candidate genes. (A) Developmental expression pattern of genes upregulated in microarrays. (B) Developmental expression pattern of genes downregulated in microarrays. RNA of embryos from different developmental stages was isolated, reverse transcribed and taken for RT-PCR. (Stage (st.) 7: morula; st.9: late blastula; st.10: early gastrula; st.11: mid gastrula; st.12: late gastrula; st.17: neurula; st.21: tailbud stage; st.33: tadpole stage).

The spatial expression pattern of the target genes was investigated by whole mount *in situ* hybridisation in gastrula stage embryos (stage 10-12), and their expression patterns were compared to that of PAPC (Fig. 11). Most genes showed a ubiquitous expression pattern in the ectoderm. Hemisections of stage 10 embryos revealed that their expression was enhanced at the dorsal side. xOct-91 expression was also found in the involuted mesendoderm, where PAPC and xFz7 are normally expressed. xGit2 and xRhoGAP 11A, two of the downregulated candidates, were only seen in the dorsal ectoderm. The involuted mesendoderm, where PAPC and xFz7 expression overlap, was devoid of xGit2 or xRhoGAP 11A mRNA. At stage 12, FNIII like (BC077967) was expressed very strongly in the notochord, where PAPC is excluded. Interestingly, Xnlrr-1 shows a similar exclusion from the notochord as PAPC in stage 12.

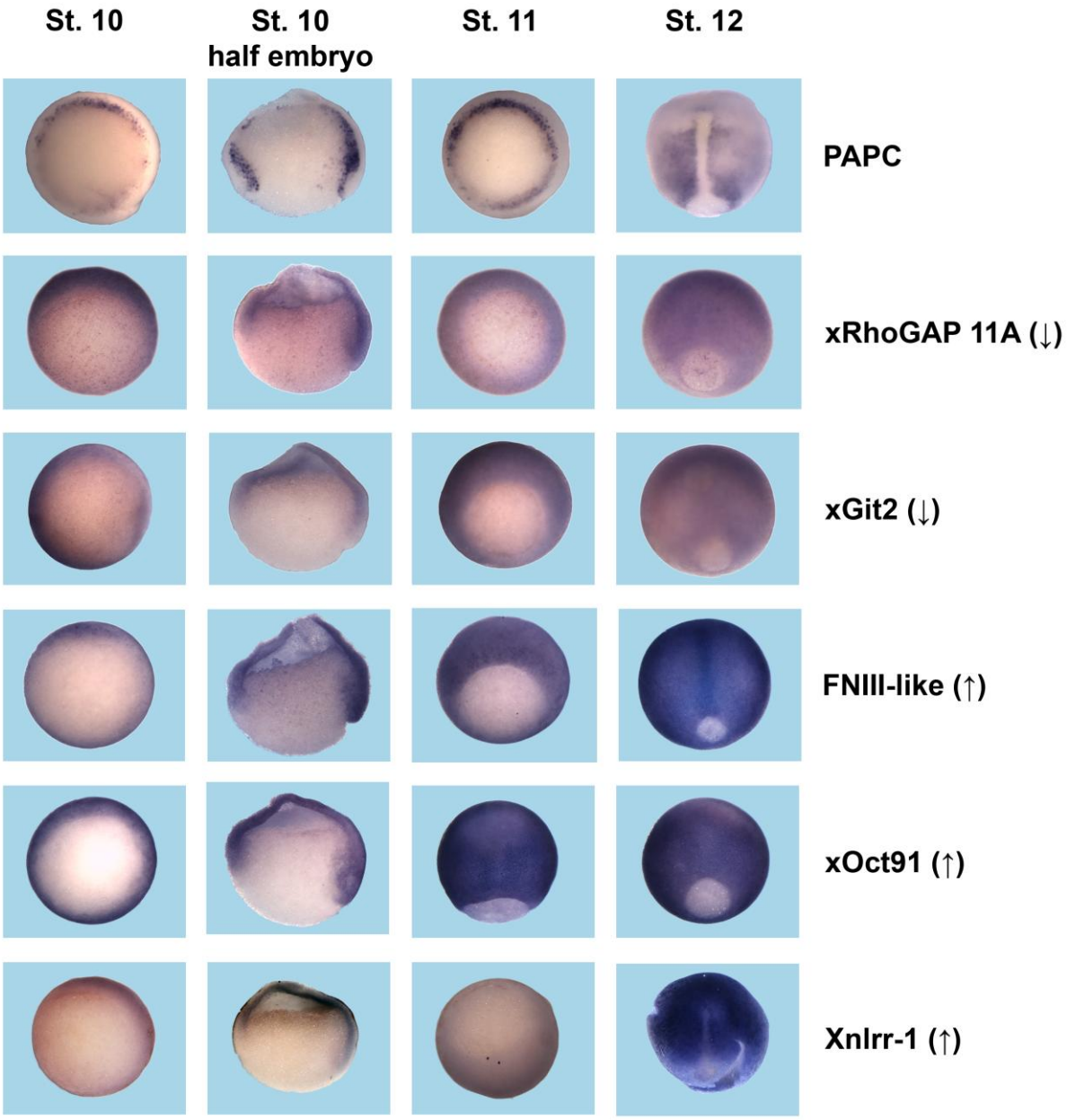

Fig. 11: Spatial expression pattern of candidate genes during gastrulation in comparison to the expression pattern of PAPC. Most of the genes show a ubiquitous but dorsally enriched expression pattern. Gene expression was visualised by whole mount *in situ* hybridisation. Dorsal is up (whole embryos) or to the right (half embryos). (↓) downregulated gene, (↑) upregulated gene.

3.1.4 Influence of PAPC and xFz7 knockdown on target genes

In order to analyse whether PAPC and xFz7 function is required for the regulation of the target genes, I investigated the influence of their knockdown on the target genes by qRT-PCR and whole mount *in situ* hybridisations. Knockdown of target genes in the tetraploid genome of *Xenopus laevis* is achieved by antisense morpholino oligonucleotides (morpholinos, Mo) that bind to their target mRNA and specifically block its translation. 4-cell-stage embryos were injected dorsally with 0.5 mM each of MoPAPC and MoxFz7, alone or in combination, and grown until stage 10. Total RNA was isolated from the dorsal halves and subsequently quantitative RT-PCR was performed.

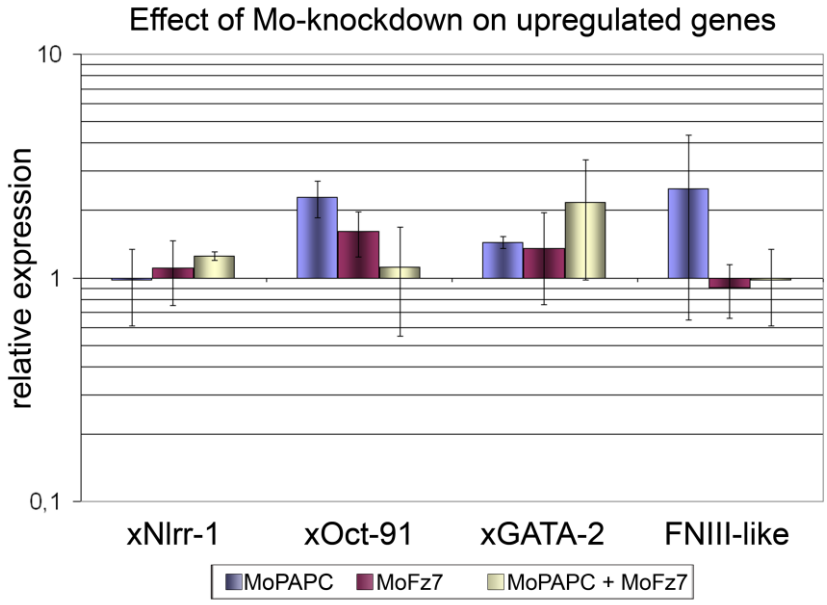

Fig. 12: Influence of PAPC and xFz7 knockdown on upregulated target genes. Neither MoPAPC nor MoxFz7 had a strong influence on the expression levels of Xnlrr-1, xOct-91, xGATA-2 or FNIII like. Standard error is indicated.

Knockdown of neither PAPC nor xFz7 by morpholino oligonucleotides had a strong influence on the expression levels of the upregulated target genes (Fig. 12). MoPAPC was able to upregulate xOct-91 2-fold. xGATA-2 was also upregulated 2-fold by the combination of the two morpholinos. But altogether the loss of PAPC and xFz7 showed only a faint effect on the positively regulated target genes. This lead to the conclusion that PAPC and xFz7 are able to upregulate these genes, but their regulation also depends on other factors. Furthermore, if the expression of these genes would strictly depend on PAPC and xFz7, a downregulation of these genes after PAPC and xFz7 knockdown would be expected. This data indicates that PAPC and xFz7 are sufficient to upregulate the genes, but they do not seem to be required for their expression in the embryo.

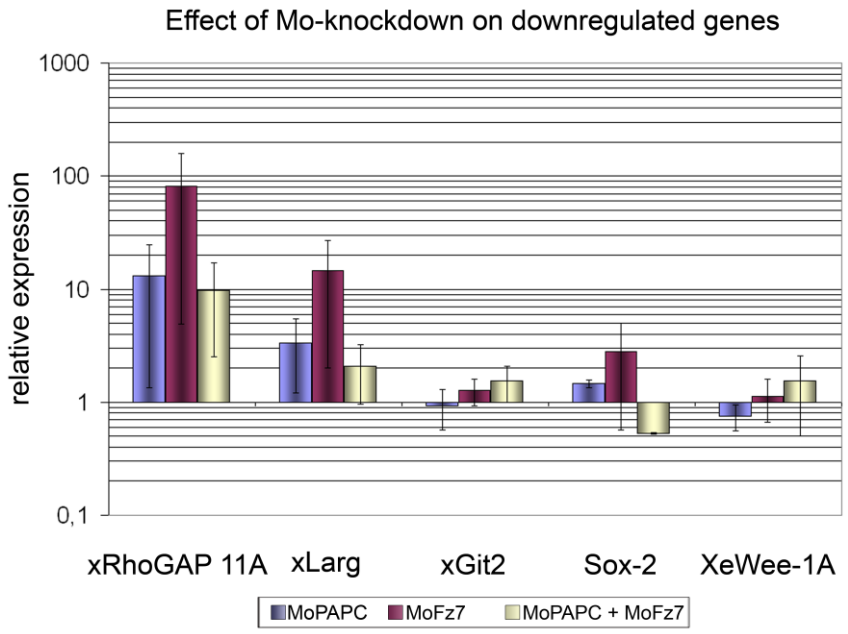

Fig. 13: Influence of PAPC and xFz7 knockdown on downregulated target genes. Standard error is indicated.

xRhoGAP 11A was strongly upregulated in PAPC- and xFz7-depleted embryos. Its expression levels were increased about 10-fold after MoPAPC and MoPAPC plus MoxFz7 injection. The knockdown of xFz7 alone even increased xRhoGAP 11A levels 80-fold (Fig. 13). The same tendency was seen for xLarg, another gene which was downregulated by PAPC and xFz7 gain of function. MoPAPC and the combination of MoxFz7 and MoPAPC upregulated the gene to the same extend, whereas loss of xFz7 had much greater effect on xLarg. As the loss of PAPC and xFz7 had the opposite effect as their gain of function, I conclude that their expression is dependent on PAPC and xFz7 function.

xGit2 was not influenced by the single loss of PAPC or xFz7, but the combined knockdown of both lead to a very weak upregulation. Sox-2 was weakly upregulated by MoxFz7 but not by MoPAPC and the combination even decreased its levels. XeWee-1A wasn't influenced very much by both morpholinos.

The influence of MoPAPC on target gene expression was also analysed by *in situ* hybridisation (Fig. 14). 4-cell embryos were injected dorsally with 0.5 mM MoPAPC and embryos were grown until gastrula stages, fixed in MEMFA and taken for *in situ* hybridisation. As loss of PAPC inhibits the constriction of the mesoderm (Unterseher et al., 2004), a lateral expansion of the notochord and the PAPC expression domain was seen in stage 12 embryos (Fig. 14, right column). But like in the qRT-PCRs, the overall expression pattern of the upregulated candidate genes was hardly changed compared to their wildtype expression pattern (Fig. 11). In hemisectioned embryos an expansion of xGit2 and xRhoGAP 11A into the dorsal involuted mesendoderm was noticeable and further characterised in chapter 3.2.3.

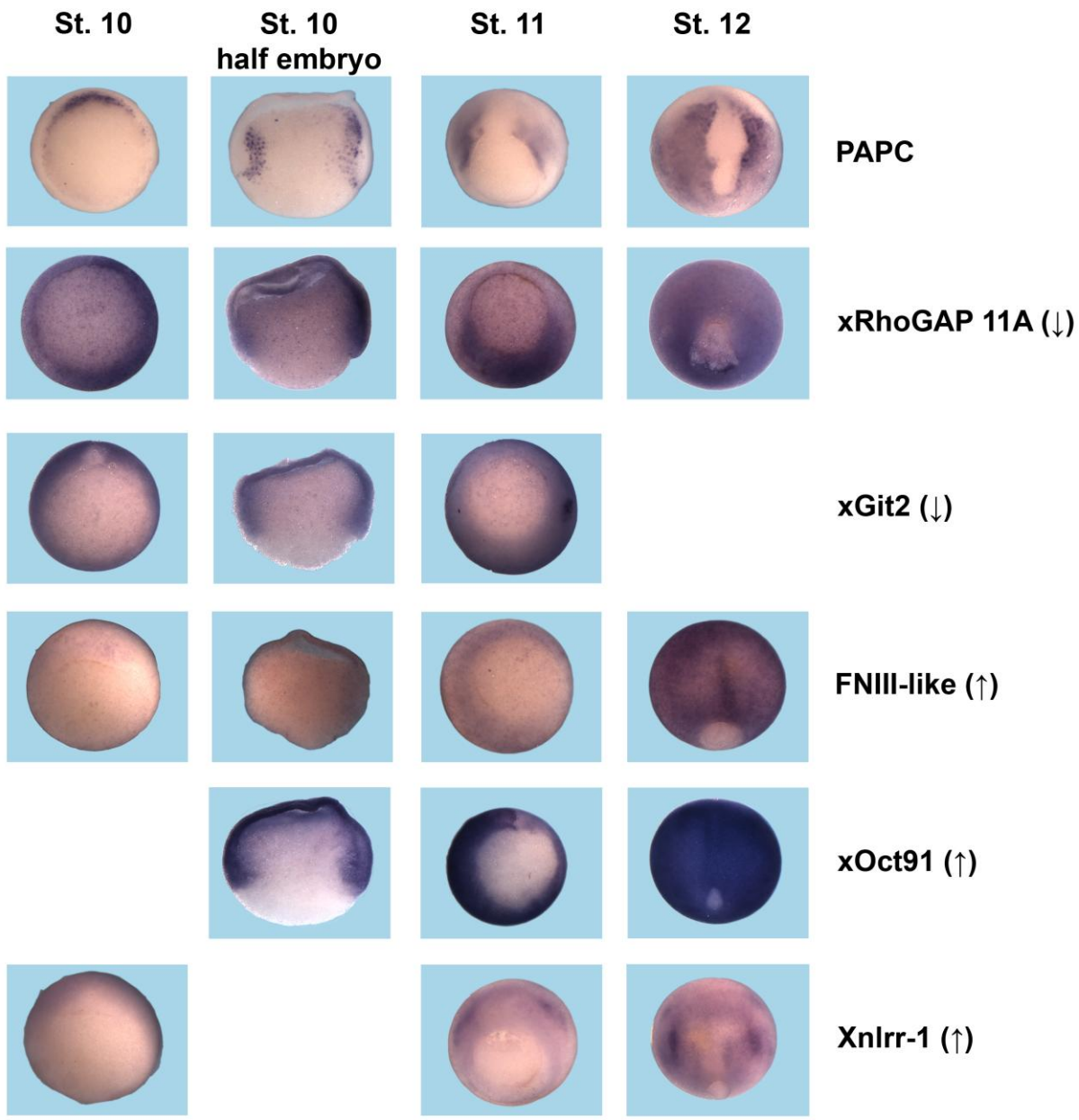

Fig. 14: Spatial expression pattern of candidate genes after morpholino knockdown of PAPC. Gene expression was visualised by whole mount *in situ* hybridisation. Dorsal is up (whole embryos) or to the right (half embryos). (↓) downregulated gene, (↑) upregulated gene.

3.2 xGit2 and xRhoGAP 11A regulate morphogenesis during *Xenopus* gastrulation

Among the genes downregulated by PAPC and xFz7, I found two novel *Xenopus* GTPase activating proteins (GAPs) for small GTPases. Since PAPC and xFz7 mediate Rho signalling and separation behaviour is sensitive to the modulation of Rho signalling, I chose these genes for additional functional analysis. One of these genes encodes a GTPase-activating protein for RhoA which is homologous to human RhoGAP 11A and was therefore named xRhoGAP 11A. Functional data on the human homologue does not exist (Fig. 15, top).

The other protein, xGit2, is homologous to the human protein Git2 (G-protein-coupled receptor kinase interacting protein2). It contains a GAP-domain for the small GTPase Arf followed by three ankyrin repeats, a Spa2-homology domain, a coiled-coil domain and a Paxillin-binding site (Fig. 15, bottom). Git proteins are ubiquitous multidomain proteins involved in multiple cellular processes such as modulating cellular structures, membrane trafficking and scaffolding signalling cascades (Hoefen and Berk, 2006).

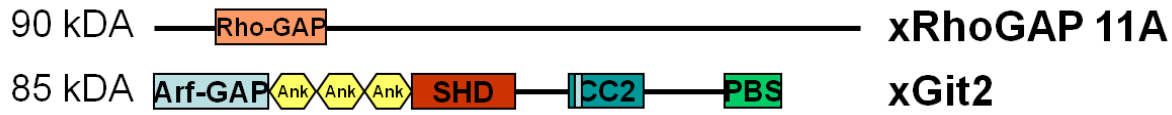

Fig. 15: Domain structure of xRhoGAP 11A and xGit2. Apart from the GTPase-activating domain, xRhoGAP 11A does not possess any conserved protein domains. xGit2 contains a GAP-domain for the small GTPase Arf followed by three ankyrin (Ank) repeats, a Spa2-homology domain (SHD), a coiled-coil domain (CC2) and a Paxillin-binding site (PBS).

3.2.1 xGit2 and xRhoGAP 11A inhibit convergent extension movements and tissue separation

To investigate the function of xGit2 and xRhoGAP 11A, I performed overexpression studies of both proteins. The two dorsal blastomeres of 4-cell stage embryos were injected with either 800 pg xGit2 mRNA or 60 pg xRhoGAP 11A mRNA. The embryos were then cultured until tailbud stages (stage 30). Overexpression of xGit2 led to spina bifida and shortened body axes (Fig. 16). These are typical phenotypes observed after the perturbation of morphogenetic movements like convergent extension or tissue separation. Embryos overexpressing xRhoGAP 11A also showed spina bifida, but in addition I also observed embryos that were posteriorised and showed smaller head structures compared to wildtype embryos (Fig. 16).

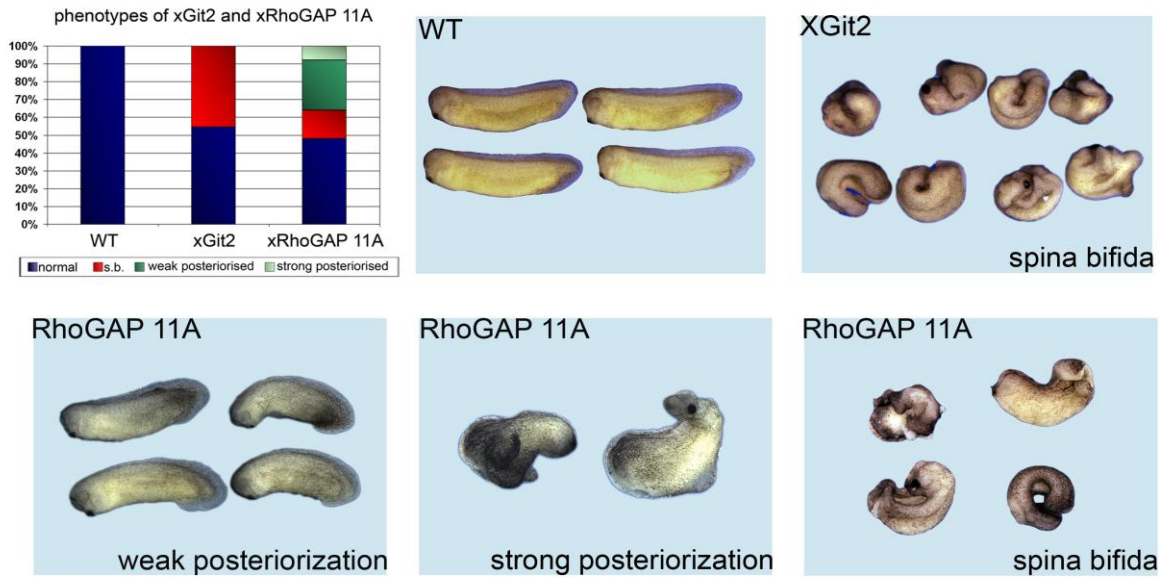

Fig. 16: Overexpression of both XGit2 and xRhoGAP 11A leads to gastrulation defects like shortened body axes and spina bifida. Gain of xRhoGAP 11A also led to posteriorised phenotypes. Embryos were injected dorsally with either 800 pg of xGit2 or 60 pg xRhoGAP 11A mRNA.

Neither xGit2 overexpression nor xRhoGAP 11A overexpression affected the differentiation of the mesoderm. In RT-PCRs of xGit2 or xRhoGAP 11A injected embryos, the expression of mesodermal marker genes like xBra and xChd was unchanged (Fig. 17A). The same result was obtained by *in situ* hybridisation analysis of xGit2 or xRhoGAP 11A injected embryos. Overexpression of xGit2 and xRhoGAP 11A did not alter the expression domain of xBrachyury (xBra) and xChordin (xChd) (Fig. 17B). This suggests that the phenotypes induced by gain of xGit2 and xRhoGAP 11A are indeed due to defective morphogenetic movements.

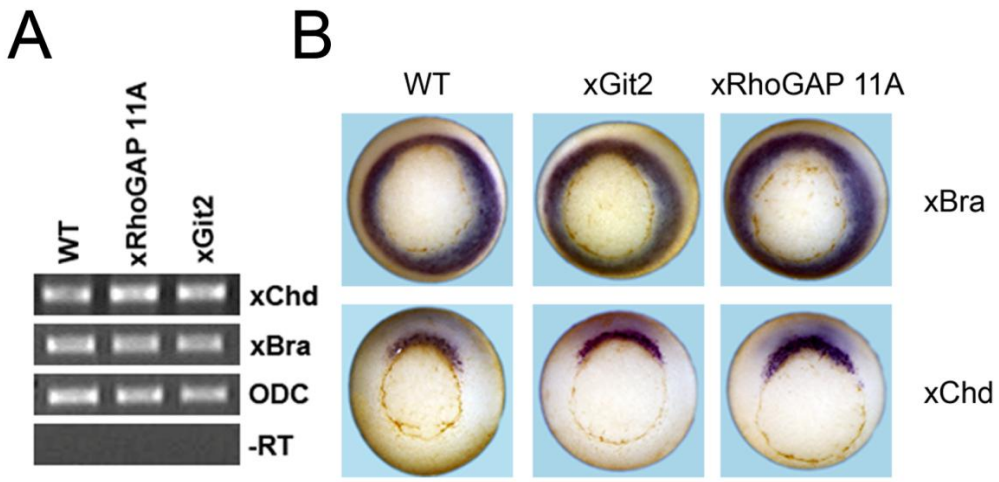

Fig. 17: xRhoGAP 11A and xGit2 do not affect mesoderm differentiation. (A) Injection of 60pg xRhoGAP 11A or 800 pg xGit2 does not change expression levels of the mesoderm markers xChd or xBra in RT-PCRs. (B) Overexpression of 60pg xRhoGAP 11A or xGit2 does not change the expression domains of the mesoderm markers xChd and xBra in whole mount *in situ* hybridisations.

To test whether gain of xGit2 and xRhoGAP 11A function inhibits CE movements, I analysed the morphogenetic movements in dorsal marginal zone (DMZ) explants and animal caps (AC) stimulated with TGF-β growth factors. Inhibition of convergent extension movements blocks the elongation of DMZ explants, so-called Keller open face explants (Keller et al., 1992). According to their elongation state, DMZ explants were categorised into three groups: fully, partially or not elongating. Overexpression of 800 pg xGit2 or 60 pg xRhoGAP 11A in the two dorsal blastomeres reduced the elongation of Keller explants dramatically (Fig. 18). About 50% of the xRhoGAP 11A or xGit2-injected DMZs failed to elongate at all. In contrast, more than 90% of uninjected DMZ explants elongated either fully or partially. In addition xGit2 R39K, which contains a point mutation in the ArfGAP domain of xGit2 and lacks GAP activity (Di Cesare et al., 2000; Matafora et al., 2001), inhibited elongation to the same extent as wildtype xGit2, indicating that the inhibition of CE movements is independent of the ArfGAP-activity of xGit2.

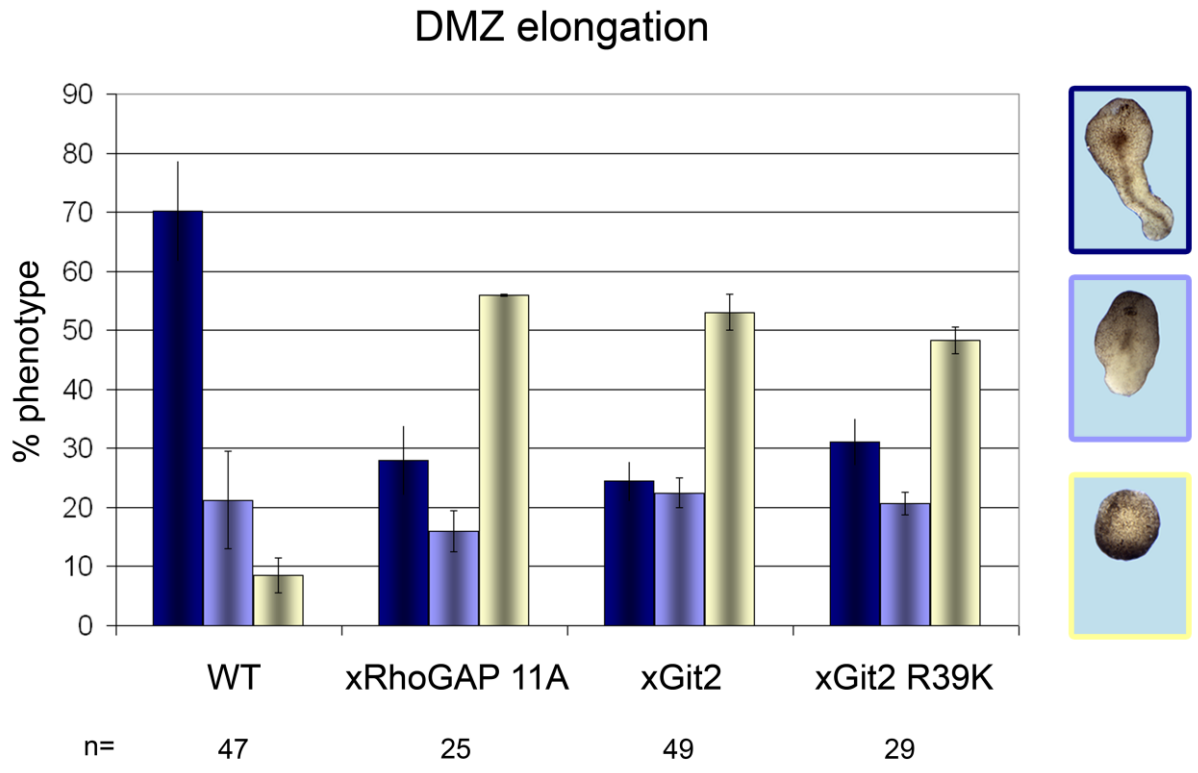

Fig. 18: xGit2 and xRhoGAP 11A inhibit convergent extension movements in DMZ explants. Microinjection of xRhoGAP 11A (60 pg/embryo), xGit2 (800 pg/embryo) and xGit2 R39K (800 pg/embryo), a protein with a mutated ArfGAP domain into the dorsal blastomeres of 4-cell embryos reduced the number of elongating Keller explants. Explants were categorised into three groups: fully elongating (dark blue), partial elongating (light blue) and not elongating (yellow).

A similar result was obtained in TGF-β-induced AC explants. Overexpression of Bvg1, a TGF-β family member, induced dorsal mesoderm in the AC tissue (Green and Smith, 1990; Green et al., 1992; Green et al., 1997a) and 85% of the explants elongated due to convergent extension movements. Coexpression with xRhoGAP 11A or xGit2 reduced the percentage of elongating animal caps to 40% and 50% respectively (Fig. 19). Based on the morphogenesis defects in the embryos and the

inhibition of elongation in DMZ and AC explants I conclude that overexpression of xRhoGAP 11A or xGit2 inhibits CE movements.

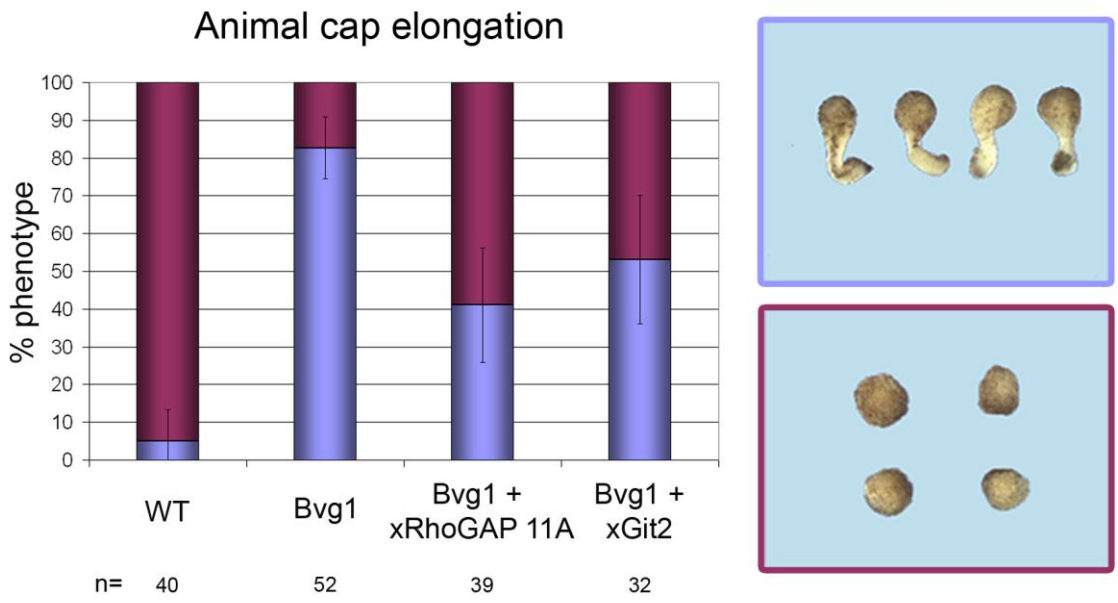

Fig. 19: Overexpression of xRhoGAP 11A (60 pg RNA/embryo) and xGit2 (800 pg RNA/embryo) inhibits CE in Bvg1 (200 pg RNA/embryo) induced animal cap explants. Elongation of the explants was scored when control siblings had reached st. 22. AC explants were categorised in two groups: elongating (blue) and not elongating (red). Standard error is indicated.

PAPC and xFz7 induce tissue separation and downregulate both xGit2 and xRhoGAP 11A. Knockdown of PAPC and xFz7 abolishes the posterior part of Brachet's cleft (Winklbauer et al., 2001; Medina et al., 2004). Therefore I investigated whether gain of xGit2 or xRhoGAP 11A would inhibit the formation of Brachet's cleft like knockdown of PAPC and xFz7 does. Embryos were injected at the 4-cell stage with 800 pg xGit2 mRNA or 60 pg xRhoGAP 11A mRNA, grown until stage 10.5, fixed and cut sagitally through the dorsal midline to investigate Brachet's cleft formation. Indeed, 55% of the xGit2-injected and about 80% of the xRhoGAP 11A injected embryos showed a loss of the posterior part of Brachet's cleft (Fig. 20).

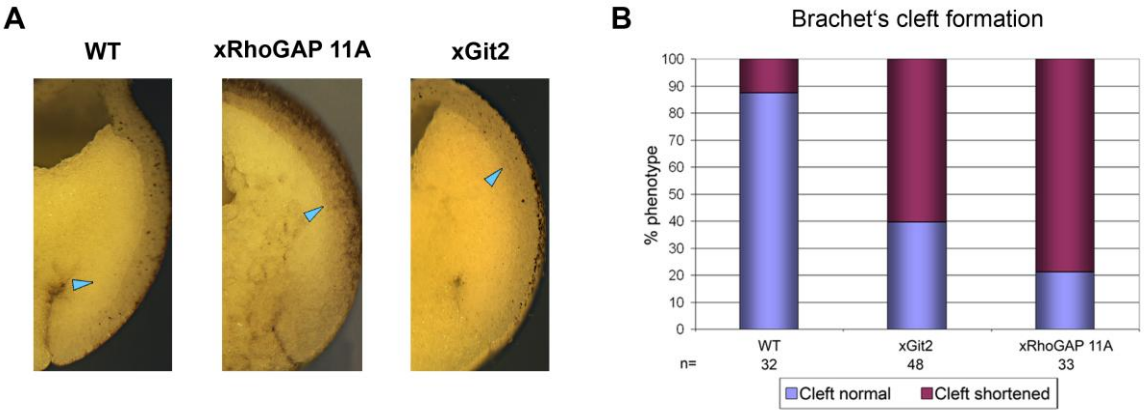

Fig. 20: xGit2 and xRhoGAP 11A inhibit the formation of the posterior Brachet's cleft. (A) Synthetic RNA for xRhoGAP 11A (60 pg/embryo) and xGit2 (800 pg/embryo) were injected into the dorsal blastomeres of 4-cell stage *Xenopus* embryos. Overexpression of both xRhoGAP 11A and xGit2 abolished the posterior part of Brachet's cleft. Blue arrowheads indicate the posterior end of Brachet's cleft. (B) Statistical evaluation of Brachet's cleft formation.

The role of xGit2 and xRhoGAP 11A in tissue separation was also demonstrated in the blastocoel roof (BCR) assay (Wacker et al., 2000). Dorsal mesoderm, which is able to separate from ectoderm tissue of the BCR, was induced by injection of synthetic Bvg1 RNA into animal blastomeres of 4-8-cell stage embryos and fluorescein dextran was coinjected as a lineage tracer. Clusters of Bvg1-induced cells from stage 10.5 embryos were placed on the BCR substratum and tissue separation was observed in 60% of these clusters (Fig. 21). When Bvg1-injected animal caps were coinjected with xGit2 or xRhoGAP 11A only 20-30% of the clusters remained separated from the BCR and the majority of cells sank into the substratum.

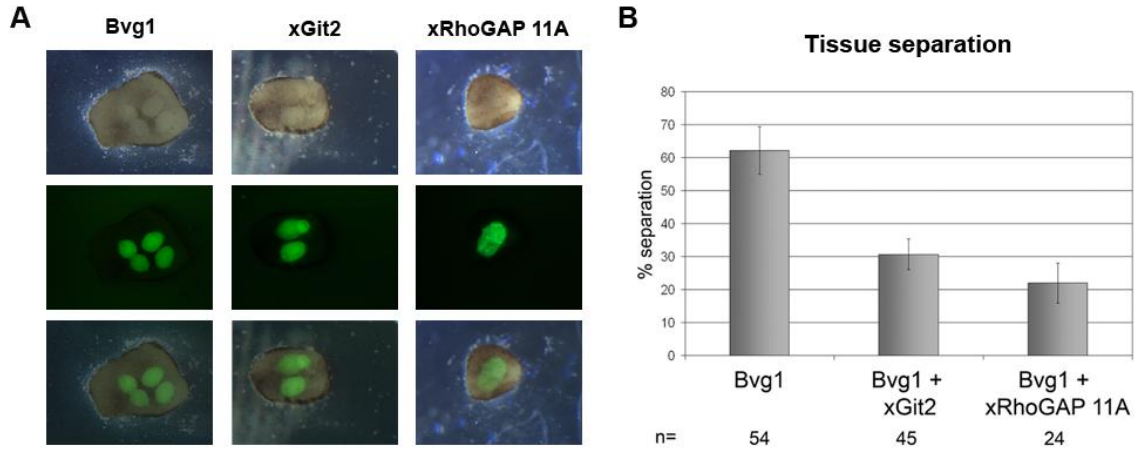

Fig. 21: xGit2 and xRhoGAP 11A inhibit tissue separation in the blastocoels roof assay. (A) xGit2 (800 pg/embryo) and xRhoGAP 11A (60 pg/embryo) reduced separation in the BCR assay in Bvg1-induced animal cap tissue (200 pg/embryo). Embryos were coinjected with fluorescein dextran to make the injected animal cap cell clusters visible. Upper row: brightfield picture, middle row: fluorescence picture, lower row: overlay. (B) Statistical evaluation of the BCR assays.

The loss of Brachet's cleft and the inhibition of separation behaviour in dorsal mesoderm after overexpression of xRhoGAP 11A or xGit2 indicate that these proteins negatively regulate tissue separation.

3.2.2 Characterisation of xGit2 and xRhoGAP 11A loss of function

Morpholinos have been designed against xGit2 and xRhoGAP 11A mRNAs (MoGit and MoRhoGAP) to specifically knockdown xGit2 and xRhoGAP 11A in the embryo and learn about their function *in vivo*. The specificity of MoGit and MoRhoGAP was tested in a TNT *in vitro* translation assay. Plasmid-DNA of myc-tagged xGit2 and xRhoGAP 11A constructs containing the specific target sequences of the morpholinos were transcribed into RNA and translated into protein in the presence of RNA polymerases and ribosomes in a rabbit reticulocyte lysate. By addition of the morpholinos, translation of both proteins was blocked efficiently, indicating that both antisense morpholino oligonucleotides are specific for their targets (Fig. 22).

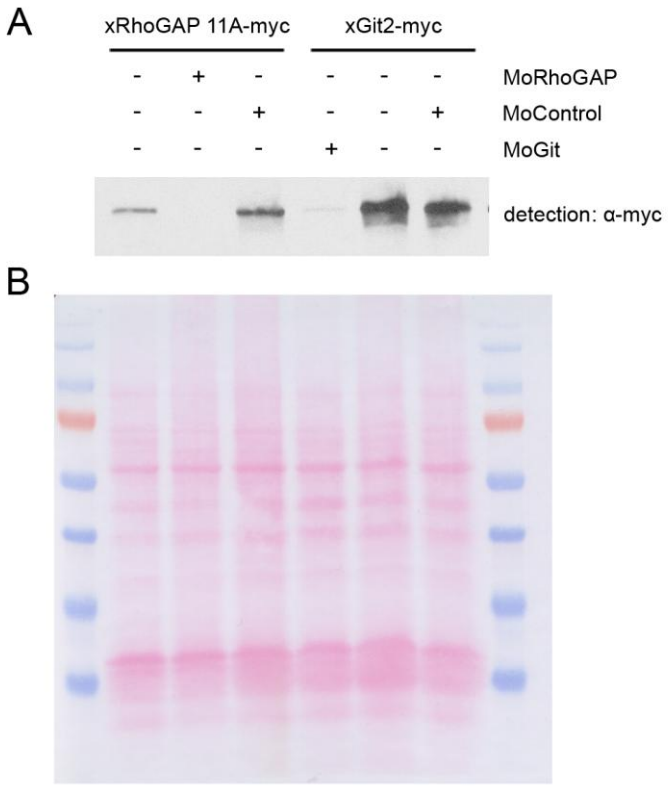

Fig. 22: MoRhoGAP and MoGit specifically block translation of xRhoGAP 11A and xGit2, respectively. (A) TNT *in vitro* translation showing the specific block of translation by antisense morpholino oligonucleotides against xRhoGAP 11A and xGit2. MoRhoGAP blocks translation of myc-tagged xRhoGAP 11A. MoGit2 blocks translation of xGit2. Control-morpholino does not inhibit translation of targets. (B) PonceauS staining of Western blot showing loading of equal protein amounts.

Like overexpression of xGit2 and xRhoGAP 11A, knockdown of both proteins by morpholinos caused gastrulation defects (Fig. 23). Injected *Xenopus* showed spina bifida, shortened body axes and posteriorisation. Injection of a control morpholino (MoControl) didn't show an effect on the embryos. Only about 50% of the xGit2 or xRhoGAP 11A depleted embryos looked normal after injection of the appropriate morpholino. However, no influence on Brachet's cleft formation was observed in earlier stage embryos. Another ArfGAP in *Xenopus* has previously been described, that also shows the same gastrulation typical phenotype both in gain and loss of function (Hyodo-Miura et al., 2006)

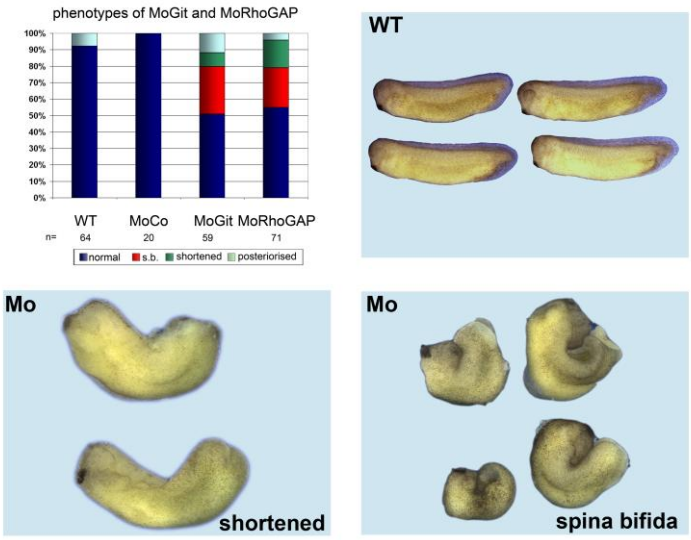

Fig. 23: Knockdown of both XGit2 and xRhoGAP 11A leads to gastrulation defects like shortened body axes and spina bifida. Embryos were injected dorsally with either 0.25 mM of MoGit2, MoRhoGAP or MoCo.

3.2.3 Knockdown of PAPC upregulates xGit2 and xRhoGAP 11A

Transcription of xGit2 and xRhoGAP 11A is downregulated in PAPC and xFz7-expressing animal caps, and neither gene is expressed endogenously in the involuting mesendoderm where PAPC and xFz7 mRNAs are localised. *In situ* hybridisations showed that xGit2 and xRhoGAP 11A mRNAs were present in the entire ectoderm, but were enriched dorsally (Fig. 11, Fig. 24). The involuting mesendoderm, where PAPC is expressed, was almost devoid of xGit2 and xRhoGAP 11A transcripts. Additionally, qRT-PCRs revealed that xRhoGAP 11A is dependent on PAPC and xFz7 expression, as loss of both genes upregulates xRhoGAP 11A. The combined knockdown of PAPC and xFz7 also resulted in a weak upregulation of xGit2 (Fig. 13). Therefore I analysed the expression patterns of xGit2 and xRhoGAP 11A after knockdown of PAPC.

The expression domains of PAPC on the one hand and xGit2 and xRhoGAP 11A on the other hand are mutually exclusive and adjacent to each other. When PAPC was knocked down by morpholino oligonucleotides, 80 to 85% of the analysed embryos showed an expansion of both xGit2 and xRhoGAP 11A expression domains into the area where PAPC would normally be expressed (Fig. 24A, B). Measurements of the domains showed that the area of expression of xRhoGAP 11A was enlarged 3.2-fold compared to uninjected WT embryos. The domain of xGit2 was increased 2.6-fold into the involuted mesendoderm in MoPAPC injected embryos (Fig. 24C). For this quantification, the area of the xGit2 and xRhoGAP 11A expression in the involuted mesendoderm (blue staining inside Brachet's cleft) was measured using ImageJ software and was divided by the total area of the involuted mesendoderm. PAPC-mRNA was still detectable after knockdown with morpholino antisense oligonucleotides, because the mRNA is not degraded after binding of the morpholino oligonucleotide.

These experiments demonstrate that the expression of xGit2 and xRhoGAP 11A in the *Xenopus* gastrula is regulated by PAPC. They also show that the expression domains of xGit2 and xRhoGAP 11A on the dorsal side of the embryo are defined in part by PAPC.

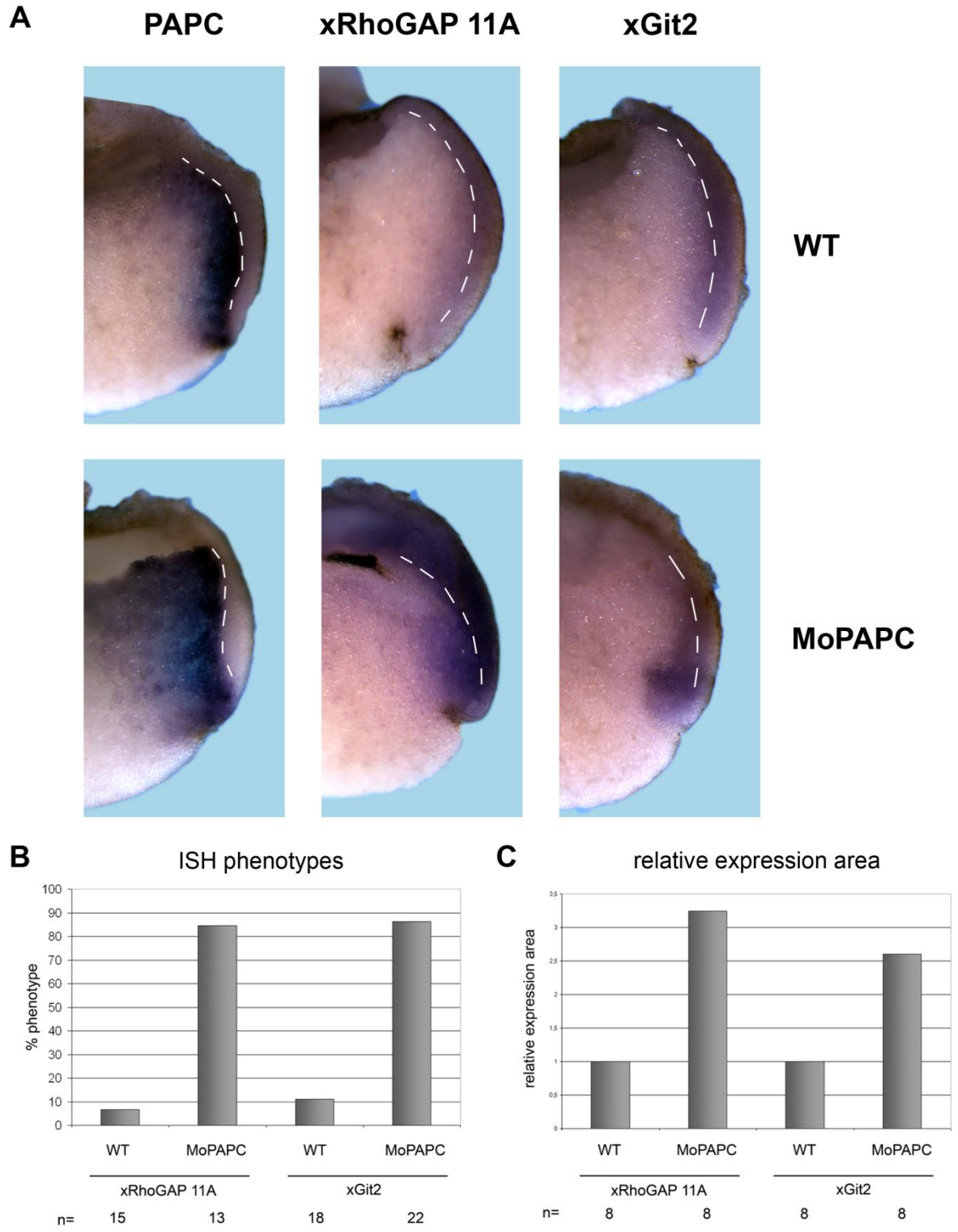

Fig. 24: Knockdown of PAPC upregulates xGit2 and xRhoGAP 11A in the involuting mesendoderm. (A) Analysis of xRhoGAP 11A and xGit2 expression by whole mount *in situ* hybridisation in hemisectioned *Xenopus* gastrula embryos (st. 10.5). In wild type embryos the expression domains of PAPC and xGit2 or xRhoGAP mRNAs are adjacent to each other. xGit2 and xRhoGAP 11A transcripts are localised in the ectoderm but not in the dorsal lip and the involuting mesoderm (upper row). In PAPC depleted embryos the expression domains were extended into the involuting mesoderm, where PAPC would be expressed normally. Knockdown of PAPC by antisense morpholino oligonucleotides did not cause PAPC-mRNA degradation, so that PAPC could still be detected by *in situ* hybridisation. (B, C) Quantification of *in situ* hybridisation-data. (B) 85% of the MoPAPC-injected embryos showed an expansion of the xRhoGAP 11A and xGit2-expression domains. (C) In these embryos the expression area of xRhoGAP 11A was increased 3.2-fold compared to wildtype embryos, the expression area of xGit2 was increased 2.6-fold.

3.2.4 xGit2 and xRhoGAP 11A negatively regulate RhoA activity

PAPC and xFz7 are part of non-canonical Wnt-signalling and are able to regulate downstream effectors. It has been shown previously that PAPC is able to activate RhoA and JNK, but to inhibit Rac1 (Unterseher et al., 2004; Medina et al., 2004; Berger et al., 2009). Because overexpression of xGit2 and xRhoGAP 11A and Mo-knockdown of PAPC and xFz7 inhibit CE movements and tissue separation, I hypothesised that xGit2 and xRhoGAP 11A could also negatively regulate β-catenin-independent Wnt signalling. Since Rho is an effector of this signalling cascade, I tested whether xGit2 and xRhoGAP 11A could modulate RhoA activity in a classical Rho pulldown experiment (Ren et al., 1999).

100 pg of a myc-tagged RhoA construct was injected dorsally into 4-cell stage embryos alone or in combination with 800 pg synthetic xGit2 or 60 pg xRhoGAP 11A mRNA. Activated, RhoA-myc was pulled down with RBD-GST, the GST-tagged Rho-binding domain of rhotekin that binds only GTP-bound, active RhoA, and analysed in a Western blot using an anti-myc antibody (Fig. 25A). As expected, xRhoGAP 11A, which carries a GTPase-activating domain specific for RhoA, reduced RhoA-activity. RhoA activity was also significantly reduced in xGit2-expressing embryos. Interestingly a similar result was obtained when the xGit2 mutant R39K was expressed. xGit2 R39K carries a point mutation in the ArfGAP domain, which abolishes GAP activity (Di Cesare et al., 2000; Matafora et al., 2001). This suggests again that the inhibition of RhoA signalling by xGit2 is independent of its GAP activity. Quantification of the Western blot confirmed the inhibition of RhoA activity by xGit2, xRhoGAP 11A and xGit2 R39K. Ratios of active Rho and total Rho were taken and the relative Rho-activity of embryos injected only with RhoA-myc was set to 100% (Fig. 25B).

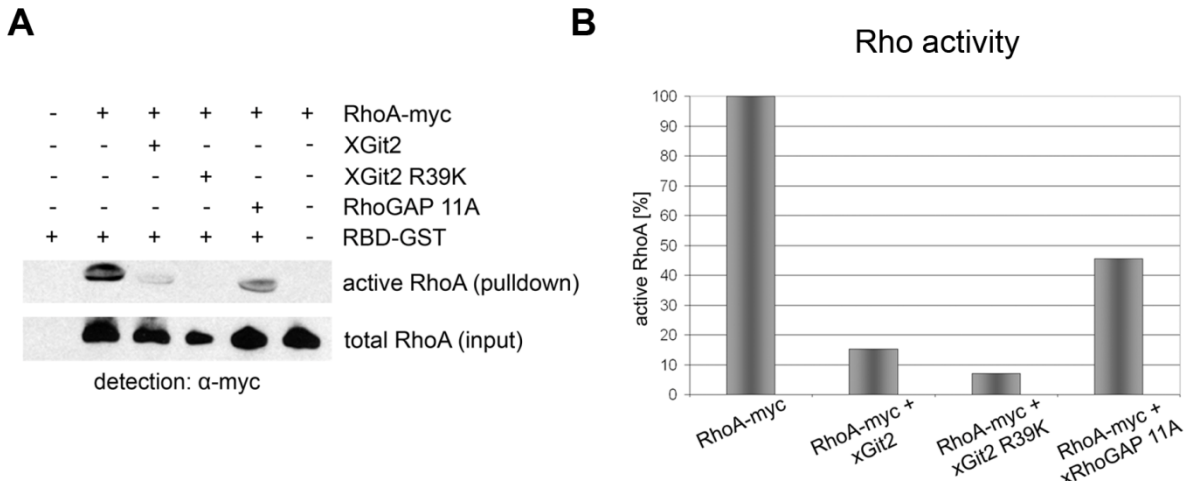

Fig. 25: xGit2 and xRhoGAP 11A reduce RhoA activity. (A) Synthetic mRNAs for xGit2 (800 pg/embryo), xGit2 R39K (800 pg/embryo), which lacks ArfGAP activity, and xRhoGAP 11A (60 pg/embryo) were injected in combination with RhoA-myc (200 pg/embryo) into the animal region of 4-cell-stage *Xenopus* embryos. GTP-bound Rho was recovered from embryo extracts at stage 11 by RBD-GST fusion protein and detected on a Western blot using an anti-myc antibody. RhoA activity was inhibited by xGit2, xGit2 R39k and xRhoGAP11A. (B) Quantification of the Western blot shown in (A). Ratios of pulldown and input were taken. The relative Rho-activity of embryos injected only with RhoA-myc was set to 100%.

The inhibition of endogenous Rho signalling after overexpression of xGit2 and xRhoGAP 11A was demonstrated in DMZ explants using confocal microscopy. Synthetic xGit2 or xRhoGAP 11A mRNAs

were injected into the right dorsal blastomere of 4-cell stage embryos. Histone 2B-RFP (H2B-RFP) mRNA was co-injected to mark the nuclei of the injected cells. The uninjected left side of the embryo served as an internal control. DMZs were fixed at stage 11.5 and stained with RBD-GFP, the Rho-binding domain of rhotekin fused to GFP which specifically binds GTP-bound, activated Rho (Goulimari et al., 2005; Berger et al., 2009). Confocal microscopy revealed that the amount of active Rho was considerably lower in the xGit2 and xRhoGAP 11A-injected sides compared to the control side (Fig. 26). Images were taken on the uninjected and injected sides with the same exposure times. To exclude bleaching effects the injected side was imaged first.

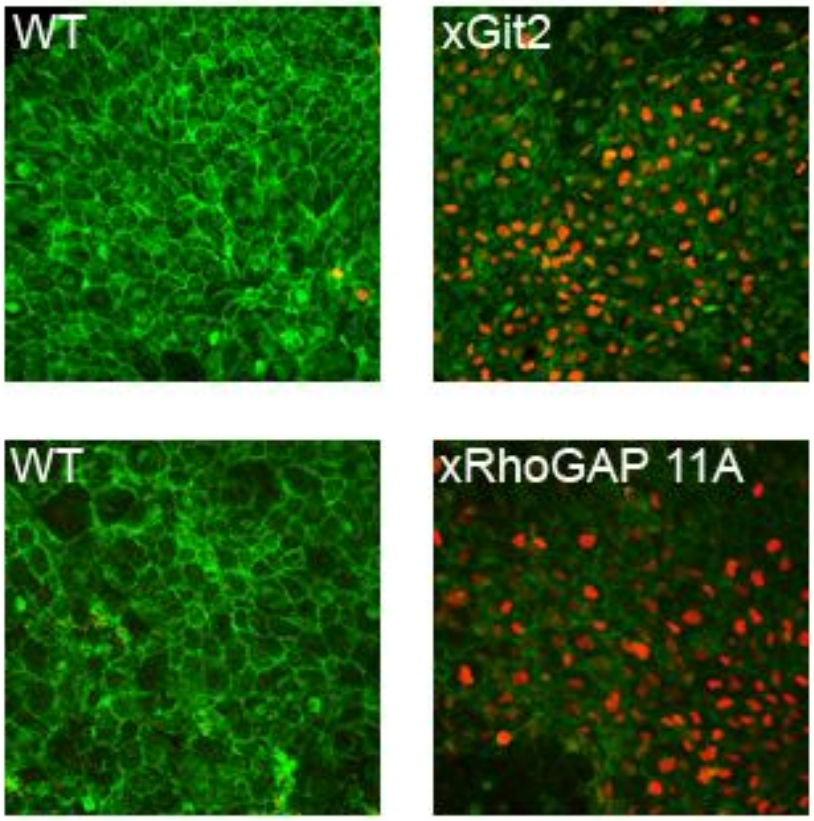

Fig. 26: xGit2 and xRhoGAP 11A negatively regulate endogenous RhoA activity. mRNA for xRhoGAP 11A (30 pg/embryo) and xGit2 (400 pg/embryo) was injected in combination with Histone 2B-RFP mRNA (200 pg/embryo) into the dorsal right blastomere of 4-cell stage *Xenopus* embryos. Dorsal marginal zones were explanted at stage 10.5 and incubated with RBD-GFP protein to visualise endogenous activated Rho. Injected cells were identified by nuclear Histone 2B-RFP. Endogenous RhoA activity was inhibited by xRhoGAP11A and xGit2 compared to uninjected dorsal marginal zone tissue (WT).

These experiments corroborate the pulldown experiments of exogenous myc-tagged RhoA using the RBD-GST fusion protein and demonstrate that endogenous Rho signalling can be inhibited by xGit2 and xRhoGAP11A. Since PAPC and xFz7-mediated signalling negatively regulates transcription of the Rho inhibitors xRhoGAP 11A and xGit2, I hypothesise that the activation of Rho in the involuting mesoderm could be due to inhibition of xRhoGAP 11A and xGit2.

To see whether the influence of xGit2 and xRhoGAP 11A on RhoA activity is direct, I investigated whether constitutively active RhoA (caRhoA) could rescue Brachet's cleft formation in xGit2 and

xRhoGAP 11A expressing embryos. Indeed, expression of caRhoA rescued the loss of Brachet's cleft induced by xRhoGAP 11A but not by xGit2 (Fig. 27), indicating that xRhoGAP 11A modulates tissue separation through inhibition of RhoA. xGit2, which is a multidomain protein with different protein functions (Frank et al., 2006; Hoefen and Berk, 2006), could influence tissue separation via additional mechanisms.

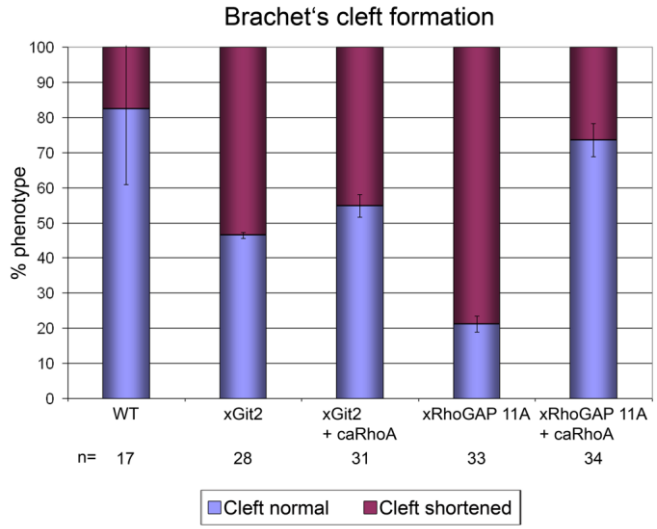

Fig. 27: Constitutively active RhoA rescues the overexpression of xRhoGAP 11A, but not of xGit2. mRNAs of xGit2 and xRhoGAP 11A were injected either alone or in combination with 100pg mRNA of caRhoA, and Brachet's cleft formation was analysed. xGit2 reduced the length of the posterior Brachet's cleft in 55% of the embryos. This could not be significantly rescued by coexpression of caRhoA. Only 20% of xRhoGAP 11A injected embryos showed a normal cleft and this could be rescued to 73% by the coinjection of caRhoA. Standard error is indicated.

3.2.5 Loss of xGit2 and xRhoGAP 11A rescues knockdown of PAPC and xFz7

xGit2 and xRhoGAP 11A can inhibit Rho activity, CE movements and tissue separation. These are the same effects that are seen after loss of PAPC and xFz7 by antisense morpholino oligonucleotides (Medina et al., 2000; Unterseher et al., 2004; Medina et al., 2004). To find out whether xGit2 and xRhoGAP 11A indeed act downstream of PAPC and xFz7 signalling, I investigated whether the inhibitory effect of MoPAPC on morphogenetic movements and Rho activation could be rescued by co-knockdown of the two proteins. Injection of Bvg1 mRNA induced elongation in 60-85% of the explants and PAPC knockdown reduced the percentage of elongated animal caps to 30-45%. Elongation of animal caps was rescued in 70-90% of the Bvg1-induced, MoPAPC-injected explants, when antisense morpholino oligonucleotides that block translation of xGit2 and xRhoGAP 11A (MoGit and MoRhoGAP) were coinjected (Fig. 28A, B).

This finding is supported by a RT-PCR of Bvg1-induced animal caps. Injection of Bvg1 mRNA induces dorsal mesoderm and upregulates the expression of PAPC. Like in whole embryos injected with PAPC mRNA (Fig. 9), this causes a strong decrease in xGit2 expression (Fig. 28C). After morpholino knockdown of PAPC, a faint increase in xGit2 mRNA can be observed, whereas xRhoGAP 11A mRNA is highly upregulated. The same results were obtained in qRT-PCRs of PAPC-depleted embryos as shown in Fig. 9.

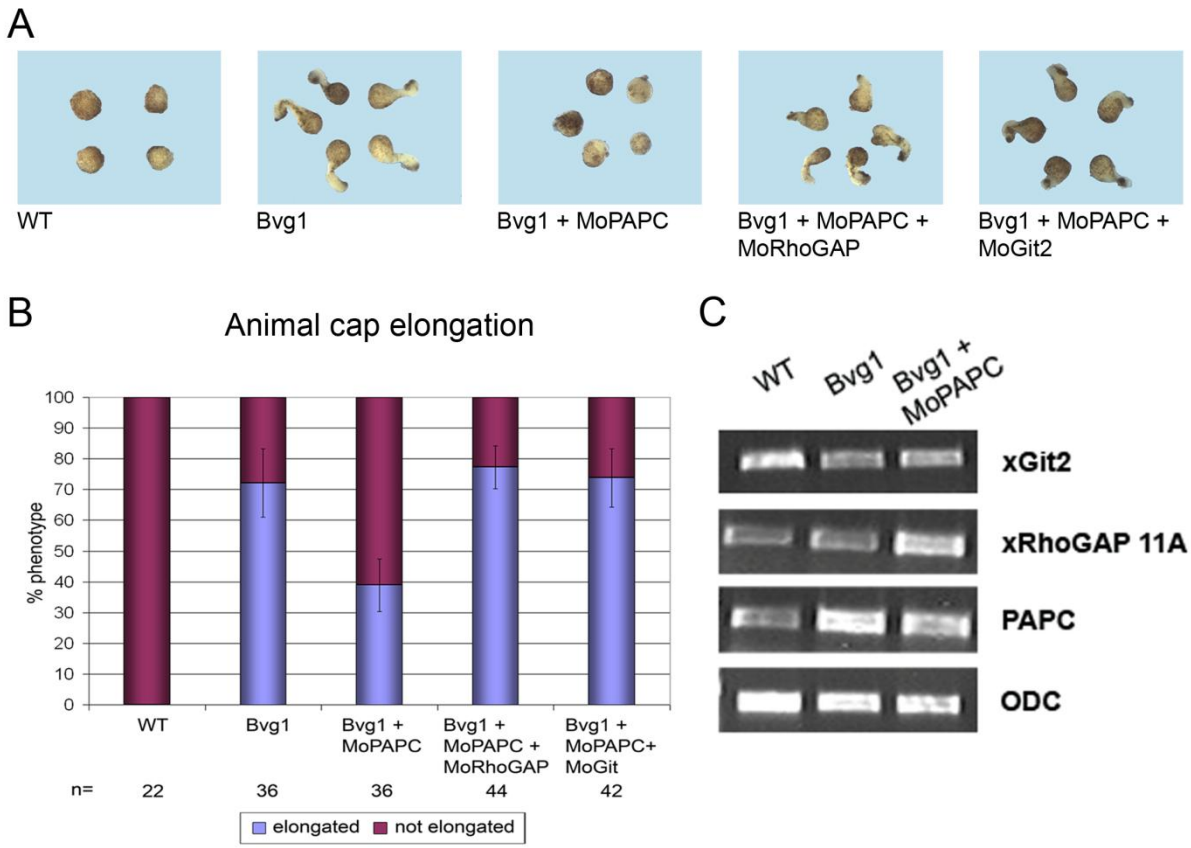

Fig. 28: Knockdown of xRhoGAP 11A and xGit2 rescue knockdown of PAPC. (A) Mesoderm differentiation and elongation of animal caps was induced by injection of synthetic Bvg1 RNA (200 pg/embryo) into the animal blastomeres of 4-cell-stage embryos. Elongation was blocked by coinjection of 0.5 mM PAPC antisense morpholino oligonucleotide (MoPAPC). Knockdown of xRhoGAP and xGit2 after injection of antisense morpholino oligonucleotides (MoRhoGAP 0.5 mM, MoGit2 0.5 mM) rescued animal cap elongation in PAPC-depleted ACs. (B) Statistical evaluation of animal cap elongation. Standard error is indicated. (C) RT-PCR in Bvg1 induced animal caps. xGit2 is downregulated when PAPC is expressed. After knockdown of PAPC, xGit2 expression increases slightly. MoPAPC in Bvg1-induced animal caps upregulates xRhoGAP 11A.

To investigate whether xGit2 and xRhoGAP 11A act in a linear signalling pathway and to find out which of the two acts upstream of the other, I overexpressed xGit2 in PAPC- and xRhoGAP 11A depleted animal caps. Vice versa xRhoGAP 11A was overexpressed in PAPC- and xGit2-depleted animal caps. Interestingly, overexpression of xGit2 could inhibit the rescue of animal cap elongation by MoRhoGAP, and vice versa xRhoGAP 11A inhibited the rescued PAPC knockdown by MoGit (Fig. 29). This indicates that xRhoGAP 11A and xGit2 exert their function on β-catenin independent Wnt-signal not in an epistatic signalling pathway but interfere with it on different levels.

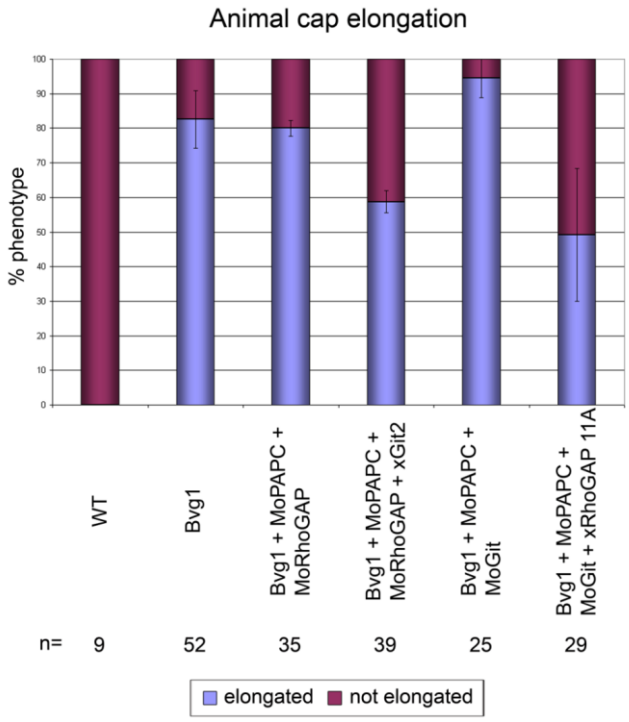

Fig. 29: xGit2 and xRhoGAP 11A do not act in an epistatic signalling pathway. Mesoderm differentiation and elongation of animal caps was induced by injection of synthetic Bvg1 mRNA (200 pg/embryo) into the animal blastomeres of 4-cell-stage embryos. Knockdown of xRhoGAP 11A and xGit2 after injection of antisense morpholino oligonucleotides (MoRhoGAP 0.5 mM, MoGit2 0.5 mM) rescued animal cap elongation in PAPC-depleted ACs (MoPAPC 0.5 mM). Co-expression of either xGit2 (800 pg) or xRhoGAP 11A (60 pg) could abolish animal cap elongation of the rescue experiment.

Rescue of PAPC knockdown by the co-knockdown of either xRhoGAP 11A or xGit2 was also seen in a blastocoel roof assay (Fig. 30). Knockdown of both PAPC and xFz7 in Bvg1-induced animal cap cells reduced tissue separation behaviour to 0-15%. The combined knockdown of xRhoGAP 11A or xGit2 could rescue tissue separation in 50-80% of animal cap explants (Fig. 30A). These experiments demonstrate that inhibition of CE and tissue separation after knockdown of PAPC is caused by elevated levels of xGit2 and xRhoGAP 11A.

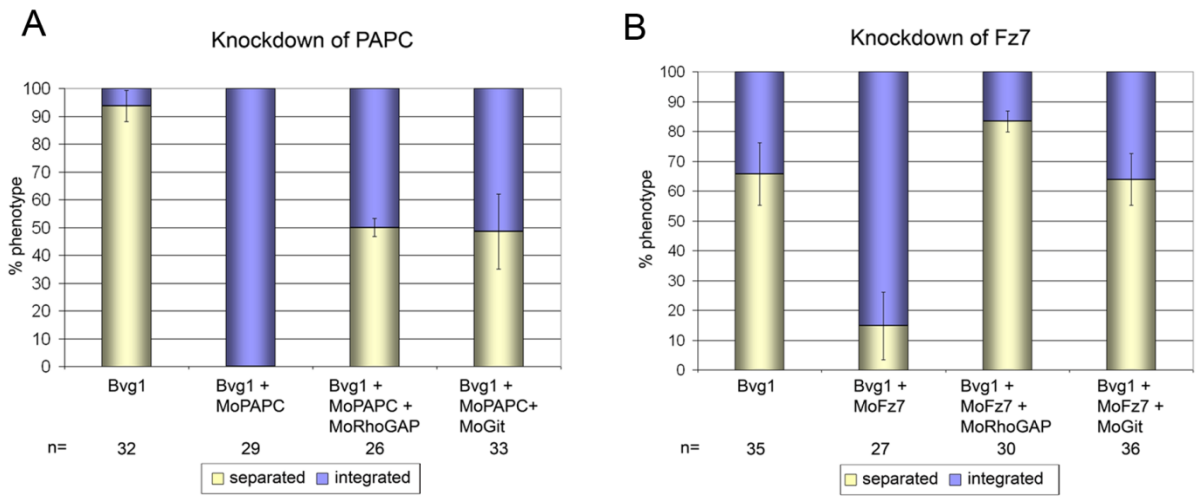

Fig. 30: Knockdown of xRhoGAP 11A and xGit2 rescues tissue separation in PAPC-depleted (A) and xFz7-depleted (B) embryos. Tissue separation behaviour was induced in animal cap cells by injection of Bvg1 mRNA (200 pg/ embryo) and injected either alone or in combination with MoPAPC (0.5 mM), MoGit (0.5 mM) and MoRhoGAP (0.5 mM).

This conclusion was supported by the analysis of Rho activity in embryos in which PAPC, xGit2 and xRhoGAP 11A function were knocked down. As already shown before (Unterseher et al., 2004; Medina et al., 2004), Rho pulldown assays revealed reduced levels of activated Rho in MoPAPC injected embryos. In embryos with combined knockdown of PAPC and xRhoGAP 11A or xGit2, the levels of activated Rho were elevated again (Fig. 31). These rescue experiments demonstrate that the regulation of Rho activity in the involuting mesoderm by PAPC is mediated by xRhoGAP 11A and xGit2.

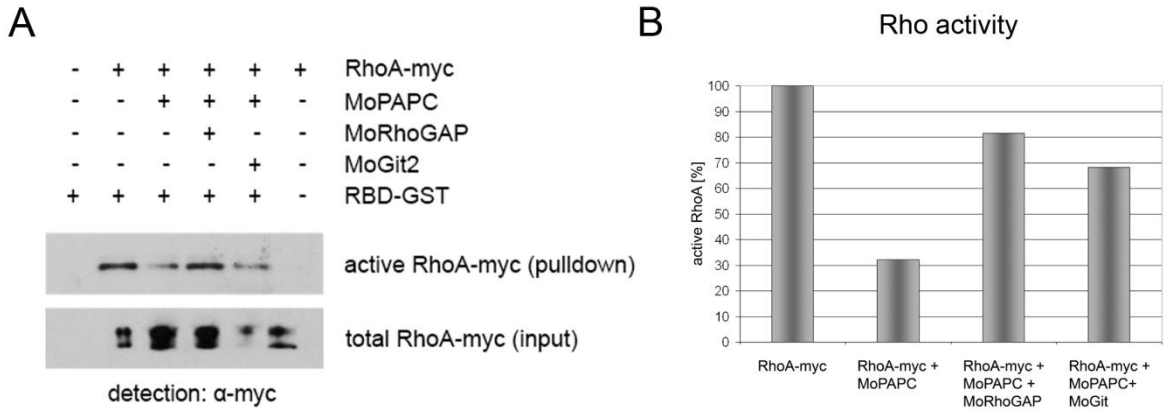

Fig. 31: (A) Morpholino oligonucleotid–mediated knockdown of xRhoGAP 11A rescues RhoA activity in PAPC-depleted embryos in RhoA-activity assay. RhoA-myc RNA (200 pg/embryo) was either injected alone or in combination with MoPAPC (0.4 mM), MoRhoGAP (0.5 mM) or MoGit2 (0.5 mM). GTP-bound RhoA-myc was recovered from embryos lysed at stage 11 and visualised in a Western blot using an anti-myc antibody. (B) Quantification of Rho activity assay shown in (A).

Furthermore knockdown of xGit2 and xRhoGAP 11A alone could change levels of active Rho. Rho activity in RhoGAP-depleted embryos was more than two times higher than in embryos injected only with RhoA-myc (Fig. 32). In xGit2-depleted embryos active Rho levels were only elevated to 130%.

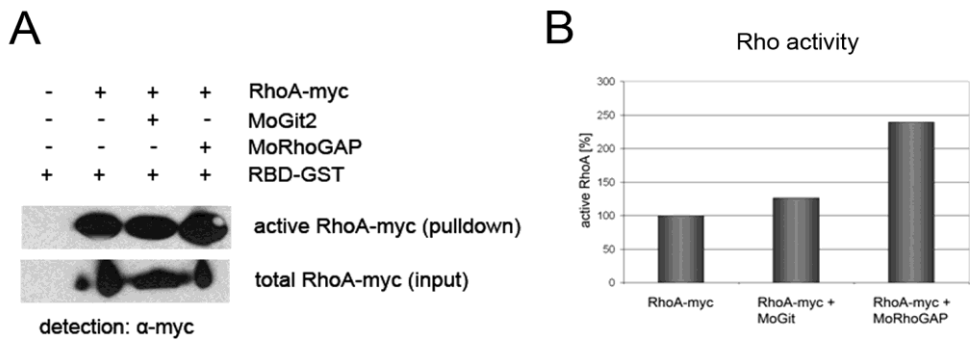

Fig. 32: Knockdown of xRhoGAP 11A and xGit2 increase levels of active RhoA. (A) Western Blot of Rho activity assay. (B) Quantification of Western Blot shown in (A). Ratios of pulldown and input were taken. The relative Rho-activity of embryos injected only with RhoA-myc was set to 100%.

Loss of xGit2 and xRhoGAP 11A is able to rescue the knockdown of PAPC in animal caps, tissue separation and Rho pulldown assays. Furthermore it is able to rescue knockdown of xFz7 in tissue separation. These experiments show that both proteins xGit2 and xRhoGAP 11A act downstream of PAPC/xFz7 mediated signalling *in vivo*.

4 Discussion

4.1 PAPC and xFz7 regulate gene transcription in the involuting mesoderm

In a search for genes that regulate tissue separation of the involuting mesoderm during *Xenopus* gastrulation, I performed microarray analysis in *Xenopus* animal cap cells overexpressing PAPC and xFz7 and compared their transcriptomes to wildtype cells. PAPC and xFz7 induce ectopic separation in those cells in the absence of mesoderm induction (Winklbauer et al., 2001; Medina et al., 2004). It has been shown, that for the PAPC and xFz7 induced separation behaviour the signalling function of both proteins is necessary and indispensable. The molecular mechanism by which they regulate tissue separation, however, is as yet unclear. As tissue separation behaviour only starts after stage 9, when zygotic gene transcription has started, it is likely that PAPC and xFz7 mediated signalling alters the transcription of target genes that are involved in this process.

Further evidence that altered gene transcription plays a role in the regulation of tissue separation comes from recent data in our group. If zygotic gene translation is blocked in early animal caps by cycloheximide, these cells fail to repel mesodermal cells that have already acquired proper separation behaviour. This shows that zygotic gene transcription is essential for the development of the repulsion behaviour in the ectoderm (Jungwirth, 2009).

Indeed, I found about 120 genes encoding transcription factors, signal transducers and novel hypothetical proteins whose expression was changed significantly in PAPC and xFz7 overexpressing animal cap cells in the microarray screen. The settings for data analysis were very stringent, so that only genes that were regulated in all three biological replicates with a p-value of 0.01 were considered as true candidates. Therefore the number of regulated genes was rather limited, although the microarray consists of 20.000 different transcripts. A comparable number of regulated genes (143) was identified by microarray analysis in animal cap explants after stimulation with activin and angiopoietin (Nagamine et al., 2005). In another study, 77 regulated genes were found after inhibition of BMP signalling in *Xenopus* ectoderm (Shin et al., 2005). Spot tests of the candidates by qRT-PCRs revealed that 9 out of 10 genes were regulated by PAPC and xFz7.

Because PAPC and xFz7 stimulate β-catenin-independent Wnt signalling, it is reasonable to assume that transcription of the identified genes is regulated by this signalling cascade. Non-canonical Wnt signalling has to date only rarely been linked to a transcriptional readout. JNK, which is a downstream effector of Wnt/PCP-signalling, has been suggested to activate the transcription of target genes via the transcription factor jun in *Drosophila* (Weber et al., 2000; Fanto et al., 2000b). PAPC expression itself is activated by Wnt-5A in a β-catenin-independent Wnt-pathway. For this alternative non-canonical pathway Wnt-5A interacts with the tyrosine receptor kinase Ror2 and signals through PI3 and cdc42 to activate JNK signalling and subsequently the transcription factors c-jun and ATF2 (Schambony and Wedlich, 2007). Besides, EAF2, a component of the ELL-mediated RNA polymerase II elongation factor complex, has been identified as a target of a β-catenin-independent

Wnt4-signalling pathway (Maurus et al., 2005). How the transcription of target genes is actually activated by these signalling cascades is unclear.

There is also some evidence, that PAPC could mediate gene transcription directly. Recent publications show an involvement of γ-protocadherins in nuclear gene transcription. γ-Protocadherins are cleaved extracellularly by metalloproteases followed by intracellular cleavage by the γ-secretase presenilin, which releases the cytoplasmic domains of these protocadherins so that the cleavage products can enter the nucleus where they activate gene transcription (Hambsch et al., 2005; Haas et al., 2005; Bonn et al., 2007). Recent results from our group suggest that PAPC might also be subject to this sequential cleavage (Berger, 2009). Western blots of c-terminal tagged PAPC-myc overexpressing embryo and oocyte lysates showed a 50 and a 60 kDa band besides the 150 kDa tagged full length protein. These fragments might be the fragments of PAPC-myc after extracellular and intracellular protein shedding. The bigger 60kDa fragment would comprise the ΔN-PAPC-myc fragment after extracellular cleavage by metalloproteases, and the smaller 50 kDa fragment the tagged cytoplasmic domain of PAPC after γ-secretase cleavage. However, the proof that PAPC indeed is processed by this mechanism remains to be shown.

In addition, a yeast-two-hybrid screen for interaction partners of PAPCc revealed the nuclear protein SMARCD1 as potential binding partner (Wang, 2007). SMARCD1 (Baf60) is a factor of the SWI/SNF chromatin remodelling complex that is involved in remodelling of active gene promoters and hence is active in transcription processes (Hsiao et al., 2003; Oh et al., 2008). SMARCD1 binds to the very last 13 amino acids of PAPCc. Recent results from our group suggest, that the transcriptional activation of XGATA-2 is inhibited, when PAPCcΔ966, a deletion construct of PAPCc that lacks the last 13 amino acids and cannot bind SMARCD1 any more, is overexpressed (Kietzmann, 2008); Mickael Edelmann, unpublished data).

There is additional evidence that PAPC influences gene expression of canonical Wnt-target genes. The above mentioned yeast-two-hybrid screen also identified casein kinase 2β (CK2β) as intracellular interaction partner of PAPC (Wang, 2007). CK2β is a positive regulator of the canonical Wnt-signalling-pathway and stabilizes β-catenin in the cell. Indeed results of our group show, that knockdown of PAPC by morpholino oligonucleotides upregulates Xnr3, a target gene of the Wnt/β-catenin-pathway, suggesting that PAPC is able to inhibit Wnt/β-catenin-signalling by sequestering CK1 from the cytoplasm in a mechanism that is similar to the sequestration of sprouty by PAPC to inhibit its negative function on PCP-signalling (Wang et al., 2008; Kietzmann, 2008).

PAPC and xFz7 are both able to up- or downregulate the candidate genes that have been investigated more closely on their own or in combination. In downregulating the candidates like xGit2 or XeWee-1A alone, however, xFz7 is not so potent as PAPC (see Fig. 8, Fig. 9). The mechanism by which PAPC and xFz7 regulate these candidates might by different for each of these genes. Possibly, some are activated or inhibited directly by PAPC in a γ-secretase-dependent way. Others might be regulated indirectly via the Rho signalling pathway or other Wnt-signalling pathways.

4.2 Microarray experiments give a chance to find unknown mediators of morphogenesis

Genome wide expression studies in the amphibian *Xenopus laevis* are yet in their infancy. Other organisms like human and mouse are well annotated, and microarray experiments in these organisms are standardised and easily evaluated by numerous softwares. For *Xenopus*, only two commercially available platforms exist. As the Affymetrix *Xenopus* Gene Chip covers only about 4,400 transcripts, my choice fell to the Agilent *Xenopus* oligo microarray, which comprises 20,000 transcripts. About 120 genes of them were significantly regulated by PAPC and xFz7 overexpression. Only about 30% of those genes were annotated at all. The other proteins were categorised according to their predicted gene function after sequence analysis. One quarter of both the up- and the downregulated candidate genes are unknown or hypothetical proteins. Sequence analysis did not reveal any homologues in other organisms, which makes the evaluation of the array results difficult.

Most recently, the genome of *Xenopus tropicalis* was published (Hellsten et al., 2010). This species of the clawed frogs is closely related to *Xenopus laevis*, but as it is diploid, it is better suited for genetic approaches. The *X. tropicalis* genome consists of 20,000 protein-coding genes. Comparison of the microarray results to the recently annotated genome might give new insights into the functions of the microarray candidates.

In search for genes, which are involved in morphogenetic processes like convergent extension or tissue separation, I focussed on candidates with an obvious connection to these mechanisms like cell adhesion molecules or transcription factors. I chose proteins with a connection to small GTPase signalling, as their involvement in these processes is already well described (Wunnenberg-Stapleton et al., 1999; Tahinci and Symes, 2003; Habas et al., 2003; Unterseher et al., 2004; Raftopoulou and Hall, 2004; Hyodo-Miura et al., 2006; Habas and He, 2006). XGit2 and xRhoGAP 11A were functionally characterised in more detail. And indeed, I could show that both genes negatively regulate CE and TS and have an inhibitory effect on RhoA activity.

Furthermore, I looked for molecules with a connection to the cell adhesion machinery and found Xnlrr-1 (*Xenopus laevis* neuronal leucine-rich repeat protein). Homologous proteins with leucine rich repeats have been described as cell adhesion molecules (Hayata et al., 1998). Functional analysis of Xnlrr-1 remains to show whether this protein is actually involved in cell adhesion and tissue separation. The coincident expression pattern with PAPC, however, is promising.

Recently, Fletcher and co-workers have shown that GATA transcription factors are involved in the cell migration during gastrulation. *Xenopus* embryos expressing a mutant active form of GATA6 show a disturbed Brachet's cleft morphology (Fletcher et al., 2006).Therefore a closer look on the regulation of GATA family members by PAPC and xFz7 is surely rewarding.

Among all these interesting candidates, the hypothetical proteins with unknown protein domains and gene functions remain unresolved. Surely, some of them are completely unconnected to gastrulation movements. However, there could be a novel gene among them which would answer many open questions, which still consist. Although, with the discovery of xGit2 and xRhoGAP 11A, I

could add new components to Rho signalling, convergent extension and tissue separation and elucidate the mechanism behind these processes a little further.

4.3 xRhoGAP 11A and xGit2 are negative regulators of RhoA

Among the genes which are downregulated by PAPC/FZ7 were two novel *Xenopus* proteins, which I called xGit2 and xRhoGAP 11A according to their human homologous proteins. Overexpression of xGit2 and xRhoGAP 11A inhibits Rho activity and impairs convergent extension movements as well as tissue separation behaviour. Both proteins encode GTPase activating proteins (GAPs) for small GTPases and catalyse GTP bound to the active GTPase to GDP. xRhoGAP 11A comprises a GAP domain that is specific for the small GTPase RhoA. By RhoA activity assays and staining of endogenous active Rho in *Xenopus* tissue explants, I could show that xRhoGAP 11A actually has an inhibitory effect on Rho signalling (Fig. 25, Fig. 26). Apart from this GAP domain, no other conserved functional domain can be detected. Therefore, it can be assumed that xRhoGAP 11A has a direct catalytic GAP activity for RhoA (Tcherkezian and Lamarche-Vane, 2007). Furthermore, the effects of xRhoGAP 11A on Brachet's cleft formation could be rescued by constitutively active RhoA, which shows that xRhoGAP 11A regulates tissue separation by modulation of Rho signalling.

xGit2 is also a GTPase activating protein, but its GAP domain is specific for the small GTPase Arf (ADP ribosylation factor), a member of the Ras superfamily (Randazzo et al., 2000). The GAP domain of xGit2 has no direct catalytic activity for Rho, but overexpression of xGit2 reduces RhoA activity in the *Xenopus* embryo. Interestingly, this inhibiting activity for Rho is independent of a functional GAP domain. A point mutation in the GAP domain, that abolishes GAP activity, inhibits Rho activity like the wildtype xGit2 protein (Fig. 25) (Di Cesare et al., 2000; Matafora et al., 2001).

Previously another ArfGAP, xGAP, has been described to play a role in *Xenopus* gastrulation by regulating the cell intercalations occurring during CE movements. Most importantly the effect of xGAP on morphogenetic movements is also independent of its GAP activity, arguing in favour of the involvement of another functional domain of the protein (Hyodo-Miura et al., 2006).

Git proteins are multidomain proteins that are involved in a variety of intracellular processes. They interact via PIX (p21-activated kinase interacting exchange factor) with PAK (p21-activated kinase) and the small GTPases Rac1 and Cdc42 (Frank et al., 2006). Another interacting protein is Paxillin, a focal adhesion adaptor protein which links Git proteins to the adhesion machinery and to the regulation of cell migration (Mazaki et al., 2001). These are functions that need to be regulated tightly in convergent extensions as well as tissue separation. In contrast to in xRhoGAP 11A expressing embryos, constitutively active RhoA could not rescue Brachet's cleft formation in xGit2 overexpressing embryos (Fig. 27). The negative effect of xGit2 on Rho signalling therefore seems to be indirect, and xGit2 regulates tissue separation and Rho signalling via additional mechanisms.

Git proteins, mainly Git1, have an impact on the disassembly of Rho dependent focal adhesions (Mazaki et al., 2001; Shikata et al., 2003; van Nieuw Amerongen et al., 2004). Git1 is recruited to focal adhesion complexes in a Rho dependent manner (van Nieuw Amerongen et al., 2004). Phosphorylation of Git1 requires Rho kinase (ROK), Src and FAK (focal adhesion kinase). At the same

time RhoA activity is suppressed by FAK to promote focal adhesion turnover (Ren et al., 2000). Rho signalling and Git proteins clearly are connected. a downregulation of Rho activity, however, could not be shown by van Nieuw Amongen and co-workers (van Nieuw Amerongen et al., 2004). Arf1, the in vivo substrate of Git2 (Mazaki et al., 2001), potentiates RhoA activated stress fibers and Mazaki and co-workers state, that Arf1 and RhoA activate complementary pathways (Mazaki et al., 2001). As a negative regulator of Arf activity, Git2 might inhibit the Arf1-dependent RhoA activity potentiation. However, involvement of the ArfGAP activity would be contradictory to the result that the GAP domain is dispensable for the inhibition of Rho activity.

It has been shown, that Git proteins disrupt the normal internalisation of G-protein coupled receptors (Premont et al., 1998; Premont et al., 2000; Claing et al., 2000). In the past, endocytosis has been considered mainly as terminator of signalling pathways by receptor downregulation, but by now, it is evident that endocytosis is a positive key player in many signalling cascades. It has been shown for example, that endocytosis also contributes positively to Wnt signalling, as interfering with clathrin-mediated endocytosis actually blocks active Wnt/β-catenin signalling (Seto et al., 2002; Blitzer and Nusse, 2006; Seto and Bellen, 2006; Gagliardi et al., 2008). There is also some evidence that receptor internalisation plays a role in PCP signalling, as this branch of the Wnt-signalling cascades involves AP-2 and β-arrestin, two proteins that modulate endocytosis (Gagliardi et al., 2008). Additionally, it is evident that Fz7 shows a turnover at the plasma-membrane which is regulated in a Ca^{2+} dependent manner (Struewing et al., 2007). However, it is not clear yet if this turnover is necessary for proper Wnt/Ca^{2+}-signalling. If active Wnt/Fz7 signalling requires internalisation of the receptor, it is possible that this is the point where xGit2 exerts its inhibiting effect on this signalling cascade. By blocking xFz7-internalisation, xGit2 would inhibit the pathway in the ectoderm, which is necessary for tissue separation and convergent extension movements. By the downregulation of xGit2 in the involuting mesendoderm, PAPC and xFz7 enhance non-canonical Wnt-signalling in these cells. Thus convergent extension movements and tissue separation can take place. Cell surface biotinylation assays could give a hint, whether Fz7-internalisation is impeded in the presence of xGit2 and whether this also has a functional influence on Frizzled-signalling.

4.4 Rho-signalling is regulated on a transcriptional level

The small GTPase RhoA is an important regulator of cellular processes like cytoskeleton dynamics, cell migration, cell growth, cell adhesion and intracellular membrane trafficking (Kaibuchi et al., 1999; Kaibuchi, 1999; Fanto et al., 2000a; Burridge and Wennerberg, 2004; Raftopoulou and Hall, 2004). RhoA acts as a molecular switch and cycles between an active, GTP-bound state and an inactive, GDP-bound state which is tightly regulated by two kinds of protein families: GAP (GTPase activating protein) and GEF (guanine nucleotide exchange factor) proteins. GEF proteins activate RhoA and catalyse the exchange of GDP to GTP, whereas GTPase activating proteins enhance the intrinsic GTPase activity of the small GTPase and promote the hydrolisation of GTP to GDP, leading to an inactivation of the small GTPase (Cerione and Zheng, 1996; Tcherkezian and Lamarche-Vane, 2007).

It has been shown, that Rho-signalling is indispensable for proper regulation of morphogenetic movements during *Xenopus* gastrulation, as it is a downstream component of Wnt/PCP-signalling

and is required for convergent extension and tissue separation (Habas et al., 2001; Tahinci and Symes, 2003; Habas et al., 2003; Unterseher et al., 2004; Medina et al., 2004; Habas and He, 2006; Bikkavilli et al., 2008). The level of Rho-signalling during gastrulation movements must be tightly regulated, as both activation and inhibition of Rho leads to a disturbance in convergent extension movements (Tahinci and Symes, 2003). But little is known about the GAPs and GEFs that keep the right balance of Rho-signalling in the mesodermal tissue undergoing morphogenetic movements. Recently, a RhoGEF called WGEF was described in *Xenopus* as being involved in *Xenopus* PCP-signalling (Tanegashima et al., 2008). WGEF is expressed dorsally in the region of the prospective notochord. It activates RhoA in the PCP-pathway and it is required for CE movements. In addition, a RhoGAP (XrGAP) with unknown function has been described that is localised specifically in the notochord and the brain (Kim et al., 2003). Despite the conserved function of Rho in the regulation of morphogenesis, there are no RhoGAPs or RhoGEFs known in zebrafish that are specifically expressed during gastrulation.

xRhoGAP 11A has been identified as negative regulator of RhoA activity (Köster et al., 2010). xRhoGAP 11A expression is downregulated *in vivo* by both PAPC and xFz7 in the involuting mesendoderm, where convergent extension and tissue separation take place. I showed that xRhoGAP 11A negatively regulates RhoA activity both *in vitro* and *in vivo* (Fig. 25, Fig. 26) and overexpression of xRhoGAP 11A has an inhibitory effect on both CE and TS (Fig. 18, Fig. 21). I therefore conclude that the elevated levels of RhoA in the involuting mesendoderm are regulated by the inhibition of the Rho inhibitor xRhoGAP 11A by PAPC and xFz7. This shows for the first time, that regulation of RhoA is mediated by the transcriptional repression of its inhibitor in the involuting mesoderm.

4.5 PAPC and xFz7 define the expression domains of target genes

The specification of the three germ layers requires precision in order to maintain the proportions of the cells that belong to either ecto-, meso- or endoderm. Therefore, the spatial and temporal expression patterns of genes involved in germ layer specification must be tightly regulated. It has been shown, that the confinement of a cell to a specific germ layer is a gradual process during gastrulation. At the beginning of gastrulation, the transition between the prospective germ layers is smooth and there are cells expressing marker genes that belong to more than one germ layer. As gastrulation proceeds, the cells are more and more specified to one germ layer and rogue cells expressing marker genes of a foreign tissue are becoming less frequent (Wardle and Smith, 2004).

There are several possible mechanisms that regulate the commitment of cells to one specific germ layer or tissue. One possibility is that those cells expressing marker genes of an extrinsic tissue disappear by apoptosis when they are surrounded by another tissue. During gastrulation, a limited number of apoptotic cells can be identified (Hensey and Gautier, 1998). Another mechanism is the regulation of gene expression patterns by local feedback loops. For example, xBra and eFGF in the marginal zone are regulated in a positive feedback loop to maintain each other's expression. As eFGF is not expressed in the ectoderm, xBra expression in a rogue ectodermal cell would not be maintained in this area (Isaacs et al., 1994; Casey et al., 1998). Furthermore, by limiting the number

of mesoderm inducing signals, the homeodomain protein Mixer is involved in forming the boundary between mesoderm and endoderm (Kofron et al., 2004).

In this work, I identified PAPC and xFz7 as factors that are able define the expression domains of genes in the involuting mesendoderm. xGit2 and xRhoGAP 11A are strongly expressed in the dorsal ectoderm, but only weak expression is seen in the involuting mesoderm, where PAPC and xFz7 are expressed and active Rho-signalling is detected (Berger et al., 2009). When PAPC is knocked down by morpholino antisense oligonucleotides, expression of xGit2 and xRhoGAP 11A is no longer suppressed in the involuting mesoderm and their expression domains are extended into this region (Fig. 24). Rho-signalling is inhibited in this area by xRhoGAP 11A and xGit2 leading to defects in morphogenetic cell behaviours like tissue separation and convergence and extension. This indicates that xRhoGAP 11A and xGit2 act downstream of PAPC/xFz7-signalling. This view is supported by the finding that overexpression of xGit2 and xRhoGAP 11A in the dorsal mesendoderm phenocopies the inhibitory effect of PAPC and xFz7 knockdown on tissue separation and convergent extension (Winklbauer et al., 2001; Medina et al., 2004). Furthermore, knockdown of PAPC in TGF-β-induced animal caps inhibits CE movements, a defect that can be rescued by simultaneous knockdown of PAPC and xGit2 or xRhoGAP 11A (Fig. 28), indicating that the regulation of CE by PAPC is mediated by inhibition of xGit2 and xRhoGAP 11A expression *in vivo*. Finally, knockdown of xRhoGAP 11A and xGit2 restores RhoA activity in PAPC-depleted embryos, demonstrating that PAPC-mediated Rho activation is achieved by suppression of xRhoGAP 11A and xGit2. This study suggests that PAPC and xFz7 together suppress the transcription of the two Rho-inhibitors and proper PCP-signalling can take place in the involuting mesoderm. I propose that Rho-signalling in the dorsal involuting mesoderm is regulated by the restriction of its inhibitors to the dorsal ectoderm (Fig. 33).

A similar mechanism could form the basis of Sox-2 expression in the involuting mesoderm. Sox-2 is expressed in the dorsal marginal zone and refined during gastrulation to the prospective neural tissue (Kishi et al., 2000; Sasai, 2001). Although it is upregulated during gastrulation, it was downregulated in PAPC and xFz7 expressing animal cap cells in the microarray experiment (Table 2). PAPC and xFz7 might downregulate the expression of Sox-2 locally in the involuting mesoderm and thus restricting its expression to the prospective neural tissue. The downregulation of target genes in the involuting mesoderm by PAPC and xFz7 might provide a general mechanism for the confinement of cells to this tissue. Therefore, PAPC and xFz7 are not only important keyplayers of non-canonical Wnt-signalling and morphogenetic movements like convergent extension and tissue separation, but they also play a role in the specification of the germ layers by defining the expression domains of their target genes.

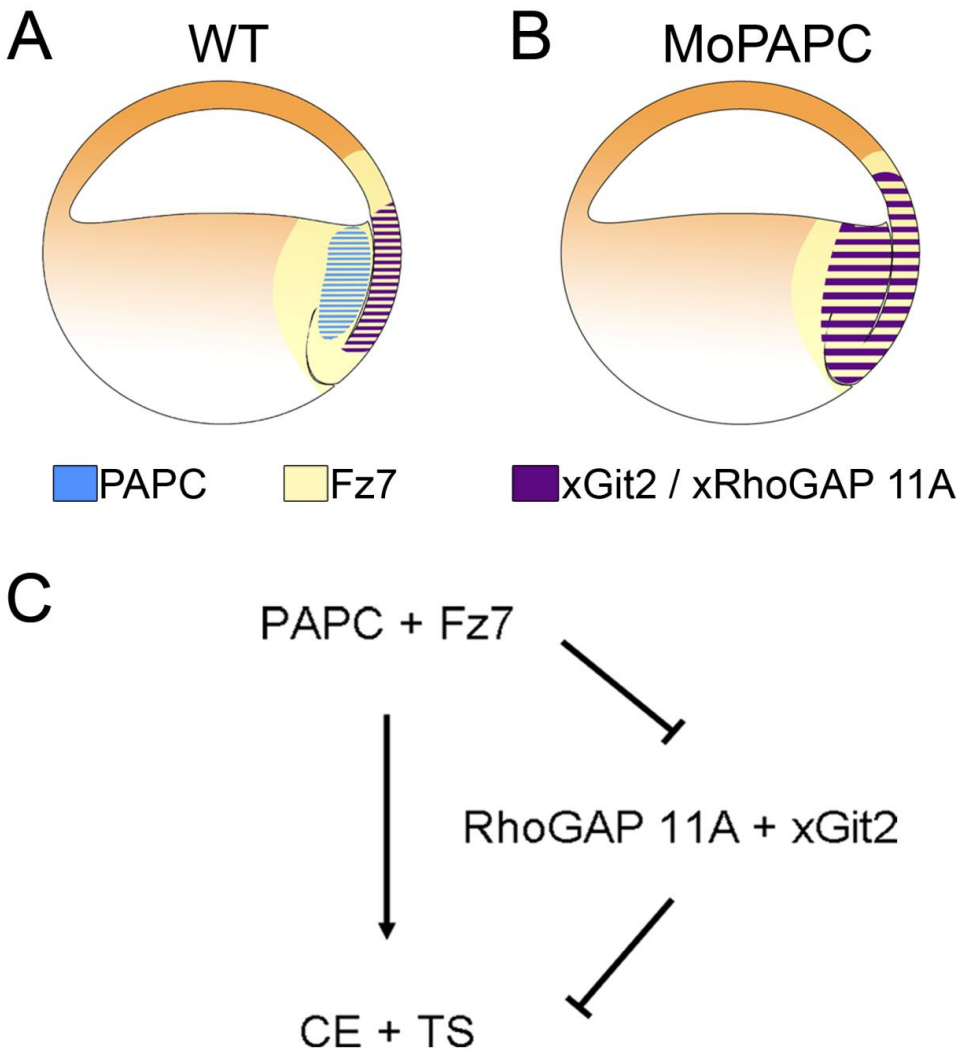

Fig. 33: Model of PAPC and xFz7-mediated regulation of xRhoGAP 11A and xGit2. (A) PAPC and xxFz7 inhibit the expression of XGit2 and xRhoGAP 11A in the involuted mesoderm and promote proper convergent extension movements and tissue separation. (B) After knockdown of PAPC by morpholino antisense oligonucleotides, the expression of both xGit2 and xRhoGAP 11A is extended to the involuted mesoderm, where PAPC normally is expressed. (C) The regulation of convergent extension (CE) and tissue separation (TS) by PAPC and xFz7 may be attributable to inhibition of xRhoGAP 11A and xGit2 in the involuting mesoderm.

5 Materials and Methods

5.1 Materials

5.1.1 Chemicals

All chemicals, if not stated otherwise, were obtained from Applichem, Merck, Roth and Sigma-Aldrich.

Agarose	Biozym
BMPurple AP-substrate	Roche
Complete protease inhibitor cocktail	Roche
Digoxigenin-labelling mix	Roche
dNTP-mix, 2 and 10 mM	Fermentas
Ethidium bromide	Merck
Fluorescein-labelling mix	Roche
GeneRuler 1 kb DNA Ladder	Fermentas
GeneRuler 100 bp DNA Ladder	Fermentas
PageRuler Prestained Protein Ladder	Fermentas
RNAse-free water	Ambion
Sheep serum	Sigma
Stabilization and Drying Solution	Agilent
TRIZOL reagent	Invitrogen

5.1.2 Buffers and Solutions

All chemicals, if not stated otherwise, were obtained from Applichem, Merck, Roth and Sigma-Aldrich.

Bacteria lysis buffer	50 mM Tris-HCl pH 7.4, 150mM NaCl, 5 mM $MgCl_2$, 1 mM DTT, 1x complete protease inhibitor
BBR (10%)	10% (w/v) Boehringer blocking reagent, 1x MAB
BBR/MABT (2%)	1v 10% BBR, 4v MABT
Bleaching solution	1% H_2O_2, 5% formamidee, 0.5x SSC
Blocking solution (ISH)	2% BBR, 20% heat treated sheep serum in MABT
Blocking solution (RBD-GFP)	3% BSA, 20% normal goat serum (NGS), 0.1 M glycine
Blocking solution (Western blot)	5% powdered milk in PBS/0.1% Tween-20
Cystein solution	2% l-cystein, pH 8.0
DNA loading buffer (6x)	40% glycerol (v/), 0.25% Bromphenol blue
Hybridisation buffer (ISH)	5x SSC, 50% (v/v) formamidee, 1% (w/v) Boehringer blocking reagent, dissolve 1h at 65°C, 1 mg/ml yeast tRNA, 0.1 mg/ml

	heparin, 0.1% (v/v) Tween-20, 0.1% (w/v) CHAPS, 5 mM EDTA, filtered, stored at -20°C
LB medium	1%(w/v) bactotryptone, 1%(w/v) NaCl, 0. 5% (w/v) yeast extract
LB-Amp	LB-Medium, 50 mg/ml Ampicillin
LB-Amp-agarplates	1.5% agarose, LB-Medium, 50 mg/ml ampicillin
MAB (10x)	1 M maleic acid, 1.5 M NaCl, pH 7.5
MABT	1x MAB, 0.1% (v/v) Tween-20
MBS	88 mM NaCl, 2.4 mM $NaHCO_3$, 1 mM KCl, 0.82 mM $MgSO_4$, 0.41 mM CaCl, 0.33 mM $CaNO_3$, 10 mM HEPES, 10 µg/ml streptomycinsulfate, 10 µg/ml penicillin, pH 7.5
MEM (10x)	1 M MOPS, 20 mM EGTA, 10 mM $MgSO_4$, pH 7.4
MEMFA	3.7% formaldehyde, 1x MEM
Mowiol	20 mg Mowiol, 80 ml PBS, 50 ml glycerol
NuPAGE running buffer (20x)	1 M Mops, 1 M Tris, 86.3 mM SDS, 20.5 mM EDTA, pH 7.7, do not adjust pH
PBS (10x)	27 mM KCl, 1.37 mM NaCl, 20 mM KH_2PO_4, 100 mM Na_2HPO_4, pH 7.4
PBST	1x PBS, 0.1% (v/v) Tween-20
4% PFA/PBS	4% (w/v) PFA (dissolved in 60% final volume H_2O at 60°C and neutralised with 1 M NaOH to pH 7.0). 1xPBS
pH 9-buffer	0.1 M NaCl, 0.1 M Tris pH 9.5, 50 mM $MgCl_2$
Rho lysis buffer	50 mM Tris-HCl pH 7.2, 500 mM NaCl, 10 mM $MgCl_2$, 1% Triton-X100, 1x complete protease inhibitor
Rho wash buffer	50 mM Tris-HCl pH 7.2, 150 mM NaCl, 10 mM $MgCl_2$, 1% Triton-X100, 1x complete protease inhibitor
SDS-PAGE running buffer	24.8 mM Tris, 192 mM glycine, 0.1% SDS
SDS-sample buffer (3x)	150 mM Tris-HCl pH 6.8, 6% SDS (w/v), 0.3% bromphenol blue (w/v), 30% glycerol (v/v). 300 mM DTT
SSC (20x)	3 M NaCl, 0.3 M sodium citrate, pH 7.5
TBE (10x)	890 mM Tris-borate, 0.2 mM EDTA, pH 8.0
TE	10 mM Tris-HCl, 1 mM EDTA, pH 8.0
Western blot transfer buffer	24.8 mM Tris, 192 mM glycine, 20% methanol

5.1.3 Oligonucleotides

The following oligonucleotides were ordered from Operon, Metabion and Sigma-Aldrich.

Bam_rhogap_fwd	ATGCGGATCCATGAGGGCAACTGG	cloning
Xho_rhogap_rev	ATCGCTCGAGTTAACTGATTGGTTCC	cloning
Bam_larg_fwd	ATCGGGATCCATGAGTGGAACACAGTC	cloning
Eco_larg_rev	CAATGCTTCCTACAGATAAGGGTTAA	cloning
Eco_git_fwd	ATGCGAATTCATGTCCAAGCGGCTGA	cloning
Xho_git_rev	CCAAAGAAAACACCAACTGA	cloning
Bam_XeWee1A_fwd	ATGCGGATCCATGAGGACGGCCATGT	cloning
Xho_XeWee1A_rev	GCTGAGCTTCACCTGCGGAGGGTATTAA	cloning
BamH I_rhogap_f	ATGCGGATCCAGCTGAGACGACCATGA	cloning
XbaI_rhogap_r	GGGCTCTAGAAAAATCGATTAAGTCACTGATTGG	cloning
EcoRI_git2-f	GCGAATTCTACCATGTCCAAGCGGCTGA	cloning
XbaI-git2_r	AGGCTCTAGAGTTGGTGTTTTCTTTGGTC	cloning
ODC_ABI_fwd	TGCACATGTCAAGCCAGTTC	qRT-PCR
ODC_ABI_rev	GCCCATCACACGTTGGTC	qRT-PCR
H4_ABI_fwd	AGGAAGGTGCTTAGGGACAAC	qRT-PCR
H4_ABI_rev	CAGAGATGCGCTTGACTCC	qRT-PCR
RhoGAP_ABI_fwd	AGCCACAATCTTGGTGACG	qRT-PCR
RhoGAP_ABI_rev	CATCCGGTTTTCACTGCAC	qRT-PCR
Xlarg_ABI_fwd	CCAGAAGCTGGATATACTGATGAA	qRT-PCR
Xlarg_ABI_rev	GCCTCTGTGATGGAGTAGTATGAA	qRT-PCR
Git2_ABI_fwd	CTTCGTGTAATGCAGAAAAAGC	qRT-PCR
Git2_ABI_rev	TCCGGGTTGGACCTGATA	qRT-PCR
Sox2_ABI_fwd	CGAGTGAAGAGACCCATGAAC	qRT-PCR
Sox2_ABI_rev	TTGCTGATCTCCGAGTTGTG	qRT-PCR
XeWee1A_ABI_fwd	ACTGGATGGATGTTTCTACGC	qRT-PCR
XeWee1A _ABI_rev	TGAGCGTACACTTCTCTCAACG	qRT-PCR
Xnlrr1_ABI_fwd	GGGTTCTAACCAAACCAGCA	qRT-PCR
Xnlrr1_ABI_rev	TCTTGAGCCAATGCTTCCTT	qRT-PCR
Xoct91_ABI_fwd	TGAAAACAATAAAAACCTCCAAGA	qRT-PCR
Xoct91_ABI_rev	AAGGTGCATTTCACGTTGTTC	qRT-PCR
XGATA-2_ABI_fwd	TCTTACAGCCAGGCTCACG	qRT-PCR
XGATA-2_ABI_rev	AGCGCAGTCTTCCCACTCT	qRT-PCR
FNIII like_ABI_fwd	AGCCGCCAAAAATGATATTG	qRT-PCR
FNIII like _ABI_rev	AGCTTTGGTGGCAGTGGA	qRT-PCR
XGATA-3_ABI_fwd	CAAAACTCGCTCAAGCACAG	qRT-PCR
XGATA-3_ABI_rev	TGCATTGCATAGATAATGTCCA	qRT-PCR
RhoGAP_fwd	AAGGTACAGGCGCAGAAGAG	RT-PCR
RhoGAP_rev	AGCTTCCGTACGCTTCGATA	RT-PCR
Xlarg_fwd	CACGAGATCAAGCAACAGGA	RT-PCR

Xlarg_rev	CAACTGCAGGCGCTTACATA	RT-PCR
Git_fwd	GAAGCCTTGGTCGTCACATT	RT-PCR
Git_rev	ATGAAGAGGCGTGCTACCTT	RT-PCR
Sox2_fwd	TCTGCACATGAAGGAGCATC	RT-PCR
Sox2_rev	GAGCTGGATTCCGACTTGAC	RT-PCR
Xe-Wee1A_fwd	TCTCCTCTGGCAGTGTCCTC	RT-PCR
Xe-Wee1A_rev	CAGATCCGAACACTCGTCCT	RT-PCR
xnlrr1_fwd	TCATCCATTCCACTCAACGA	RT-PCR
xnlrr1_rev	GATAAGGCCACCACAGAAGG	RT-PCR
xoct91_fwd	CCACCTTCTGGTCTCAGGTC	RT-PCR
xoct91_rev	ATGGTGGTCTGGCTGAATGT	RT-PCR
XGATA-2_fwd	CTCAGCTCTTGCCTCCTGAT	RT-PCR
XGATA-2_rev	ACTGCCTCCTTCCATCTTCA	RT-PCR
FNIII like_fwd	GGCCAGCAACAGACTACCAT	RT-PCR
FNIII like_rev	AGGTGATGCCAGAATGAAGG	RT-PCR

5.1.4 Morpholino antisense oligonucleotides

The following morpholino antisense oligonucleotides were purchased from Gene Tools LLC. For MoPAPC a mixture of two morpholinos targeting both PAPC alleles (MoPAPC_1 and MoPAPC_2) was injected (Unterseher et al., 2004; Medina et al., 2004).

MoPAPC_1	CCTAGAAACAGTGTGGCAATGTGAA
MoPAPC_2	CTTGCCTAGAAAGAGTGCTGCTGTG
MoxFz7	CCAACAAGTGATCTCTGGACAGCAG
MoGit2	GCTCCTCAGCCGCTTGGACATGGTA
MoRhoGAP11A	AGGTCCAGTTGCCCTCATGGTCG
MoControl	CCTCTTACCTCAGTTACAATTTATA

5.1.5 Plasmids

pSP64T-Bvg1	D. Melton
p13-pCS-h2B-mRFP	J.B. Wallingford
pCMV-Sport6-xGit2	RZPD; IRBHp990B0339D2
pCMV-Sport6-xRhoGAP 11A	RZPD; IRBHp990A0355D2
pCS2 + PAPCc-flag	(Wang et al., 2008)
pCS2+	(Rupp et al., 1994; Turner and Weintraub, 1994)
pCS2+ FL-PAPC (-UTR)	(Medina et al., 2004)
pCS2+ xFz7	(Medina et al., 2000)
pCS2+ M-PAPC	(Kim et al., 1998)
pCS2+ mt	(Rupp et al., 1994; Turner and Weintraub, 1994)
pCS2+ RhoA-myc	(Medina et al., 2004)
pCS2+ V14-RhoA	(Medina et al., 2004)

pCS2+xGit2	Using primers Eco_git_fwd and Xho_git_rev the open reading frame of RZPD clone pCMV-Sport6-xGit2 was amplified and cloned into EcoR I/Xho I restriction sites of pCS2+.
pCS2+xGit2-myc	
pCS2+xRhoGAP 11A	Using primers Bam_rhogap_fwd and Xho_rhogap_rev the open reading frame of RZPD clone pCMV-Sport6-xRhoGAP 11A was amplified and cloned into BamH I/Xho I restriction sites of pCS2+.
pCS2+xRhoGAP 11A-myc	
pCS+ xGit2 R39K	The clone was created from pCS2+ xGit2 by site-directed mutagenesis using primer R39K_fwd and R39K-rev.

5.1.6 Proteins and Enzymes

DNAse I	Fermentas
EuroTaq DNA Polymerase	BioOne
FastDigest® restriction enzymes	Fermentas
Human chorionic gonadotropine	Sigma
Pfu DNA polymerase	Promega
Phusion high fidelity DNA polymerase	Finnzymes
Proteinase K	Sigma
RevertAidH-Minus M-MuLV Reverse Transcriptase	Fermentas
RiboLock RNAse inhibitor	Fermentas
shrimp alkaline phosphatase (SAP)	Fermentas
T3, T7 and Sp6 RNA polymerases	Roche
T4 DNA Ligase	Fermentas

5.1.7 Kits

Absolute™ QPCR SYBR® Green Rox Mix	Thermo Scientific
Big Dye Terminator Cycle Kit	Applied Biosystems
Gene Expression Hybridisation Kit	Agilent
Gene Expression Wash Buffer Kit	Agilent
Low RNA Input Linear Amplification Kit	Agilent
mMessage mMachine High Yield Capped RNA Transcription Kit	Ambion
Qiagen Plasmid Midi Kit	Qiagen
QIAquick Gel Extraction Kit	Qiagen
QIAquick PCR Purification Kit	Qiagen
Rneasy Mini Kit	Qiagen
SuperSignal West Femto Maximum Sensitivity Substrate Trial Kit	Thermo Scientific
Two-Color RNA Spike-In Kit	Agilent
TNT SP6 Coupled Reticulocyte Lysate System	Promega

5.1.8 Antibodies

α-Digoxigenin-AP (Fab fragments)	sheep	1:10000	Roche
α-Fluorescein-AP (Fab fragments)	sheep	1:10000	Roche
α-GST	mouse	1:200	Santa Cruz
α-mouse-HRP	goat	1:10000	Biorad
α-myc 9E10 supernatant	mouse	1:1000	

5.1.9 Equipment

5415 D tabletop centrifuge	Eppendorf
595 ½ Folded Filters	Schleicher & Schuell
A1R laser scanning microscope	Nikon
ABI 7500 Fast Real-Time PCR cycler	Applied Biosystems
ALF Sequencer	Amersham Pharmacia Biotech
CC-12 digital camera	Olympus
Cellstar Tissue culture dishes	Greiner Bio-one
Cold plate	Julabo
Cronex 5 film	Agfa
Dumont Nr. 5, forceps	NeoLab
EasyCast electrophoresis system	Owl Scientific
Epi Chemi II Darkroom gel documentation system	UVP Laboratory Product
Eppi-pestle, stainless steel, for 1.5 ml reaction vessels	Schuett biotec
IM300 Microinjector	Narishige
JC-5 centrifuge	Beckman Coulter
KL 1500 electronic cold light source	Zeiss
LE-80K ultracentrifuge	Beckmann Coulter
Micromanipulator	Micro Instruments
NanoDrop ND-1000 Spectrophotometer	Thermo Scientific
NC2010 Gel cassettes 1.0 mm	Invitrogen
Novex xCell SureLock Mini-cell system	Invitrogen
Optimax Typ TR x-ray film processor	Protec Medizintechnik
PCR Plate cover foil Star Seal	Star Lab
PCR strips	Sarstedt
PD-5 Puller for producing microneedles	Narishige
Peltier Thermocycler PTC-200	MJ Research
Petri dishes	Greiner bio-one
Pipettes	Gilson
Power Pac 300	BioRad
PROTRAN BA 85 membrane	Whatman
PROTRAN Nitrocellulose Transfer Membrane	Whatman
Reaction tubes 0.5, 1.0 and 2.0 ml	Sarstedt

Reaction tubes 15 and 50 ml	Greiner bio-one
Self-adhesive hole reinforcements	Zweckform
Stemi SV6	Zeiss
Stripette	Costar
SZX12 fluorescence microscope	Olympus
Thermo Fast 96-well PCR Plates	Applied Biosystems

5.1.10 Bacteria

E. coli XL-1 Blue	*rec*A1 *end*A1 *gyr*A96 *thi*-1 *hsd*R17 *sup*E44 *rel*A1 *lac*
E. coli BL21(DE3) Rosetta	*E. coli B dcm ompT hsdS*($r_B^-m_B^-$) *gal*
E. coli SCS 110	rpsL thr leu endA thi-1 lacY galK 53thylene tonA tsx dam dcm supE44 Δ(lac-proAB)

5.1.11 Software

Agilent Feature extraction software	Agilent
Combine ZM	Alan Hadley http://www.hadleyweb.pwp.blueyonder.co.uk/CZM
ImageJ 1.41n	NIH, USA
LabWorks analysis software	UVP laboratory product
Office Excel 2003	Microsoft
Office Word 2003	Microsoft
Photoshop CS3 Extended Version 10.0.1	Adobe
Reference Manager 11	Adept Science
Rosetta Resolver	Rosetta Biosoftware
Vector NTI Advance 10.3	Invitrogen

5.2 Molecular biology

5.2.1 Isolation of nucleic acids

5.2.1.1 Isolation of DNA

DNA was isolated from bacteria, agarose gels or PCR reaction with the appropriate kits (see 5.1.7) according to the manufacturer's instructions. For isolation of plasmid DNA form bacteria, 2 ml (mini prep) or 50 ml (midi prep) of LB-amp were inoculated with a single colony and cultured overnight at 37°C with shaking.

5.2.1.2 Isolation of RNA

Total RNA from *Xenopus* embryos was isolated using TRIZOL reagent. To 5 embryos, 10 dorsal halves or 15 animal caps 1 ml Trizol reagent was added and samples were homogenised using an Eppi-pestle for reaction vessels. Homogenised samples were incubated at RT for five minutes. Subsequently 200 µl of chloroform were added and samples were mixed thoroughly by vortexing. After centrifugation (15 min, 13.000 rpm, RT) the upper aqueous phase was transferred to a new tube and RNA was precipitated by isopropanol and subsequent centrifugation (15 min, 13.000 rpm, 4°C). The pellet was washed twice with 75% ethanol and resuspended in a suitable volume of nuclease-free H_2O. Quantity of total RNA was measured using a NanoDrop ND-1000 and quality of RNA was assessed by gel electrophoresis.

5.2.1.3 Phenol-chloroform purification of nucleic acids

To separate nucleic acids from proteins and lipids phenol-chloroform extraction was used. Aqueous solutions were mixed with the same volume of phenol-chloroform-isoamylalcohol and centrifuged for five minutes at 4°C with 13.000 rpm. The upper aqueous phase was transferred to a new reaction tube and the same volume of chloroform-isoamylalcohol (1:24) was added. The solution was mixed and centrifuged again for five minutes. The upper aqueous phase was transferred to a new tube and precipitated by isopropanol.

5.2.1.4 Precipitation of nucleic acids

To precipitate nucleic acids from aqueous solutions 1/10 V 3 M sodium acetate pH 5.2 and 2.5 V 100% ethanol or 0.7 V isopropanol were added and the mixture was incubated on ice for 15 minutes or overnight at -20°C and centrifuged at 13.000 rpm. The precipitate was washed with 75% ethanol and resolved in a suitable volume of water or TE buffer.

5.2.2 Restriction of DNA

Restriction enzymes are prokaryotic endonucleases that recognise specific DNA sequences of four to eight basepairs and cut double-stranded DNA in a specific manner. Depending on the enzyme DNA ends with a 5'-overhang, a 3'-overhang or blunt end forms after the digestion.

Plasmids were digested using FastDigest restriction enzymes (Fermentas) in the following reaction volume, or the volume was scaled up according to the amount of DNA:

1	µg	DNA
2	µl	FastDigest restriction buffer
1	µl	FastDigest restriction enzyme
x	µl	H_20
20	µl	

Reactions were incubated for 15 minutes at 37°C and subsequently stopped by either heat inactivation at 80°C or ethanol precipitation of the DNA. Analysis of the restriction was performed by agarose gel electrophoresis.

5.2.3 Agarose gel electrophoresis

DNA or RNA samples were mixed with 6x DNA loading buffer and loaded onto 0.5 to 2% agarose gels containing 5 µg/ml ethidium bromide. DNA or RNA fragments were then electrophoretically separated in TBE buffer at 100 V. To visualise nucleic acids, the gel was illuminated by UV light and imaged on a gel documentation system (Epi Chemie II Darkroom, UVP laboratory product).

To isolate DNA fragments from a preparative agarose gel, the appropriate DNA band was cut out under UV light using a scalpel. Purification of the DNA was performed using the QIAquick Gel extraction kit (Qiagen) according to the manufacturer's instructions.

5.2.4 Cloning of DNA fragments

Cloning was performed using the standard protocols of PCR-based fragment amplification, restriction, ligation and plasmid transformation. DNA was isolated from bacterial clones using the appropriate kit and analysed by restriction and sequence analysis.

5.2.4.1 Dephosphorylation of linear DNA at the 5'-end

To avoid religation of a linearised DNA fragment, shrimp alkaline phosphatase (SAP) was used to dephosphorylate 5'-ends. 2 µl of SAP were directly added to a restriction reaction and incubated for 15 minutes at 37°C. The reaction mix was subsequently heat inactivated for 15 minutes at 65°C.

5.2.4.2 Ligation of DNA fragments

Digested DNA fragments and vectors were ligated in a molecular ratio of 1:1 to 1:3 using T4 DNA ligase (Fermentas) in the following reaction volume:

5	µl	restricted DNA fragment
3	µl	restricted vector
1	µl	10x reaction buffer
1	µl	T4 DNA ligase
10	µl	

The ligation reaction mix was incubated for 1 hour at RT or at 16°C overnight and transformed into competent *E. Coli* XL-1 Blue.

5.2.5 Transformation of competent bacteria

50 µl of competent bacteria were transformed with 50-200 µg of purified plasmid DNA or 3 µl of ligation mix. Electrocompetent cells were transformed by an electropulse of 1.8 V, chemocompetent cells were heatshocked for 45 seconds in a 42°C water bath and subsequently placed on ice for five minutes. 500 µl LB medium were added and bacteria were cultured for one hour shaking at 37°C without antibiotics. 50 to 100 µl of transformed bacteria were plated on LB-ampicillin agar plates and cultured overnight at 37°C.

5.2.6 Polymerase Chain Reaction (PCR)

5.2.6.1 Cloning PCR

For cloning purposes the proofreading DNA polymerase Phusion was used. Specific primers containing restriction sites were used to introduce these restriction sites into the DNA fragments. To avoid retransformation of the template plasmid, it was linearised prior to the PCR reaction. The following reaction volume was used for amplification:

10	ng	DNA linearised plasmid
10	µl	5x HF buffer
5	µl	Primer Mix (10 µM each)
5	µl	dNTPs (2 mM)
x	µl	H_2O
1	µl	Phusion
50	µl	

For addition of restricition sites the first five cycles were performed at a low annealing temperature which was specific for the primer sequence without the restriction site sequence. After 5 cycles, when enough PCR product was formed, the annealing temperature of the program was set to the specific melting temperature of the whole primer sequence including the restriction sites. The following PCR program was used:

	Temperature	Time
	98°C	2min
5x	98°C	10sec
	low annealing temperature	15sec
	72°C	15sec
25x	95°C	10sec
	high annealing temperature	15sec
	72°C	15sec
	72°C	7min
	4°C	∞

Table 3: PCR program used for addition of restriction sites

5.2.6.2 Site-directed mutagenesis

Single nucleotide point mutations were introduced into DNA sequences by PCR-based site-directed mutagenesis. Primers suitable for mutagenesis where designed to have about 20 nucleotides flanking the mutated sites on each side and forward and reverse primers were complementary to each other. The proofreading polymerase Pfu (Promega) was used for the following PCR reaction:

1	µl	DNA template plasmid (100 ng/µl)
5	µl	10x Pfu reaction buffer + $MgSO_4$
5	µl	dNTPs (2 mM)
1	µl	Primer_fwd (10 µM)
1	µl	Primer_rev (10 µM)
1	µl	Pfu DNA polymerase
36	µl	H_2O
50	µl	

The vector was amplified using the following PCR program:

	Temperature	Time
	95°C	2 min
25x	95°C	45sec
	58°C	45sec
	68°C	10min
	68°C	10 min
	4°C	∞

Table 4: PCR program used for mutagenesis

5.2.6.3 Sequence analysis

Sequence analysis was performed using the Big Dye Terminator Cycle kit (Applied Biosystems). 400 ng of Plasmid DNA were amplified in the following reaction volume:

400	ng	Plasmid-DNA
1	µl	Primer (5 µM)
2	µl	5x Buffer
1	µl	Big Dye
x	µl	H_20
10	µl	

The target sequence was amplified by PCR according to the following protocol:

	Temperature	Time
	95°C	2min30sec
28x	95°C	30sec
	55°C	4min15sec
	4°C	∞

Table 5: PCR program used for sequencing

5.2.6.4 RT-PCR and qRT-PCR

To detect the expression of a target gene in the *Xenopus* embryo reverse transcription (RT) PCR was used. Total RNA was isolated using TRIZOL reagent (Invitrogen) and reverse transcribed using M-MuLV reverse transcriptase (see 5.2.7). The primers used for RT-PCR and qRT-PCR are listed in 0.

RT-PCR was performed in a 10 µl PCR reaction. Afterwards PCR reactions were mixed with 6x DNA loading buffer and analysed on a 1% agarose gel.

1-3	µl	cDNA
0.4	µl	$MgCl_2$ (10 mM)
1	µl	10x reaction buffer
1	µl	Primer-Mix (10 µM each)
1	µl	dNTPs (2 mM)
0.15	µl	EuroTaq
x	µl	H_2O
10	µl	

Template cDNA was amplified using the following PCR program:

	Temperature	Time
	96°C	2min
25-30x	94°C	30ec
	55-65°C	30sec
	72°C	1min
	72°C	5min
	4°C	∞

Table 6: PCR program used for RT-PCR

To quantify gene expression quantitative Real-time-RT-PCR was performed on an ABI 7500 Fast Real-Time PCR cycler. The qPCR reaction was set up in the following 20 µl PCR reaction according to the PCR program listed in Table 7.

2	µl	cDNA
10	µl	Absolute™ QPCR SYBR® Green Rox Mix
0.4	µl	Primer-Mix (10µM each)
7.6	µl	H_2O
20	µl	

	Temperature	Time
	25°C	15min
	95°C	15min
40x	95°C	15ec
	60°C	1min
	100-25°C	dissociation stage

Table 7: PCR program used for qRT-PCR

5.2.7 cDNA synthesis

RNA was reverse transcribed using RevertAidH-Minus M-MuLV reverse transcriptase (Fermentas) and random hexamer primers (Fermentas). To avoid possible genomic DNA contaminations a DNAse digest was performed previously. 1 µg of total RNA was incubated in a 10 µl reaction volume with 1 µl DNAse I (Fermentas) and incubated for 30 minutes at 37°C. DNAse I was inactivated by addition of 1µl EDTA and subsequent heat inactivation at 85°C for 15 minutes. The 10 µl DNAse-reaction was directly taken for reverse transcription. RNA was mixed with 0.2µg of random hexamer primer and incubated at 79°C for 5 minutes. 4 µl of 5x reaction buffer, 2 µl 10 mM dNTP mix and 0.5 µl RiboLock RNAse inhibitor were added, the reaction was filled to 19 µl total volume by nuclease-free water and incubated for 5 minutes at 25°C, followed by chilling to 4°C. After that, 1 µl reverse transcriptase was added and the reaction was incubated at 42°C for 2 hours. The reverse transcription was stopped by incubation at 70°C for 15 minutes. For further use, the reaction was filled to a total volume of 100 µl with nuclease-free H_20.

5.2.8 *In vitro* transcription of RNA

For microinjection synthetic 5'-capped mRNA was transcribed from linearised plasmids using the mMessage mMachine High yield capped RNA Transcription kit (Ambion) according to the manufacturer's instructions in the following reaction volume. The reaction was incubated at 37°C for two hours.

1	µg	linearised template plasmid
5	µl	2x NTP/CAP
1	µl	10x reaction buffer
1	µl	Sp6, T7 or T3 enzyme mix
x	µl	H_2O
10	µl	

Subsequently, 1 µl TurboDNAse was added and the reaction was incubated for 15 minutes at 37°C. 15 µl ammonium acetate stop solution were added and the reaction was filled to a total volume with 115 µl of nuclease-free H_2O. The synthesised CAP-RNA was purified by phenol-chloroform-extraction, resuspended in 15 µl nuclease-free H_2O and stored at -80°C. RNA concentration was measured using a NanoDrop ND-1000 spectrophotometer and sample quality was checked by agarose gel electrophoresis.

Digoxigenin or fluorescein labelled antisense probes for whole mount *in situ* hybridisations were transcribed from linearised plasmids using the fluorescein/digoxigenin labelling kit (Roche) in the following reaction volume.

1	µg	linearised template plasmid
1	µl	fluorescein or digoxigenin labelling mix
1	µl	10x transcription buffer
1	µl	Sp6, T7 or T3 RNA polymerase
1	µl	RiboLock RNAse inhibitor
x	µl	H_2O
10	µl	

The reaction was incubated at 37°C for 2 hours followed by ethanol precipitation of the in vitro transcribed RNA probe. The probe was resuspended in suitable volume of RNAse-free H_20 and stored at -20°C. Sample quality was checked by agarose gel electrophoresis.

5.2.9 Microarray analysis

To compare the two transcriptomes of wildtype animal caps and animal caps in which tissue separation behaviour was induced by the ectopic expression of xPAPC and xFz7, microarray analysis was performed using the Agilent *Xenopus laevis* 60-mer oligo microarray. 4-cell stage embryos were injected animally with each 400 pg PAPC and 300 pg xFz7 mRNA. Embryos were cultured until stage 9 and animal caps were dissected and cultured until control embryos reached stage 10.5. RNA of each 40 wildtype and 40 injected animal caps was isolated using TRIZOL reagent (Invitrogen). The RNA was

amplified and cRNA was directly labelled with Cy3 (WT) and Cy5 (injected) using the Low RNA Input Linear Amplification Kit (Agilent) according to the manufacturer's instructions. Labelled cRNA was fragmented using the Gene Expression Hybridisation Kit (Agilent) and competitively hybridised to the microarrays rotating for 17h at 65°C using an Agilent SureHyb hybridisation chamber. Hybridised arrays were washed using the Gene Expression Wash Buffer Kit (Agilent) and scanned by the Agilent DNA microarray scanner. Data was obtained through the Agilent Feature extraction software. The microarray experiments were repeated in three biological replicates. Further data analysis was performed using Rosetta Resolver software. Only genes that were regulated in all three biological replicates more than 2-fold with a p-value of 0.01 were considered as true candidates.

5.3 Embryology

5.3.1 *Xenopus* embryo culture and manipulation

Xenopus eggs were obtained from females injected with 500 IU human chorionic gonadotropin (Sigma), and were fertilised *in vitro*. Embryos were dejellied with 2% cystein solution, and embryos were microinjected in 1x MBS (Modified Barth's Solution). For microinjections, *in vitro* synthesised 5'-capped RNA or antisense morpholino oligonucleotides were injected into 2- or 4-cell stage embryos by a IM300 Microinjector and using extended glass capillaries. Injection was calibrated to 5 nl by constant time and pressure settings. The embryos were cultured in 0.1x MBS and staged according to Nieuwkoop and Faber (Nieuwkoop and Faber, 1975).

5.3.2 Animal cap assay

Animal caps were explanted from blastula embryos at stage 9. In a first step, the vitelline membrane of the embryos was removed, and the pigmented animal pole was cut out using two forceps. Animal caps were cultured in 1x MBS for further use until they reached the desired stage.

For the animal cap elongation assay, 4-cell stage embryos were injected animally into two blastomeres with 200 pg Bvg1 mRNA to induce dorsal mesoderm (Tiedemann and Tiedemann, 1959; Green and Smith, 1990; Green et al., 1997b), together with MoPAPC, MoRhoGAP, MoGit or xGit2 and xRhoGAP 11A RNA. Animal caps were excised at stage 9 and cultivated in 1x MBS together with 10 ng/µl gentamycine over night. Elongation of animal cap explants was scored.

5.3.3 Dorsal marginal zone explants

To investigate convergent extension movements in vitro, explants of the dorsal marginal zone were isolated from gastrula embryos. Embryos were injected into the two dorsal blastomeres at 4-cell stage with synthetic mRNAs of interest. Keller open face explants of the dorsal marginal zone were prepared at stage 10.5 as described (Keller et al., 1992) and grown under a coverslip seated with silicone grease in the presence of 10 ng/µl gentamycine (Fig. 34). Elongated explants were classified into three subgroups: full elongation, intermediate elongation and no elongation.

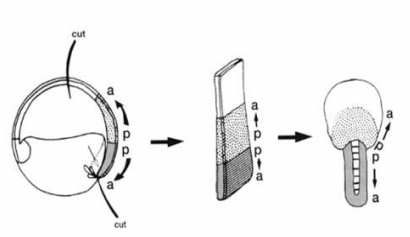

Fig. 34: Experimental procedure of preparation of dorsal marginal zone explants. Adapted from (Keller et al., 1992).

5.3.4 Tissue separation

For analysis of Brachet's cleft formation, embryos were injected at 4-cell stage into the two dorsal blastomeres with synthetic mRNAs of interest. Embryos were grown until stage 10.5, fixed with MEMFA and cut sagitally through the dorsal midline. The length of Brachet's cleft was analysed.

The blastocoel roof (BCR) assay to investigate tissue separation behaviour was performed as described (Wacker et al., 2000). Embryos were injected animally with *in vitro* synthesised mRNAs or antisense morpholino oligonucleotides together with fluorescein dextran into two opposing blastomeres at 4-cell stage. 200 pg Bvg1 mRNA was used to induce tissue separation behaviour in animal cap cell aggregates. At stage 10.5, the inner animal cap cells derived from injected embryos were dissected into small cell aggregates and placed upon an uninjected animal cap that served as a substrate. A coverslip was fixed with silicone grease to prevent the explant from rolling up of the explant. Separation behaviour was scored after 45 minutes (Fig. 35).

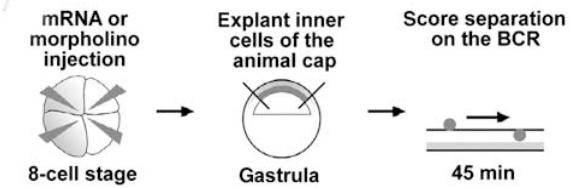

Fig. 35: Experimental procedure of BCR assay. Adapted from (Medina et al., 2004).

5.3.5 Whole mount *in situ* hybridisation

By whole mount *in situ* hybridisation the spatial expression pattern of endogenous mRNA in the embryo was analysed. For this method, an epitope-marked antisense RNA probe , e.g. digoxigenin or fluorescein, is hybridised to the endogenous RNA of interest and the probe can be visualised by the epitope-specific antibody that is coupled to alkaline phosphatase.

Hemi-section *in situ* hybridisation and antisense probe preparation were carried out as described (Epstein et al., 1997). Anti-Digoxigenin-AP and Anti-Fluorescein-AP antibodies (Roche) were used for detection. BMPurple (Roche) was used as a substrate for the alkaline phosphatase. The *in situ* hybridisation was performed as follows:

Day 1:

- Rehydration of the embryos for 5 min each in 75%, 50% and 25% MeOH in PBST
- 2x 5 min PBST
- (Bisect embryos)
- Proteinase K digest: 10 µg/ml in PBST, 30 min at RT, half embryos 10 min at RT without shaking
- Refixation of embryos in 4% PFA/PBS for 10 min at RT
- 4x 5 min PBST
- 1 ml hybridisation buffer/PBST (1:1) for 5 min at RT
- 1 ml prewarmed hybridisation buffer 5 min at RT
- 1 ml hybridisation buffer 1h at 65°C
- 1 ml fresh hybridisation buffer 2-4h at 65°C
- Hybridisation of antisense probes: 1 µl probe/1 ml hybridisation buffer overnight at 65°C

Day 2:

- 1x 5min 50% formamidee/0.1% Chaps/5x SSC (preheated to 65°C) at RT
- 1x 5min 25% formamidee/0.1% Chaps/3,5x SSC at RT
- 1x 5min 2x SSC/0.1% Chaps (preheated to 37°C) at RT
- 2x 25min 2x SSC/0.1% Chaps at 37°C
- 1x 5min 0.2x SSC/0.1% Chaps at RT
- 2x 30min 0.2x SSC/0.1% Chaps at 60°C
- 2x 5min 0.2x SSC/0.1% Chaps at RT
- 2x 10 min 0.2x SSC/0.1% Chaps at RT
- 1x 10 min 0.2x SSC/0.1% Chaps:MABT (1:1) at RT
- 2x 5min and 2x 10 min MABT at RT
- 1x 1h 1 ml MABT/2% BBR
- 1x 1h 1 ml blocking solution
- Antibody: α-Dig-AP (1:10000), α-Flu-AP (1:10000) overnight at 4°C

Day 3:

- 2x 30 min MABT at RT
- 4x 1h MABT at RT
- Staining of embryos with pH 9-buffer/BMPurple (1:1) in the dark
- Stop reaction by washing 2x in PBS
- Refix embryos in 3.7% formaldehyde/PBS overnight at 4°C

Pigmented embryos were bleached in 1% H_2O_2/5% formamidee in 0.5x SSC under intensive light.

5.4 Proteinbiochemistry

5.4.1 SDS-PAGE and Western blot

Proteins were separated by SDS-polyacrylamide gel electrophoresis (SDS-PAGE) using a Novex Xcell SureLock mini chamber. A 12% separating gel topped with 6% stacking gel was prepared by polymerisation as described (Laemmli, 1970). Stained protein molecular weight standards and protein extracts were then separated at constant voltage of 160 V in SDS-PAGE running buffer. For separation of samples from Rho activity assays, precast NuPAGE 12% Bis-Tris gels (Invitrogen) were used in NuPAGE running buffer.

After SDS-PAGE proteins were transferred to a nitrocellulose membrane by wet transfer at constant current (400 mA, 80 minutes) in Western blot transfer buffer. Transfer was checked by PonceauS staining and the membrane was blocked in 5% milk powder in PBST. Incubation of primary antibody was performed overnight at 4°C. After 6 washing steps in PBST at room temperature and incubation of the secondary antibody followed at RT for 1 hour. After washing again 6x in PBST, the specific protein bands were visualised by chemoluminescence using the SuperSignal West Femto Maximum Sensitivity Substrate Trial Kit (Thermo Scientific). The luminescence was registered on X-ray film, which was developed using an X-ray film processor (Protec Medizintechnik).

5.4.2 TNT *in vitro* translation

To test the specific inhibition of protein translation by antisense morpholino oligonucleotides, the TNT SP6 Coupled Reticulocyte Lysate System (Promega) was used. The sequence of the DNA template contained the specific target sequence of the morpholino as well as a C-terminal myc-tag to visualise the in vitro-translated protein by subsequent Western blot. The reaction volume for the TNT *in vitro* translation was set up as follows:

12.5	µl	rabbit reticulocyte lysate
1	µl	25x reaction buffer
0.5	µl	RNA polymerase (SP6)
0.25	µl	amino acid mix (-met)
0.25	µl	amino acid mix (-leu)
0.5	µl	RiboLock RNAse inhibitor (Fermentas)
1	µg	DNA template
2	µl	Morpholino (0.5 mM)
x	µl	H_2O
25	µl	

The reaction was incubated at 30°C for 90 minutes. After that 12.5 µl 3x SDS sample buffer were directly added and samples were incubated at 95°C for 5 minutes. Results were visualised by subsequent Western blot.

5.4.3 RBD-GST expression in *E. Coli*

Electrocompetent *E. Coli* BL21(DE3) Rosetta were transformed with 100 ng pGEX-RBD-GST and cultured overnight in 50 ml LB medium containing Amp (100 µg/ml) and Chloramphenicol (34 µg/ml) at 37°C with shaking. The following day 4x 500 ml LB-ampicillin-chloramphenicol were inoculated each with 5 ml of the overnight culture and grown until OD_{600} reached 0.4 to 0.5. Protein expression was then induced by 400 µl IPTG (500 mM). Induced bacteria were cultured for 3 hours at 37°C with shaking. Cells were harvested by centrifugation for 30 minutes at 5.000 rpm at 4°C. The bacterial pellet was resuspended in 20 ml total volume of bacteria lysis buffer and cells were sonicated 6 times for 15 seconds, with a 30 second break between each sonication cycle. 2 ml 10% Triton X-100 were added and the suspension was incubated shaking on ice in the cold room for 30 minutes. To clear the bacterial lysate, ultra centrifugation with 20.000 rpm was carried out for 20 minutes. The cleared supernatant was filtered using a folded filter and 2 ml glycerol and 200 µl PMSF were added. The protein lysate was aliquoted to 2 ml and shock frosted using liquid nitrogen. Aliquots were stored at -80°C until further use.

5.4.4 Rho activity assay

For the RhoA activity assay, *Xenopus* embryos were injected at 4-cell stage into the two dorsal blastomeres with 200 pg mRNA for RhoA-myc (Medina et al., 2004) either alone or together with synthetic mRNA or antisense morpholino oligonucleotide of interest. The embryos were grown until stage 10.5, washed once in ice cold Rho lysis buffer and homogenised with 15 µl/embryo of ice cold Rho lysis buffer using a syringe. The embryo homogenate was centrifuged for 5 minutes with 13.000 rpm at 4°C, the protein lysate was transferred to a new reaction tube without fat and cell debris and one volume of FREON was added. Samples were mixed and centrifuged again for five minutes (13.000 rpm, 4°C). The upper aqueous phase containing the cleared protein lysate was used for RBD-GST-pulldown of active RhoA. RBD-GST protein from bacteria lysates was coupled to Glutathione Sepharose 4B beads (Pharmacia Biotech) by adding 1 ml of bacterial lysate to 60 µl of bead-suspension, followed by rotation for one hour at 4°C. RBD-GST coupled beads were washed 3x with Rho wash buffer and 500 µl of embryo protein lysate were added. The lysate was incubated with RBD-GST-Glutathione sepharose beads for 45 minutes rotating at 4°C. The beads were washed 3x with Rho wash buffer and active Rho was eluated by directly adding 40 µl of 3x SDS sample buffer and subsequent heating to 95°C for 5 minutes. Samples were resolved using 12% SDS-PAGE and immunoblotted with a mouse anti-Myc (9E10) antibody. Whole embryo extracts were used as a loading control.

5.4.5 RBD-GFP staining

For RhoA activity staining, embryos were injected at 4-cell stage into the dorsal right blastomere with xGit2 mRNA (800 pg) or xRhoGAP 11A mRNA (60 pg) together with mRNA for H2B-RFP (200 pg) to mark the injected side. Embryos were grown until stage 10.5 and dorsal marginal zones were explanted and cultivated under a coverslip fixed with silicone grease in 1x MBS for 4 hours. Explants were fixed in MEMFA for 30 minutes and washed 6x in PBS. Then they were permeabilised with 0.3%

Triton X-100/PBS for 10 minutes and washed again with PBS for 15 minutes. Samples were blocked in blocking solution and stained overnight with 10 µg RBD-GFP in blocking solution at 4°C in the dark. DMZ were washed 6x with PBS for 10 minutes, mounted using Mowiol and subjected to 66thylene microscopy (Berger et al., 2009). Images were taken on the uninjected and injected sides with the same exposure times. To exclude bleaching effects the injected side was imaged first.

6 References

Angres, B., Muller, A.H., Kellermann, J., and Hausen, P., 1991. Differential expression of two cadherins in Xenopus laevis. Development 111, 829-844.

Axelrod, J.D., Miller, J.R., Shulman, J.M., Moon, R.T., and Perrimon, N., 1998. Differential recruitment of Dishevelled provides signaling specificity in the planar cell polarity and Wingless signaling pathways. Genes Dev. 12, 2610-2622.

Berger, C.D. Regulation of Morphogenetic Cell Behavior by Xenopus Paraxial Protocadherin. Doctoral Thesis, University of Heidelberg. 2009.

Berger, C.D., Marz, M., Kitzing, T.M., Grosse, R., and Steinbeisser, H., 2009. Detection of activated Rho in fixed Xenopus tissue. Dev. Dyn. 238, 1407-1411.

Bikkavilli, R.K., Feigin, M.E., and Malbon, C.C., 2008. G alpha o mediates WNT-JNK signaling through dishevelled 1 and 3, RhoA family members, and MEKK 1 and 4 in mammalian cells. J. Cell Sci. 121, 234-245.

Blitzer, J.T. and Nusse, R., 2006. A critical role for endocytosis in Wnt signaling. BMC. Cell Biol. 7, 28.

Bonn, S., Seeburg, P.H., and Schwarz, M.K., 2007. Combinatorial expression of alpha- and gamma-protocadherins alters their presenilin-dependent processing. Mol. Cell Biol. 27, 4121-4132.

Bouwmeester, T., Kim, S., Sasai, Y., Lu, B., and De Robertis, E.M., 1996. Cerberus is a head-inducing secreted factor expressed in the anterior endoderm of Spemann's organizer. Nature 382, 595-601.

Brannon, M. and Kimelman, D., 1996. Activation of Siamois by the Wnt pathway. Dev. Biol. 180, 344-347.

Burridge, K. and Wennerberg, K., 2004. Rho and Rac take center stage. Cell 116, 167-179.

Carnac, G., Kodjabachian, L., Gurdon, J.B., and Lemaire, P., 1996. The homeobox gene Siamois is a target of the Wnt dorsalisation pathway and triggers organiser activity in the absence of mesoderm. Development 122, 3055-3065.

Casey, E.S., O'Reilly, M.A., Conlon, F.L., and Smith, J.C., 1998. The T-box transcription factor Brachyury regulates expression of eFGF through binding to a non-palindromic response element. Development 125, 3887-3894.

Cerione, R.A. and Zheng, Y., 1996. The Dbl family of oncogenes. Curr. Opin. Cell Biol. 8, 216-222.

Chen, X. and Gumbiner, B.M., 2006. Paraxial protocadherin mediates cell sorting and tissue morphogenesis by regulating C-cadherin adhesion activity. J. Cell Biol. 174, 301-313.

Choi, Y.S., Sehgal, R., McCrea, P., and Gumbiner, B., 1990. A cadherin-like protein in eggs and cleaving embryos of Xenopus laevis is expressed in oocytes in response to progesterone. J. Cell Biol. 110, 1575-1582.

Claing, A., Perry, S.J., Achiriloaie, M., Walker, J.K., Albanesi, J.P., Lefkowitz, R.J., and Premont, R.T., 2000. Multiple endocytic pathways of G protein-coupled receptors delineated by GIT1 sensitivity. Proc. Natl. Acad. Sci. U. S. A 97, 1119-1124.

Darken, R.S. and Wilson, P.A., 2001. Axis induction by wnt signaling: Target promoter responsiveness regulates competence. Dev. Biol. 234, 42-54.

Davidson, L.A., Hoffstrom, B.G., Keller, R., and DeSimone, D.W., 2002. Mesendoderm extension and mantle closure in Xenopus laevis gastrulation: combined roles for integrin alpha(5)beta(1), fibronectin, and tissue geometry. Dev. Biol. 242, 109-129.

Di Cesare, A., Paris, S., Albertinazzi, C., Dariozzi, S., Andersen, J., Mann, M., Longhi, R., and de Curtis, I., 2000. p95-APP1 links membrane transport to Rac-mediated reorganization of actin. Nat. Cell Biol. 2, 521-530.

Djiane, A., Riou, J., Umbhauer, M., Boucaut, J., and Shi, D., 2000. Role of frizzled 7 in the regulation of convergent extension movements during gastrulation in Xenopus laevis. Development 127, 3091-3100.

Fan, M.J., Gruning, W., Walz, G., and Sokol, S.Y., 1998. Wnt signaling and transcriptional control of Siamois in Xenopus embryos. Proc. Natl. Acad. Sci. U. S. A 95, 5626-5631.

Fanto, M., Weber, U., Strutt, D.I., and Mlodzik, M., 2000b. Nuclear signaling by Rac and Rho GTPases is required in the establishment of epithelial planar polarity in the Drosophila eye. Curr. Biol. 10, 979-988.

Fanto, M., Weber, U., Strutt, D.I., and Mlodzik, M., 2000a. Nuclear signaling by Rac and Rho GTPases is required in the establishment of epithelial planar polarity in the Drosophila eye. Curr. Biol. 10, 979-988.

Fletcher, G., Jones, G.E., Patient, R., and Snape, A., 2006. A role for GATA factors in Xenopus gastrulation movements. Mech. Dev. 123, 730-745.

Frank, S.R., Adelstein, M.R., and Hansen, S.H., 2006. GIT2 represses Crk- and Rac1-regulated cell spreading and Cdc42-mediated focal adhesion turnover. EMBO J. 25, 1848-1859.

Gagliardi, M., Piddini, E., and Vincent, J.P., 2008. Endocytosis: a positive or a negative influence on Wnt signalling? Traffic. 9, 1-9.

Geng, X., Xiao, L., Lin, G.F., Hu, R., Wang, J.H., Rupp, R.A., and Ding, X., 2003. Lef/Tcf-dependent Wnt/beta-catenin signaling during Xenopus axis specification. FEBS Lett. 547, 1-6.

Gilbert, S.F., 2006. Developmental biology. Sinauer, Sunderland, Mass.

Ginsberg, D., DeSimone, D., and Geiger, B., 1991. Expression of a novel cadherin (EP-cadherin) in unfertilized eggs and early Xenopus embryos. Development 111, 315-325.

Glickman, N.S., Kimmel, C.B., Jones, M.A., and Adams, R.J., 2003. Shaping the zebrafish notochord. Development 130, 873-887.

Goulimari, P., Kitzing, T.M., Knieling, H., Brandt, D.T., Offermanns, S., and Grosse, R., 2005. Galpha12/13 is essential for directed cell migration and localized Rho-Dia1 function. J. Biol. Chem. 280, 42242-42251.

Green, J.B., Cook, T.L., Smith, J.C., and Grainger, R.M., 1997a. Anteroposterior neural tissue specification by activin-induced mesoderm. Proc. Natl. Acad. Sci. U. S. A 94, 8596-8601.

Green, J.B., Cook, T.L., Smith, J.C., and Grainger, R.M., 1997b. Anteroposterior neural tissue specification by activin-induced mesoderm. Proc. Natl. Acad. Sci. U. S. A 94, 8596-8601.

Green, J.B., New, H.V., and Smith, J.C., 1992. Responses of embryonic Xenopus cells to activin and FGF are separated by multiple dose thresholds and correspond to distinct axes of the mesoderm. Cell 71, 731-739.

Green, J.B. and Smith, J.C., 1990. Graded changes in dose of a Xenopus activin A homologue elicit stepwise transitions in embryonic cell fate. Nature 347, 391-394.

Haas, I.G., Frank, M., Veron, N., and Kemler, R., 2005. Presenilin-dependent processing and nuclear function of gamma-protocadherins. J. Biol. Chem. 280, 9313-9319.

Habas, R., Dawid, I.B., and He, X., 2003. Coactivation of Rac and Rho by Wnt/Frizzled signaling is required for vertebrate gastrulation. Genes Dev. 17, 295-309.

Habas, R. and He, X., 2006. Activation of Rho and Rac by Wnt/frizzled signaling. Methods Enzymol. 406, 500-511.

Habas, R., Kato, Y., and He, X., 2001. Wnt/Frizzled activation of Rho regulates vertebrate gastrulation and requires a novel Formin homology protein Daam1. Cell 107, 843-854.

Halbleib, J.M. and Nelson, W.J., 2006. Cadherins in development: cell adhesion, sorting, and tissue morphogenesis. Genes Dev. 20, 3199-3214.

Hambsch, B., Grinevich, V., Seeburg, P.H., and Schwarz, M.K., 2005. {gamma}-Protocadherins, presenilin-mediated release of C-terminal fragment promotes locus expression. J. Biol. Chem. 280, 15888-15897.

Hayata, T., Uochi, T., and Asashima, M., 1998. Molecular cloning of XNLRR-1, a Xenopus homolog of mouse neuronal leucine-rich repeat protein expressed in the developing Xenopus nervous system. Gene 221, 159-166.

Hellsten, U., Harland, R.M., Gilchrist, M.J., Hendrix, D., Jurka, J., Kapitonov, V., Ovcharenko, I., Putnam, N.H., Shu, S., Taher, L., Blitz, I.L., Blumberg, B., Dichmann, D.S., Dubchak, I., Amaya, E., Detter, J.C., Fletcher, R., Gerhard, D.S., Goodstein, D., Graves, T., Grigoriev, I.V., Grimwood, J., Kawashima, T., Lindquist, E., Lucas, S.M., Mead, P.E., Mitros, T., Ogino, H., Ohta, Y., Poliakov, A.V., Pollet, N., Robert, J., Salamov, A., Sater, A.K., Schmutz, J., Terry, A., Vize, P.D., Warren, W.C., Wells, D., Wills, A., Wilson, R.K., Zimmerman, L.B., Zorn, A.M., Grainger, R., Grammer, T., Khokha, M.K., Richardson, P.M., and Rokhsar, D.S., 2010. The genome of the Western clawed frog Xenopus tropicalis. Science 328, 633-636.

Hensey, C. and Gautier, J., 1998. Programmed cell death during Xenopus development: a spatio-temporal analysis. Dev. Biol. 203, 36-48.

Herzberg, F., Wildermuth, V., and Wedlich, D., 1991. Expression of XBcad, a novel cadherin, during oogenesis and early development of Xenopus. Mech. Dev. 35, 33-42.

Hinkley, C.S., Martin, J.F., Leibham, D., and Perry, M., 1992. Sequential expression of multiple POU proteins during amphibian early development. Mol. Cell Biol. 12, 638-649.

Hoefen, R.J. and Berk, B.C., 2006. The multifunctional GIT family of proteins. J. Cell Sci. 119, 1469-1475.

Hsiao, P.W., Fryer, C.J., Trotter, K.W., Wang, W., and Archer, T.K., 2003. BAF60a mediates critical interactions between nuclear receptors and the BRG1 chromatin-remodeling complex for transactivation. Mol. Cell Biol. 23, 6210-6220.

Huelsken, J. and Behrens, J., 2002. The Wnt signalling pathway. J. Cell Sci. 115, 3977-3978.

Huelsken, J. and Birchmeier, W., 2001. New aspects of Wnt signaling pathways in higher vertebrates. Curr. Opin. Genet. Dev. 11, 547-553.

Hukriede, N.A., Tsang, T.E., Habas, R., Khoo, P.L., Steiner, K., Weeks, D.L., Tam, P.P., and Dawid, I.B., 2003. Conserved requirement of Lim1 function for cell movements during gastrulation. Dev. Cell 4, 83-94.

Hyodo-Miura, J., Yamamoto, T.S., Hyodo, A.C., Iemura, S., Kusakabe, M., Nishida, E., Natsume, T., and Ueno, N., 2006. XGAP, an ArfGAP, is required for polarized localization of PAR proteins and cell polarity in Xenopus gastrulation. Dev. Cell 11, 69-79.

Irvine, K.D. and Wieschaus, E., 1994. Cell intercalation during Drosophila germband extension and its regulation by pair-rule segmentation genes. Development 120, 827-841.

Isaacs, H.V., Pownall, M.E., and Slack, J.M., 1994. eFGF regulates Xbra expression during Xenopus gastrulation. EMBO J. 13, 4469-4481.

Jenny, A. and Mlodzik, M., 2006. Planar cell polarity signaling: a common mechanism for cellular polarization. Mt. Sinai J. Med. 73, 738-750.

Jungwirth, M.S. Regulation of Repulsion Behaviour in the Ectoderm of Xenopus laevis Embryos. Master Thesis, University of Heidelberg. 2009.

Kaibuchi, K., 1999. Regulation of cytoskeleton and cell adhesion by Rho targets. Prog. Mol. Subcell. Biol. 22, 23-38.

Kaibuchi, K., Kuroda, S., Fukata, M., and Nakagawa, M., 1999. Regulation of cadherin-mediated cell-cell adhesion by the Rho family GTPases. Curr. Opin. Cell Biol. 11, 591-596.

Keller, R., 2002. Shaping the vertebrate body plan by polarized embryonic cell movements. Science 298, 1950-1954.

Keller, R., 2005. Cell migration during gastrulation. Curr. Opin. Cell Biol. 17, 533-541.

Keller, R., Davidson, L., Edlund, A., Elul, T., Ezin, M., Shook, D., and Skoglund, P., 2000. Mechanisms of convergence and extension by cell intercalation. Philos. Trans. R. Soc. Lond B Biol. Sci. 355, 897-922.

Keller, R., Shih, J., and Domingo, C., 1992. The patterning and functioning of protrusive activity during convergence and extension of the Xenopus organiser. Dev. Suppl 81-91.

Kelley, C., Yee, K., Harland, R., and Zon, L.I., 1994. Ventral expression of GATA-1 and GATA-2 in the Xenopus embryo defines induction of hematopoietic mesoderm. Dev. Biol. 165, 193-205.

Kestler, H.A. and Kühl, M., 2008. From individual Wnt pathways towards a Wnt signalling network. Philos. Trans. R. Soc. Lond B Biol. Sci. 363, 1333-1347.

Kietzmann, A. Charakterisierung der Proteininteraktionsdomänen im cytoplasmatischen Teil des Paraxialen Protocadherins von Xenopus laevis. Diplomarbeit, Universität Heidelberg. 2008.

Kim, J., Shim, S., Choi, S.C., and Han, J.K., 2003. A putative Xenopus Rho-GTPase activating protein (XrGAP) gene is expressed in the notochord and brain during the early embryogenesis. Gene Expr. Patterns. 3, 219-223.

Kim, S.H., Jen, W.C., De Robertis, E.M., and Kintner, C., 2000. The protocadherin PAPC establishes segmental boundaries during somitogenesis in xenopus embryos. Curr. Biol. 10, 821-830.

Kim, S.H., Yamamoto, A., Bouwmeester, T., Agius, E., and Robertis, E.M., 1998. The role of paraxial protocadherin in selective adhesion and cell movements of the mesoderm during Xenopus gastrulation. Development 125, 4681-4690.

Kishi, M., Mizuseki, K., Sasai, N., Yamazaki, H., Shiota, K., Nakanishi, S., and Sasai, Y., 2000. Requirement of Sox2-mediated signaling for differentiation of early Xenopus neuroectoderm. Development 127, 791-800.

Klein, T.J. and Mlodzik, M., 2005. Planar cell polarization: an emerging model points in the right direction. Annu. Rev. Cell Dev. Biol. 21, 155-176.

Kofron, M., Wylie, C., and Heasman, J., 2004. The role of Mixer in patterning the early Xenopus embryo. Development 131, 2431-2441.

Köster, I., Jungwirth, M.S., and Steinbeisser, H., 2010. xGit2 and xRhoGAP 11A regulate convergent extension and tissue separation in Xenopus gastrulation. Dev. Biol.

Kristelly, R., Gao, G., and Tesmer, J.J., 2004. Structural determinants of RhoA binding and nucleotide exchange in leukemia-associated Rho guanine-nucleotide exchange factor. J. Biol. Chem. 279, 47352-47362.

Kühl, M., 2002. Non-canonical Wnt signaling in Xenopus: regulation of axis formation and gastrulation. Semin. Cell Dev. Biol. 13, 243-249.

Kühl, M., Geis, K., Sheldahl, L.C., Pukrop, T., Moon, R.T., and Wedlich, D., 2001. Antagonistic regulation of convergent extension movements in Xenopus by Wnt/beta-catenin and Wnt/Ca2+ signaling. Mech. Dev. 106, 61-76.

Kühl, M., Sheldahl, L.C., Park, M., Miller, J.R., and Moon, R.T., 2000. The Wnt/Ca2+ pathway: a new vertebrate Wnt signaling pathway takes shape. Trends Genet. 16, 279-283.

Kwan, K.M. and Kirschner, M.W., 2005. A microtubule-binding Rho-GEF controls cell morphology during convergent extension of Xenopus laevis. Development 132, 4599-4610.

Laemmli, U.K., 1970. Cleavage of structural proteins during the assembly of the head of bacteriophage T4. Nature 227, 680-685.

Latinkic, B.V. and Smith, J.C., 1999. Goosecoid and mix.1 repress Brachyury expression and are required for head formation in Xenopus. Development 126, 1769-1779.

Lemaire, P., Darras, S., Caillol, D., and Kodjabachian, L., 1998. A role for the vegetally expressed Xenopus gene Mix.1 in endoderm formation and in the restriction of mesoderm to the marginal zone. Development 125, 2371-2380.

Logan, C.Y. and Nusse, R., 2004. The Wnt signaling pathway in development and disease. Annu. Rev. Cell Dev. Biol. 20, 781-810.

Matafora, V., Paris, S., Dariozzi, S., and de, C., I, 2001. Molecular mechanisms regulating the subcellular localization of p95-APP1 between the endosomal recycling compartment and sites of actin organization at the cell surface. J. Cell Sci. 114, 4509-4520.

Maurus, D., Heligon, C., Burger-Schwarzler, A., Brandli, A.W., and Kühl, M., 2005. Noncanonical Wnt-4 signaling and EAF2 are required for eye development in Xenopus laevis. EMBO J. 24, 1181-1191.

Mazaki, Y., Hashimoto, S., Okawa, K., Tsubouchi, A., Nakamura, K., Yagi, R., Yano, H., Kondo, A., Iwamatsu, A., Mizoguchi, A., and Sabe, H., 2001. An ADP-ribosylation factor GTPase-activating protein Git2-short/KIAA0148 is involved in subcellular localization of paxillin and actin cytoskeletal organization. Mol. Biol. Cell 12, 645-662.

McKendry, R., Hsu, S.C., Harland, R.M., and Grosschedl, R., 1997. LEF-1/TCF proteins mediate wnt-inducible transcription from the Xenopus nodal-related 3 promoter. Dev. Biol. 192, 420-431.

Medina, A., Reintsch, W., and Steinbeisser, H., 2000. Xenopus frizzled 7 can act in canonical and non-canonical Wnt signaling pathways: implications on early patterning and morphogenesis. Mech. Dev. 92, 227-237.

Medina, A. and Steinbeisser, H., 2000. Interaction of Frizzled 7 and Dishevelled in Xenopus. Dev. Dyn. 218, 671-680.

Medina, A., Swain, R.K., Kuerner, K.M., and Steinbeisser, H., 2004. Xenopus paraxial protocadherin has signaling functions and is involved in tissue separation. EMBO J. 23, 3249-3258.

Miller, J.R., 2002. The Wnts. Genome Biol. 3, REVIEWS3001.

Mueller, P.R., Coleman, T.R., and Dunphy, W.G., 1995. Cell cycle regulation of a Xenopus Wee1-like kinase. Mol. Biol. Cell 6, 119-134.

Munro, E.M. and Odell, G.M., 2002. Polarized basolateral cell motility underlies invagination and convergent extension of the ascidian notochord. Development 129, 13-24.

Myers, D.C., Sepich, D.S., and Solnica-Krezel, L., 2002. Bmp activity gradient regulates convergent extension during zebrafish gastrulation. Dev. Biol. 243, 81-98.

Nagamine, K., Furue, M., Fukui, A., and Asashima, M., 2005. Induction of cells expressing vascular endothelium markers from undifferentiated Xenopus presumptive ectoderm by co-treatment with activin and angiopoietin-2. Zoolog. Sci. 22, 755-761.

Nakatsuji, N. and Johnson, K.E., 1983. Comparative study of extracellular fibrils on the ectodermal layer in gastrulae of five amphibian species. J. Cell Sci. 59, 61-70.

Nieuwkoop, P.D. and Faber, J., 1975. Normal table of Xenopus laevis. Daudin, North Holland:Amsterdam.

Oh, J., Sohn, D.H., Ko, M., Chung, H., Jeon, S.H., and Seong, R.H., 2008. BAF60a interacts with p53 to recruit the SWI/SNF complex. J. Biol. Chem. 283, 11924-11934.

Premont, R.T., Claing, A., Vitale, N., Freeman, J.L., Pitcher, J.A., Patton, W.A., Moss, J., Vaughan, M., and Lefkowitz, R.J., 1998. beta2-Adrenergic receptor regulation by GIT1, a G protein-coupled receptor kinase-associated ADP ribosylation factor GTPase-activating protein. Proc. Natl. Acad. Sci. U. S. A 95, 14082-14087.

Premont, R.T., Claing, A., Vitale, N., Perry, S.J., and Lefkowitz, R.J., 2000. The GIT family of ADP-ribosylation factor GTPase-activating proteins. Functional diversity of GIT2 through alternative splicing. J. Biol. Chem. 275, 22373-22380.

Raftopoulou, M. and Hall, A., 2004. Cell migration: Rho GTPases lead the way. Dev. Biol. 265, 23-32.

Randazzo, P.A., Nie, Z., Miura, K., and Hsu, V.W., 2000. Molecular aspects of the cellular activities of ADP-ribosylation factors. Sci. STKE. 59, RE1.

Ren, X.D., Kiosses, W.B., and Schwartz, M.A., 1999. Regulation of the small GTP-binding protein Rho by cell adhesion and the cytoskeleton. EMBO J. 18, 578-585.

Ren, X.D., Kiosses, W.B., Sieg, D.J., Otey, C.A., Schlaepfer, D.D., and Schwartz, M.A., 2000. Focal adhesion kinase suppresses Rho activity to promote focal adhesion turnover. J. Cell Sci. 113 (Pt 20), 3673-3678.

Rupp, R.A., Snider, L., and Weintraub, H., 1994. Xenopus embryos regulate the nuclear localization of XMyoD. Genes Dev. 8, 1311-1323.

Sasai, Y., 2001. Roles of Sox factors in neural determination: conserved signaling in evolution? Int. J. Dev. Biol. 45, 321-326.

Sausedo, R.A. and Schoenwolf, G.C., 1994. Quantitative analyses of cell behaviors underlying notochord formation and extension in mouse embryos. Anat. Rec. 239, 103-112.

Schambony, A. and Wedlich, D., 2007. Wnt-5A/Ror2 regulate expression of XPAPC through an alternative noncanonical signaling pathway. Dev. Cell 12, 779-792.

Schoenwolf, G.C. and Alvarez, I.S., 1989. Roles of neuroepithelial cell rearrangement and division in shaping of the avian neural plate. Development 106, 427-439.

Seto, E.S. and Bellen, H.J., 2006. Internalization is required for proper Wingless signaling in Drosophila melanogaster. J. Cell Biol. 173, 95-106.

Seto, E.S., Bellen, H.J., and Lloyd, T.E., 2002. When cell biology meets development: endocytic regulation of signaling pathways. Genes Dev. 16, 1314-1336.

Sheldahl, L.C., Slusarski, D.C., Pandur, P., Miller, J.R., Kühl, M., and Moon, R.T., 2003. Dishevelled activates Ca2+ flux, PKC, and CamKII in vertebrate embryos. J. Cell Biol. 161, 769-777.

Shikata, Y., Birukov, K.G., and Garcia, J.G., 2003. S1P induces FA remodeling in human pulmonary endothelial cells: role of Rac, GIT1, FAK, and paxillin. J. Appl. Physiol 94, 1193-1203.

Shin, Y., Kitayama, A., Koide, T., Peiffer, D.A., Mochii, M., Liao, A., Ueno, N., and Cho, K.W., 2005. Identification of neural genes using Xenopus DNA microarrays. Dev. Dyn. 232, 432-444.

Struewing, I.T., Barnett, C.D., Zhang, W., Yadav, S., and Mao, C.D., 2007. Frizzled-7 turnover at the plasma membrane is regulated by cell density and the Ca(2+) -dependent protease calpain-1. Exp. Cell Res. 313, 3526-3541.

Sumanas, S. and Ekker, S.C., 2001. Xenopus frizzled-7 morphant displays defects in dorsoventral patterning and convergent extension movements during gastrulation. Genesis. 30, 119-122.

Sumanas, S., Strege, P., Heasman, J., and Ekker, S.C., 2000. The putative wnt receptor Xenopus frizzled-7 functions upstream of beta-catenin in vertebrate dorsoventral mesoderm patterning. Development 127, 1981-1990.

Tada, M., Concha, M.L., and Heisenberg, C.P., 2002. Non-canonical Wnt signalling and regulation of gastrulation movements. Semin. Cell Dev. Biol. 13, 251-260.

Tahinci, E. and Symes, K., 2003. Distinct functions of Rho and Rac are required for convergent extension during Xenopus gastrulation. Dev. Biol. 259, 318-335.

Tanegashima, K., Zhao, H., and Dawid, I.B., 2008. WGEF activates Rho in the Wnt-PCP pathway and controls convergent extension in Xenopus gastrulation. EMBO J. 27, 606-617.

Tcherkezian, J. and Lamarche-Vane, N., 2007. Current knowledge of the large RhoGAP family of proteins. Biol. Cell 99, 67-86.

Tiedemann, H. and Tiedemann, H., 1959. [Experiments on the extraction of a mesodermal inductor from chick embryo.]. Hoppe Seylers. Z. Physiol Chem. 314, 156-176.

Torres, M.A., Yang-Snyder, J.A., Purcell, S.M., DeMarais, A.A., McGrew, L.L., and Moon, R.T., 1996. Activities of the Wnt-1 class of secreted signaling factors are antagonized by the Wnt-5A class and by a dominant negative cadherin in early Xenopus development. J. Cell Biol. 133, 1123-1137.

Turner, D.L. and Weintraub, H., 1994. Expression of achaete-scute homolog 3 in Xenopus embryos converts ectodermal cells to a neural fate. Genes Dev. 8, 1434-1447.

Unterseher, F., Hefele, J.A., Giehl, K., De Robertis, E.M., Wedlich, D., and Schambony, A., 2004. Paraxial protocadherin coordinates cell polarity during convergent extension via Rho A and JNK. EMBO J. 23, 3259-3269.

van Nieuw Amerongen, G.P., Natarajan, K., Yin, G., Hoefen, R.J., Osawa, M., Haendeler, J., Ridley, A.J., Fujiwara, K., van, H., V, and Berk, B.C., 2004. GIT1 mediates thrombin signaling in endothelial cells: role in turnover of RhoA-type focal adhesions. Circ. Res. 94, 1041-1049.

Veeman, M.T., Slusarski, D.C., Kaykas, A., Louie, S.H., and Moon, R.T., 2003. Zebrafish prickle, a modulator of noncanonical Wnt/Fz signaling, regulates gastrulation movements. Curr. Biol. 13, 680-685.

Wacker, S., Grimm, K., Joos, T., and Winklbauer, R., 2000. Development and control of tissue separation at gastrulation in Xenopus. Dev. Biol. 224, 428-439.

Wallingford, J.B., Fraser, S.E., and Harland, R.M., 2002. Convergent extension: the molecular control of polarized cell movement during embryonic development. Dev. Cell 2, 695-706.

Wallingford, J.B. and Harland, R.M., 2001. Xenopus Dishevelled signaling regulates both neural and mesodermal convergent extension: parallel forces elongating the body axis. Development 128, 2581-2592.

Wallingford, J.B. and Harland, R.M., 2002. Neural tube closure requires Dishevelled-dependent convergent extension of the midline. Development 129, 5815-5825.

Wallingford, J.B., Rowning, B.A., Vogeli, K.M., Rothbacher, U., Fraser, S.E., and Harland, R.M., 2000. Dishevelled controls cell polarity during Xenopus gastrulation. Nature 405, 81-85.

Wang, J., Hamblet, N.S., Mark, S., Dickinson, M.E., Brinkman, B.C., Segil, N., Fraser, S.E., Chen, P., Wallingford, J.B., and Wynshaw-Boris, A., 2006. Dishevelled genes mediate a conserved mammalian PCP pathway to regulate convergent extension during neurulation. Development 133, 1767-1778.

Wang, Y. Identification and characterization of interacting partners of cytoplasmic domain of Xenopus Paraxial Protocadherin. Doctoral Thesis, University of Heidelberg. 2007.

Wang, Y., Janicki, P., Köster, I., Berger, C.D., Wenzl, C., Grosshans, J., and Steinbeisser, H., 2008. Xenopus Paraxial Protocadherin regulates morphogenesis by antagonizing Sprouty. Genes Dev. 22, 878-883.

Wardle, F.C. and Smith, J.C., 2004. Refinement of gene expression patterns in the early Xenopus embryo. Development 131, 4687-4696.

Weber, U., Paricio, N., and Mlodzik, M., 2000. Jun mediates Frizzled-induced R3/R4 cell fate distinction and planar polarity determination in the Drosophila eye. Development 127, 3619-3629.

Winklbauer, R., Medina, A., Swain, R.K., and Steinbeisser, H., 2001. Frizzled-7 signalling controls tissue separation during Xenopus gastrulation. Nature 413, 856-860.

Winklbauer, R. and Schurfeld, M., 1999. Vegetal rotation, a new gastrulation movement involved in the internalization of the mesoderm and endoderm in Xenopus. Development 126, 3703-3713.

Wunnenberg-Stapleton, K., Blitz, I.L., Hashimoto, C., and Cho, K.W., 1999. Involvement of the small GTPases XRhoA and XRnd1 in cell adhesion and head formation in early Xenopus development. Development 126, 5339-5351.

7 Appendix

7.1 Abbreviations

(v/v)	volume-volume ratio
(w/v)	weight-volume ratio
AC	animal cap
Amp	ampicillin
Ank	ankyrin repeat
AP	alakaline phosphatase
APC	*Adenomatous polyposis coli*
APS	ammonium persulphate
Arf	ADP ribosylation factor
BCR	blastocoel roof
BSA	bovine serum albumine
CC	coiled-coil
cDNA	copy-DNA
CE	convergent extension
cRNA	copy-RNA
DMSO	dimethylsulfoxid
DMZ	dorsal marginal zone
dNTP	2'-desoxy-nucleoside-5'-triphosphate
Dsh	dishevelled
DTT	Dithiothreitol
E. coli	Escherichia coli
EC	extracellular cadherin domain
EDTA	ethylene-diamin-tetraacetate
EST	expressed sequence tag
Fz	frizzled
GAP	GTPase activating protein
GDP	guanosine diphosphate
GEF	guanine nucleotide exchange factor
GFP	green fluorescent protein
GSK-3β	glycogen synthase kinase 3β
GST	gluthatione-S-transferase
GTP	guanosine triphosphate
HEPES	2-[4-(2-Hydroxyethyl)-1-piperazinyl]-ethansulfonic acid
HMG	high mobility group
HRP	horse radish peroxidase
IPTG	isopropyl-β-D-thiogalactopyranoside

ISH	whole mount *in situ* hybridisation
JNK	c-Jun N-terminal kinase
LB	Luria Bertani Medium
MBS	Modified Barth`s Solution
MBT	midblastula transition
MEM	Modified Eagle´s Medium
Mo	antisense morpholino oligonucleotide
mRNA	messenger RNA
NGS	normal goat serum
OD	optic density
ODC	ornithin decarboxylase
PAGE	polyacrylamide gel electrophoresis
PAPC	Paraxial Protocadherin
PBS	Paxillin-binding site
PCP	planar cell polarity
PCR	polymerase chain reaction
PKC	proteinkinase C
qRT-PCR	quantitative reverse transcription-PCR
RBD	Rho-binding domain of rhotekin
RFP	red fluorescent protein
rpm	revolutions per minute
RT	room temperature
RT-PCR	reverse transcription-PCR
SDS	sodium-dodecyl-sulfate
SHD	Spa2-homology domain
SSC	standard saline citrate
TBE	Tris-boracic acid-EDTA
TEMED	N,N,N',N'-Tetramethylethylendiamin
TGF-β	Transforming Growth Factor β
TS	tissue separation
u	Unit
WT	wildtype
xBra	*Xenopus* brachyury
xChd	*Xenopus* chordin
X-Gal	5-Bromo-4-Chloro-3-Indolyl-β-D-Galactopyranosid
xGit2	*Xenopus* G-protein-coupled receptor kinase interacting protein2

7.2 Table of Figures

Für Hendrik

Auf diesem – nicht immer geraden – Weg haben mich viele Menschen begleitet und unterstützt, denen ich danken möchte:

- **Prof. Thomas Holstein** für die Übernahme des Zweitgutachtens
- **Dr. Henner Friedle** von Agilent für seine Unterstützung bezüglich aller Fragen zu den Microarray-Experimenten
- **Dr. Vladimir Benes**, **Sabine Schmidt** und **Tomi Ivacevic** von der EMBL Genetic Core Facility, für die Möglichkeit die Microarrays in ihrem Labor durchzuführen und die nötigen technischen Geräte nutzen zu dürfen, sowie die fachliche Unterstüztung dabei.

Neben diesen Menschen gibt auch einige, an die ich ein paar ganz persönliche Worte richten möchte:

- **Herbert**, ich möchte dir danken, dass du zu jeder Zeit ein wirklicher Doktorvater warst. Du hast mir ein spannendes Thema gegeben und mir wissenschaftliches Denken vermittelt, mich immer wieder zum Diskutieren angeregt und Interesse an meinem Projekt gezeigt. Das hat mich sowohl wissenschaftlich als auch menschlich geprägt.
- **Anja, Anne, Conny, Inge, Katharina, Kirsten, Maria**: Ihr wart eine zweite Familie für mich, habt mich immer wieder aufgebaut, wenn es nicht so gut lief, oder euch mit mir über Erfolge gefreut. Danke für unzählige Kaffestunden, Geburtstagsessen, Ausgeh-Abende, Gespräche, gemeinsame Sportstunden... Ich vermisse euch!
- **Kirsten** möchte ich noch mal persönlich für ihre technische Unterstützung bei dieser Arbeit danken.
- **Meine Eltern**: Ihr habt an mich geglaubt und mir den Rücken freigehalten, damit ich diese Arbeit beenden konnte. Danke fürs Babysitten. Ohne euch, hätte ich das nicht geschafft!
- **Thorsten**, um dir zu danken reicht der Platz in dieser Arbeit nicht aus, aber du weißt auch so, was ich dir sagen möchte!